Alma Mater Studiorum - Università di Bologna
DEI - Dipartimento di Ingegneria dell'Energia Elettrica e dell'Informazione
"Guglielmo Marconi"

Dottorato di Ricerca in Automatica e Ricerca Operativa
Ciclo XXVII

Settore concorsuale di afferenza: 01/A6 - RICERCA OPERATIVA
Settore scientifico disciplinare: MAT/09 - RICERCA OPERATIVA

# Mathematical Optimization Applied to Thermal and Electrical Energy Systems

Chiara Bordin

Coordinatore
Prof. Daniele Vigo

Relatore
Prof. Daniele Vigo

Esame Finale 2015

# Contents

# Acknowledgments

To everyone who truly loves me and fills my life with friendship, love and kindness. To everyone who will come soon into my life.

Durham, 2015

# Keywords

- Optimization
- Mathematical Modeling
- Mixed Integer Linear Programming
- Graph Theory
- Network Design
- Network Flows
- Energy Systems
- District Heating Systems
- Thermal Energy Distribution
- Off-Grid Systems
- Renewable Energy
- Solar Energy
- Storage
- Battery Degradation

# List of Figures

# List of Tables

# Chapter 1

# Preface

The present Thesis aims at building and discussing mathematical models applications focused on Energy problems, both on the thermal side and on the electrical side. The objective is to show how mathematical programming techniques developed within Operational Research can give useful answers in the Energy Sector, how they can provide tools to support decision making processes of Companies operating in the Energy production and distribution and how they can be successfully used to make simulations and sensitivity analyses to better understand the state of the art and convenience of a particular technology by comparing it with the available alternatives.

The scientific sector of mathematical modeling techniques applied to the Energy field is quite ample, as the Energy field includes a wide variety of systems, plants and technologies. Furthermore, the continuous research of new and renewable Energy alternatives, as well as the increasing interest towards intelligent techniques for a better use and control of the available resources, is motivating more and more the research both in Academia and Industry.

Broadly speaking, the research in the Energy field can be classified into two main very big approaches. The first one is the research of complete new technologies for a better energy generation in terms of safe, efficient and environmentally friendly alternatives; this approach can be classified in the field of *radical innovation*, as it focuses on the creation of processes and products with unprecedented performance features.

The second approach is the research of new methods to better control and use what is already available in a more intelligent or "smart" way. That is to say, sometimes the problem doesn't really lie in what we have, but in how we are using what we already have. An intelligent use of the available Energy resources and technologies can make a huge difference in terms of economical and environmental advantages, with long term positive consequences on the whole society. This latter approach can be classified in the field of *incremental innovation* as it exploits the existing technology, focusing on costs or feature improvements in existing processes and products. It generally makes a massive use of marketing or business models; the main objective is the improvement of competitiveness within current markets or industries.

The Operational Research techniques lie in the second of the two approaches outlined above. Informally known as *the science of better*, Operational Research can give interesting answers and inputs on the best use of Energy resources and technologies, both on the systems design side and on the operational management side. Through the use of mathematical techniques such as mathematical modeling, optimization, deterministic algorithms or heuristics algorithms, it is possible to find optimal or suboptimal solutions

to complex decision making problems. The focus is generally the determination of the maximum profit/performance or the minimum cost/risk/loss of an objective function that might involve both linear or non-linear variables.

This Thesis is organized in three main parts. Part I will be dedicated to a general introduction to the main background of mathematical programming together with a comprehensive literature review in the field of optimization and mathematical modeling for the Energy Sector. Part II and III will discuss mathematical programming formulations for some specific Energy applications in the thermal field and in the electrical field.

Part I is split into three main chapters. Chapter 2 will briefly introduce the most important concepts of Linear Programming and Mixed Integer Linear Programming, followed by some Non-linear Programming peculiarities and related solving techniques with particular focus to separable programming.

Chapter 3 is dedicated to mathematical background as well. The attention here is on Graph theory, which represents the main approach used along the Thesis in order to study and modeling Energy Networks.

The topics for the background theory have been selected according to the content of following chapters. Hence, the general mathematical background outlined in these two chapters is focused on those concepts that are essential for the best comprehension of the models discussed in Part II and III.

In Chapter 4 a comprehensive literature review about mathematical modeling in the Energy Sector is presented. This is made to give an overview of the current state of the art of the scientific production in the field of Energy optimization, and consequently motivate the selected topics for the present Thesis, in light of the current available literature.

A scientific paper titled *Mathematical Modeling in the Energy Sector: a Literature Review* has been prepared and is going to be submitted to the *European Journal of Operational Research*.

Part II is dedicated to mathematical models for the thermal Energy distribution. This is the output of a work that started from a collaboration between the DEI Department of Bologna University and the Multi-Utility HERA, an Energy company based in Bologna. It is important to underline the precious contribution given by OPTIT Optimal Solutions, which is an academic spin-off of the Operations Research group of the University of Bologna and which provided essential background and real world material to carry on with the scientific research.

This part is split into two main chapters. Chapter 5 contains an introduction to the main theory in the field of District Heating networks, as well as thermodynamics and hydraulic concepts that need to be considered when building models for such systems.

Mathematical models for the District Heating strategic network design and incremental network design will be discussed in Chapter 6 with particular regard to instances characterized by big networks dimensions.

This study has been presented at the *YoungOr18 Conference* held in Exeter (UK) in April 2013 and at the *Ecomondo Conference* held in Rimini (Italy) in November 2013. Other Conference presentations has been made at the *EURO-INFORMS26* Conference held in Rome in July 2013 as well as at the *IFORS20 Conference* held in Barcelona (Spain) in July 2014. A poster session has been joined at the *Risk and Reliability Modelling of Energy Systems Day* held in Durham (UK) in November 2013.

An extended abstract titled *Mathematical Optimization for the Strategic Design and Extension of District Heating Systems* will be published in the *Conference Proceeding of the Ecomondo Event*.

Moreover, a scientific paper titled *An Optimization Approach for District Heating Strategic Network Design* has been submitted to the *European Journal of Operational Research*.

Part III is dedicated to mathematical models for the Electrical Energy field. In particular the objective is the development of linear programming approaches for optimal battery operation in off-grid solar power schemes, with consideration of battery degradation. This is the output of a whole year of research period abroad, during which I've had the opportunity to be a visiting PhD student at the School of Engineering and Computing Sciences of Durham University (UK). The work was motivated by a field project on operation of off-grid storage in Rwanda, which is part of a greater set of research projects carried on by the Durham Energy Institute together with the Storage Consortium. The latter in particular is a UK academic consortium on Energy Storage for Low Carbon Grids, which include different universities among Imperial College, Cambridge, Cardiff, Durham, Leeds, Newcastle, Oxford, Sheffield, St. Andrews and University College London.

As the previous one, this part is split into two main chapters. Chapter 7 will introduce the main concepts of batteries and their integration in off-grid systems, while Chapter 8 will discuss mathematical formulations to build linear programming models for the optimal management of off-grid systems focusing on batteries degradation issues.

This work has been presented at the Storage Consortium meeting *Energy Storage for Low Carbon Grids: Boot Camp* held in Oxford in September 2014 as well as during the *Electricity Research Center ERC Research Symposium* held in Dublin (Ireland) in October 2014 and at the *Risk and Reliability Modelling of Energy Systems Day* held in Durham (UK) in November 2014.

Moreover the project has been successfully presented for a grant offered by the Excellence Initiative of the German Government for a funded participation to the *ENERstore Summer School 2014* (Energy Storages for Sustainable Energy Supply), held in Dresden in September 2014.

A scientific paper titled *A Linear Programming Approach for the Battery Degradation Analyses and Optimization in Off Grid Power Systems with Solar Energy Integration* has been prepared and is going to be submitted to an Energy Journal focused on Energy applications. The target Journals are currently *Journal of Energy Storage* and eventually the more established *Journal of Energy*.

# Part I

# Introduction to Mathematical Programming Models for the Energy Sector

# Chapter 2

# Mixed Integer Linear Programming and Non-Linear Programming

This chapter is dedicated to a brief introduction to the Linear Programming and Mixed Integer Linear Programming theory followed by some general fundamentals on the Non-Linear Programming problems and techniques.

The objective is to focus on the most important background of these main sectors of the Operational Research, because they will represent the core background for the modeling applications that will be presented in Part II and Part III. In particular, the Linear Programming and Mixed Integer Linear Programming approaches will be used in both Parts, while the Non-Linear Programming will be applied in Part II to solve the non-linearities involved in thermal distribution networks, by using Piecewise formulations.

## 2.1 LP and MILP Problems Introduction

A general Linear Programming (LP) problem has the following formulation

$$\min \sum_{j=1}^{n} c_j x_j \tag{2.1}$$

$$\sum_{j=1}^{n} a_{ij} x_j \geq b_i \qquad i = 1...m_1 \tag{2.2}$$

$$\sum_{j=1}^{n} a_{ij} x_j = b_i \qquad i = m_1 + 1...m \tag{2.3}$$

$$x_j \geq 0 \qquad j = 1...n_1 \tag{2.4}$$

where $n, n_1, m, m_1$ are known constant scalars; $c = c_j \in \mathbb{R}^n$ and $b = b_i \in \mathbb{R}^m$ are known vectors; $A = a_{ij} \in \mathbb{R}^{m*n}$ is a known matrix. While the vector $x = x_j \in \mathbb{R}^n$ represents the decision variables for which an optimal value needs to be found. For LP problems variables are supposed to be *continuous* and they can assume every value within a continuous interval.

The above formulation can be used for every Optimization Problem with a linear objective function and where constraints are expressed by linear equations or inequalities.

For maximization problems it is possible to change the objective function sign and in general if needed it is possible to change the $\geq$ inequalities into $\leq$ inequalities.

The presence of inequalities make the problem not solvable with the standard linear algebraic methodologies which might be applied if there were only equations and if the variables were not imposed $\geq 0$. Hence it is necessary to use appropriate algorithms such as the Simplex Algorithm.

An Integer Linear Programming Problem (ILP) is a variation of the Linear Programming Problem (LP) which contains a further constraint that imposes that every variable will be an integer one.

$$\begin{aligned} x_j \quad & integer \\ & j = 1...n \end{aligned} \tag{2.5}$$

A Mixed Integer Linear Programming Problem (MILP) is a generalization of LP and ILP where just a subset of variables are restricted to be integers while other variables are allowed to be non-integers.

$$\begin{aligned} x_j \quad & integer \\ & j \in S \\ & S \subseteq \{1...n\} \end{aligned} \tag{2.6}$$

A special case is the 0-1 Integer Linear Programming, in which variables are binary.

$$\begin{aligned} x_j \quad & \in \{0, 1\} \\ & j = 1...n \end{aligned} \tag{2.7}$$

Both ILP and MILP problems can be solved and they are practically solved by using $branch-and-bound$ algorithms where a continuous relaxation of the problem is iteratively solved by removing the integer constraints.

There are two main reasons for using integer variables or binary variables when modeling problems as a linear program:

- An integer variable can represent a quantity that can only assume integer values. For instance, it is not possible to build 1.5 inverters.
- An integer variable can represent decisions that can be taken or not, and therefore it should only take on the value 0 or 1; in this case it will be a binary variable. A binary variable will be equal to 1 if a certain decision is taken and it will be equal to 0 if a certain decision is not taken (for instance, a binary variable can be equal to 1 if a conventional generator is on and 0 if the conventional generator is off).

These considerations occur frequently in practice and so integer linear programming can be used in many applications areas. The Energy Sector in particular offers a wide range of applied problems where ILP and MILP can be successfully applied to facilitate the decision making process and to analyze the state of the art of some technologies, making sensitivity analyses on the most interesting parameters involved. The most important problems that can be studied through ILP and MILP in the Energy Sector are related to Energy production and Energy dispatching. In particular, the optimal generator plants management, scheduling and location and the optimal Energy distribution along optimized Energy networks are key issues. A literature review related to such topics will be presented in Chapter 4.

An interesting case that lies in the middle of the LP and ILP is related to problems where *semi-continuous* variables are considered. A semi-continuous variable is a variable that can take the value 0 or any value between its lower bound $L$ and its upper bound $U$. The semi-continuous lower bound must be finite and greater than or equal to 0 while the upper bound do not need to be finite (hence the upper bound can be equal to a defined value $U$ or to $\infty$).

$$\begin{aligned} x_j \quad & \in \{0\} \cup \{L_j, U_j\} \\ & j = 1...n \end{aligned} \tag{2.8}$$

$$\begin{aligned} x_j \quad & \in \{0\} \cup \{L_j, \infty\} \\ & j = 1...n \end{aligned} \tag{2.9}$$

Semi-continuous variables are often encountered in real-world modeling such as production planning or optimal dispatch of generating units (unit commitment) in power systems. An example of application of a semi-continuous variable can be related to the Energy production of a conventional generator during its two main modes on/off. When the conventional generator is off then its production is equal to 0, while when the conventional generator is on, then the amount of the production has to lie in a certain interval due to managerial and technological considerations. In particular, a conventional generator when active, has to respect some technical constraints related to its minimum production (lower bound) and its capacity (upper bound).

With regard to the problem complexity, there are mainly two categories:

- Polynomial Problems, for which there exist a Polynomial algorithm that can solve them
- NP-hard Problems for which there is no Polynomial algorithm available to find a solution

The LP problems belong to the class of Polynomial Problems while ILP problems belong to the class of NP-hard Problems.

NP-hard Problems are computationally harder as the required computational time to get a solution increases exponentially with the problem dimension.

## 2.2 Non-Linear Programming

A Non-Linear Programming Problem (NLP) is similar to a Linear Programming one in that it is composed of an objective function, variable bounds and general constraints that can be equalities or inequalities. The difference is that a non-linear program includes at least one non-linear function, which could be the objective function, or some or all of the constraints.

There are many examples of non-linear systems in the real world applications. We will present an example of non-linear relationships in Part II when we will deal with the hydraulic constraints of District Heating Systems. In particular, the relationship between drop of pressure along pipes and flow rate is non-linear, as further explained in Section 5.5.

A general Non-Linear Programming Problem aims at finding the optimal values of $x = (x_1, x_2...x_n)$ in such a way that

$$\min f(x) \tag{2.10}$$

$$g_i(x) \leq b_i \quad \forall i = 1...m \tag{2.11}$$

$$x \geq 0 \tag{2.12}$$

where $f(x)$ and $g_i(x)$ are known functions of the $n$ decision variables.

Non-Linear Programming can be divided usefully into *convex programming* and *non-convex programming*. A region of space is said to be convex if the portion of the straight line between any two points in the region also lies in the region.

A function $f(x)$ is said to be convex if the set of points $(x, y)$ where $y \geq f(x)$ forms a convex region. For example, the function $x^2$ is convex, while the function $2 - x^2$ is not convex. The concepts of convex and non-convex regions and function apply in as many dimensions as required.

A mathematical programming model is said to be convex if it involves the minimization of a convex function over a convex feasible region. Minimizing a convex function is equivalent to maximizing the negation of a convex function. Such a maximization problem will also therefore be convex. Clearly, Linear Programming introduced in previous section, is a special case of convex programming, as every LP model can be expressed as minimization of a linear function and linear functions satisfy the definition of a convex function. Furthermore, the feasible region defined by a set of linear constraints can easily be shown to be convex.

Non-convex programming includes all the non-linear programming problems that do not satisfy the convexity rules. In such cases, even if it is possible to find a local optimum, there is no guarantee that this will also be the global optimum.

Geometrically, non-linear programs can behave much differently from linear programs, even for problems with linear constraints. There are many reasons for which non-linear models are inherently much more difficult to optimize. It's hard to distinguish a local optimum from a global optimum; optima are not restricted to extreme points; there may be multiple disconnected feasible regions; different starting points may lead to different final solutions; it may be difficult to find a feasible starting point; it is difficult to satisfy equality constraints; different algorithms and solvers arrive at different solutions for the

same formulation. This is just to give a very broad idea of the difficulties involved in Non-Linear formulations compared to the easier Linear problems. However, as a deep theory on the Non-Linear Programming is not the main purpose of this thesis, for further readings about Non-Linear peculiarities it is possible to refer to the existing literature (i.e. Bazaraa et al. [1] or Luenberger and Ye [2]).

Different Non-Linear Programming Problems exist as a function of the different properties of the functions $f(x)$ and $g_i(x)$. While with Linear Programming a single algorithm can suit every problem, for the Non-Linear Programming field there isn't a single algorithm that can be applied for every circumstance. Hence ad hoc algorithms has been created and are used for different types of problems.

For the purpose of the present thesis, the most important Non-Linear Programming class of problems, is represented by *separable programming* which is a particular case of convex programming. As further explained in Section 2.3 these type of problems can be well approximated by a Linear Programming Problem and therefore they can be solved through the simplex algorithm.

## 2.3 Separable Programming

Separable programming is important because it allows a convex non-linear program to be approximated with arbitrary accuracy with a linear programming model. The idea is to replace each non-linear function with a piecewise linear approximation.

Consider the general Non-Linear Programming problem

$$\begin{aligned} &\min f(x) \\ &g_i(x) \leq b_i \quad \forall i = 1...m \\ &x \geq 0 \end{aligned}$$

with the additional conditions that the objective function and all constraints are separable and each decision variable $x_j$ is bounded below by 0 and above by a known constant $u_j$ for $j = 1...n$.

Remember that a function, $f(x)$, is separable if it can be expressed as the sum of functions of the individual decision variables.

$$f(x) = \sum_{j=1}^{n} f_j(x_j) \tag{2.13}$$

Separable programs are optimization problems of the following form

$$\min \sum_{j=1}^{n} f_j(x_j) \tag{2.14}$$

$$\sum_{j=1}^{n} g_{ij}(x_j) \leq b_i \quad \forall i = 1...m \tag{2.15}$$

$$0 \leq x_J \leq u_j \quad \forall j = 1...n \tag{2.16}$$

The key advantage of this formulation is that the non-linearities are mathematically independent. This property together with the finite bounds on the decision variables permits the development of a piecewise linear approximation for each function in the problem. It is then possible to use separable programming to obtain a global optimum to a convex problem or possibly only a local optimum for a non-convex problem.

Although the class of separable functions might seem to be a rather restrictive one, it is often possible to convert mathematical programming models with non-separable functions int ones with only separable functions. Ways in which this may be done are discussed in Williams [3].

An example of non-linear function $y = f(x)$ that can be treated with separable programming is depicted in Figure 2.1. In particular, Figure 2.1 represents the non-linear trend that links the drop of pressures $\Delta P$ to the water flow rate $\dot{m}$ inside District Heating Networks, so that: $\Delta P = f(\dot{m})$. This trend and the related piecewise linear approximation will be used in Chapter 6 to face the non-linearities that occur in the hydraulic modeling of District Heating Systems. See Section 5.5 for further details on hydraulic properties of District Heating Systems.

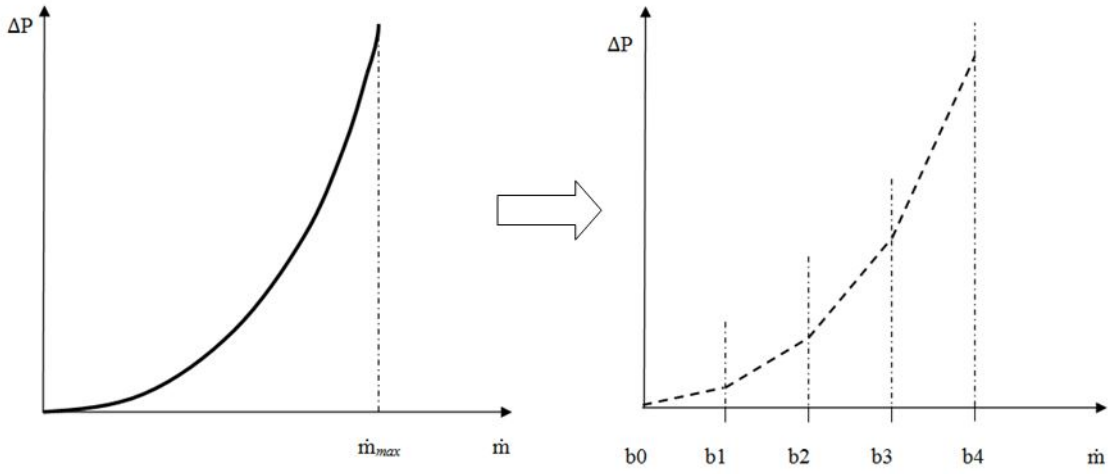


Figure 2.1: Piecewise linear approximation of a non-linear function. A representation of the relationship between drop of pressures $\Delta P$ and water flow rate $\dot{m}$ in District Heating Networks

In order to convert a non-linear programming model into a suitable form for separable programming it is necessary to make piecewise linear approximation to each of the non-linear functions of a single variable. The non-linear function $f(\dot{m})$ depicted on the left side of Figure 2.1 can be approximated into a piecewise linear $F(\dot{m})$ as represented on the right side of the figure, by using say $b$ line segments. Every discontinuity point of the polygon curve on the right is called *breakpoint*. Hence it is necessary to select at first $b + 1$ values of the scalar $\dot{m}$ within its range $0 \leq \dot{m} \leq \dot{m}_{max}$ which are $b_0, b_1, ...b_4$. At the boundaries we have $b_0 = 0$ and $b_4 = \dot{m}_{max}$. Note that the values of the $b$ interval do not have to be evenly spaced.

Every segment can be mathematically represented by the standard equation of a line.

Say we have $n$ number of segments, a possible mathematical definition of the piecewise linear function through its breakpoints, can be the following

$$f(x) = \begin{cases} f(b_0) + \dfrac{x - b_0}{b_1 - b_0}(f(b_1) - f(b_0)) & \text{x} \in [b_0, b_1[ \\ f(b_1) + \dfrac{x - b_1}{b_2 - b_1}(f(b_2) - f(b_1)) & \text{x} \in [b_1, b_2[ \\ f(b_{n-1}) + \dfrac{x - b_{n-1}}{b_n - b_{n-1}}(f(b_n) - f(b_{n-1})) & \text{x} \in [b_{n-1}, b_n] \end{cases} \tag{2.17}$$

The approximation becomes increasingly more accurate as the number of segments gets larger. Unfortunately there is a corresponding growth in the size of the resulting problem.

In order to insert a non-linear function $y = f(x)$ inside a mathematical programming model, it is necessary to introduce the concept of *Special Ordered Set of variables SOS*, which can be classified in *SOS of type One* and *SOS of type Two*.

Broadly speaking, a Special Ordered Set of type One (SOS1) is a set of variables for which no more than one member from the set may be non-zero in a feasible solution while a Special Ordered Set of type Two (SOS2) is a set of consecutive variables in which no more than two adjacent members may be non-zero in a feasible solution. In both cases, all sets are mutually exclusive of each other, the members are not subject to any other discrete conditions and each set is grouped together consecutively in the data.

The normal use of an SOS1 is to represent a set of mutually exclusive alternatives ordered in increasing values of size, cost or some other suitable units appropriate to the context of the model.

For the purpose of the present thesis the SOS2 are more important, as they were introduced to make it easier to find global optimum solutions to problems containing piecewise linear approximations to a non-linear function of a single argument (as in the Separable Programming discussed in the present section).

Let us define $n$ new decision variables $t_i$ with the following properties

$$\sum_{i=0}^{n} = 1 \tag{2.18}$$

$$t_i \geq 0 \quad \forall i = 1...n \tag{2.19}$$

and let us impose that at most two of the consecutive $t_i$ can be greater than zero. Under such conditions, we can express $x$ as follow

$$x = \sum_{i=0}^{n} t_i b_i \tag{2.20}$$

As a consequence, it is possible to approximate the value of $y = f(x)$ as follow

$$y = F(x) = \sum_{i=0}^{n} t_i f(b_i) \tag{2.21}$$

This way, the definition of $t_i$ make it possible to define $x$ as a function of the subset $[b_0, b_1[$ ... $[b_{n-1}, b_n]$ of the $f$ domain to which $x$ belongs so that $y$ will assume only the values related to the interval defined by the related breakpoints. The set of variable $t_i$ represents a Special Ordered Set of type 2 (SOS2).

Hence it is possible to manage the non-linearities, even though the above trick requires the introduction of $n$ new variables of the set SOS2 together with two further constraints.

The key of the procedure is a good choice of breakpoints that means find a compromise to represent a good approximation of the problem without making it too hard from a computational point of view.

# Bibliography

[1] M. S. Bazaraa, H. D. Sherali, and C. M. Shetty. *Nonlinear programming: theory and algorithms*. John Wiley & Sons, 2013.

[2] D. G. Luenberger and Y. Ye. *Linear and nonlinear programming*, volume 116. Springer, 2008.

[3] H. P. Williams. *Model building in mathematical programming*. John Wiley & Sons, 2013.

# Chapter 3

# Graph Problems

In this chapter we will outline the fundamental theory in the field of Graph problems as the Graph theory will represent the main approach used to model the Energy problems described in Part II and III.

The Graph theory is the most important approach used to model every type of network. For the purpose of the present thesis we are interested in Energy Networks modeling, both from a design point of view and from an operational management point of view. Network Design and Network Flow can be considered as the main classes of problems in the Energy Sector. That is because, broadly speaking, the study of an Energy Network presents three main kinds of problems that are related to how to optimally design it, how to optimally extend it and how to optimally manage its flows once the network is created. Such problems can be well classified as Network Design Problems, Incremental Network Design Problems and Network Flow Problems respectively.

In particular, we will use the theory of Network Design and Incremental Network Design in Part II where District Heating Networks will be studied in terms of optimal design; while we will use the theory of Network Flow in Part III where an Off-grid system will be modeled in terms of hourly operational management of Energy flows among the system units with particular regard to the integrated storage devices.

## 3.1 Graphs

Graphs can be classified in *undirected graphs* and *directed graphs*.

An *undirected graph* $G = (V, E)$ is defined by two sets: the set of vertexes (or nodes) $V$ and the set of arcs $E$. Every arc corresponds to a couple of nodes.

Given a couple of nodes $i, j \in V$, the related arc $e$ is defined as $e = (i, j) \in E$ and $i, j$ are the extremities of $e$.

Every arc is associated with an unordered pair of nodes $\psi(e) = \{i, j\}$ called *endpoints* of $e$.

Given a node $i \in V$, the set of arcs that contain $i$ (or arcs with an extremity in $i$) is called $\delta(i)$.

Given a subset of nodes $S \subseteq V$ the set of arcs with only one extremity in $S$ is called $\delta(S)$.

Given a subset of nodes $S \subseteq V$, the set of arcs with both extremities in $S$ is called $E(S)$.

An arc is a *loop* if its endpoints are identical.

An undirected graph is said to be *complete* if its set of arcs contains all the $|V|(|V|-1)/2$ possible couples of nodes.

A *directed graph* $G = (V, A)$ is defined by two subsets: the set of vertexes (or nodes) $V$ and the set of arcs $A$. Every arc corresponds to an *ordered* couple of nodes.

Given an ordered couple of nodes $i, j \in V$, the correspondent arc $a$ is defined as $a = (i, j) \in A$. Every arc $a \in A$ has a start node $i$ called $tail(a) \in V$ and an end node $j$ called $head(a) \in V$.

Given a node $i \in V$, the set of arcs with tail $i$ is called $\delta^+(i)$, while the set of arcs with a head $i$ is called $\delta^-(i)$.

Given a subset of nodes $S \subseteq V$, the set of arcs with a tail in $S$ and a head in $V \setminus S$ is called $\delta^+(S)$, while the set of arcs with a head in $S$ and a tail in $V \setminus S$ is called $\delta^-(S)$.

Given a subset of nodes $S \subseteq V$, the set of arcs with both extremities (head and tail) in $S$ is called $A(S)$.

An arc $a \in A$ is a *loop* if $tail(a) = head(a)$.

An oriented graph is said to be *complete* if its set of arcs contains all the $|V|(|V|-1)$ possible ordered couples of nodes.

Let $G = (V, E)$ be a graph. For a set of nodes $S \subseteq V$, we define the set of arcs $E[S] := \{e \in E : \psi(e) \subseteq S\}$ with both endpoints in $S$. A *subgraph* of $G$ is a graph $G' = (S, F)$ with $S \subseteq V$ and $F \subseteq E[V']$. In particular we define $G[S] := (S, E[S])$ to be the *subgraph induced by S*. The notions of subgraph and induced subgraph for a directed graph are defined in analogy to the undirected case.

Let $G = (V, E)$ be a graph and let $i, j \in V$. A sequence of arcs $(e_0...e_k)$ is in an *s-t-walk* if there is a sequence of nodes $(v_0...v_{k+1})$ such that $\psi(e_i) = \{v_i, v_{i+1}\}$ for $i \in [K]$. An *s-t-walk* is an *s-t-path* if the arcs $e_0...e_k$ are pairwise distinct. An *s-t-walk* is *closed* if $s = t$. A closed walk is a *cycle* if the arcs $e_0...e_k$ are pairwise distinct. An *s-t-path* or cycle is *simple* if the nodes $(v_0...v_k)$ are pairwise distinct.

A graph $G = (V, E)$ is *connected* if there is a *i-j-walk* for all $i, j \in V$. A graph $G = (V, E)$ is *strongly connected* if there is a directed i-j-walk and a directed j-i-walk for all $i, j \in V$.

A *bipartite graph* is a graph whose nodes can be divided into two disjoint sets $U$ and $V$ (often denoted as partite sets) in such a way that every arc connects a vertex in $U$ to one in $V$.

## 3.2 Network Design Problems

Network design represents one of the main theme of the present thesis, with particular regard to Part II where a mathematical model for the district heating strategic network design is presented.

Broadly speaking, network design problems aims at finding the minimum cost subgraph of a given graph, fulfilling certain constraints and usually specifying connectivity requirements. Network design problems can differ in the type of connectivity constraints

they impose; in the type of graph that can be directed or undirected; in the type of arcs that can be capacitated or not and if multiple copies of the same arc are allowed or not.

In this section we will focus on the two largest and most important problem classes: the uncapacitated and capacitated network design problems. In practical applications, most of the uncapacitated problems - at least in undirected graphs - are considered to be manageable, while capacitated problems are a great computational challenge.

The *uncapacitated network design problem* is one of the most fundamental network design problems. The purpose is to find a minimum cost tree connecting a certain set of nodes called *terminals*, possibly spanning some additional nodes called *steiner nodes*. The latter are extra intermediate nodes that can be added to the graph in order to reduce the total length of connection.

The *minimum spanning tree problem* is a special case of the uncapacitated network design problem and it can be well applied to District Heating Systems, where the task is the creation of a new network through which the thermal energy has to reach a specified set of customers within a city. The objective is to connect every customer with a minimum cost network in such a way that every couple of nodes must be connected by just one path. Hence the objective is to find the minimum cost subgraph which will be a loop free tree. A loop free tree that span all the vertices of a graph is also known as a *spanning tree*.

Given a graph $G = (V, E)$, we define $T$ a generic spanning tree; $K$ the set of all the possible spanning trees in $G$; $c(e)$ the cost of an arc $e \in E$; $x_e$ a binary variable which is equal to 1 if the arc $e \in E$ belongs to the tree $T$ and 0 otherwise.

The generic optimization problem can be mathematically described as follow

$$\min \sum_{e \in E} c_e x_e \tag{3.1}$$

$$\sum_{e \in E} x_e = |V| - 1 \tag{3.2}$$

$$\sum_{e \in E(U)} x_e \leq |U| - 1 \quad \forall U \subseteq V, U \neq \emptyset \tag{3.3}$$

$$x_e \in \{0, 1\} \qquad \forall e \in E \tag{3.4}$$

Where the first constraint imposes that the set of chosen arcs must be a subgraph, containing no more than $|V| - 1$ arcs and the second constraint is inserted to avoid loops in the resulting network.

The uncapacitated network design problem imposes simple connectivity requirements for the terminals. Every link installed in the network contributes the same unit capacity and the connecting paths of different node pairs can use this capacity independently from one another. A different approach is considered in the *capacitated network design problem* where the flow running between the terminals has to share the capacity of the installed links and the capacities provided by each link can be different.

Another important class of network design problems is represented by the *shortest path problem* which is the problem of finding a path between two nodes in a graph such that the sum of the weights of its constituent arcs is minimized.

Given an oriented graph $G = (V, E)$, a source node $s$ and a destination node $t$, the objective is to find the minimum cost path that connect $s$ to $t$. We define $R$ as the set of all the possible paths from $s$ to $t$ in $G$; $P$ as a generic path in $R$; $c_{ij}$ as the cost associated to the arc $e = (i, j)$; $x_{ij}$ as a binary variable that is equal to 1 if the arc $(i, j) \in E$ belongs to the path $P$, 0 otherwise.

The generic optimization model can be mathematically described as follow

$$\min \sum_{i,j \in E} c_{ij} x_{ij} \tag{3.5}$$

$$\sum_{j:(i,j)\in E} x_{ij} - \sum_{k:(k,i)\in E} x_{ki} = \begin{cases} 1 & \forall i = s \\ -1 & \forall i = t \\ 0 & \forall i \neq s \neq t \end{cases} \tag{3.6}$$

$$\sum_{ij \in E(U)} x_{ij} \leq |U| - 1 \quad \forall U \subseteq V, U \neq \emptyset \tag{3.7}$$

$$x_{ij} \in \{0, 1\} \quad \forall (i, j) \in E \tag{3.8}$$

where the first constraint imposes that for every node the number of outgoing arcs must be equal to the number of ingoing arcs. with the exception of the source node and the destination node, while the second constraint imposes that the resulting path must be free of loops. The latter can be eliminated for a better formulation, taking into account that an optimization model would never do a loop to move from $s$ to $t$ rather than covering a simple path.

The network design problems have been studied with a broad set of algorithmic techniques, ranging from approximation algorithms to mixed integer programming formulations and combinatorial heuristics. As an in depth analyses of such problems is not the purpose of the present thesis, for further details it possible to refer to the existing literature, in particular Crainic [3] for network design applications, Gendron et al. [8] for MIP formulations, polyhedral results and heuristics.

## 3.3 Incremental Network Design Problems

The incremental network design problem deals with the extension of existing networks by designing new additional fragments of an existing graph subject to economical/technical constraints. It is particularly important for the present Thesis as the strategic network design of District Heating Systems presented in Part II will be focused on the extension of large scale networks for the distribution of thermal Energy.

We will outline here some of the most recent works in the field of incremental network design that have been recently published for the main basic problems on Graphs: *Incremental Network Design with Shortest Paths* by Baxter et al. [2], *Incremental Network*

*Design with Minimum Spanning Trees* by Engel et al. [4] and *Incremental Network Design with Maximum Flows* by Kalinowski et al. [9]

As described in Baxter et al. [2], incremental network design problems have two characteristic features: a design feature as it is necessary to define which arcs will be part of a network and a multi-period feature as the ultimate network design is built over a number of time periods.

The general problem is formulated as follow. Given a Graph $G = (V, A)$ with nodes $V$ and arcs $A$, the set of arcs is split into two subsets: the set of existing arcs $A_e$ and the set of potential arcs $A_p$. Each arc $a \in A$ has a capacity $C_a$ and each potential arc $a \in A_p$ has an associated build-cost $c_a$; a budget $B^t$ is available to build potential arcs $a \in A_p$ in every time period $t$ with a planning horizon $T$, so that $t \in \{1...T\}$. A binary variable $y_a^t$ is defined to indicate if a potential arc has been built in time $t$ or before time $t$. Hence if $y_a^t - y_a^{t-1} = 1$ that means that the arc $a$ is built in time period $t$ and it is therefore available in period $t+1$. A continuous variable $x_a^t$ is defined to represent the flow on a generic arc $a \in A$ in time $t$. In every time step an optimization problem has to be solved over the usable arcs in time $t$ which can be the existing arcs and the potential arcs that have been built before time $t$. The objective is to minimize the total cost over the planning period.

Hence the generic mathematical formulation of an incremental network design problem is as follow

$$\min \sum_{t \in \{1...T\}} c(x)^t + \sum_{t \in \{1...T\}, a \in A_p} c_a * (y_a^t - y_a^{t-1}) \tag{3.9}$$

$$x_a^t \leq C_a * y_a^{t-1} \quad \forall a \in A_p, t \in \{1...T\} \tag{3.10}$$

$$\sum_{a \in A_p} c_a * (y_a^t - y_a^{t-1}) \leq B^t \qquad \forall t \in \{1...T\} \tag{3.11}$$

$$y_a^t \geq y_a^{t-1} \quad \forall a \in A_p, t \in \{2...T\} \tag{3.12}$$

That is, in the basic version of the problem, a single edge can be built in each period of the planning horizon and the objective is to minimize the operational costs over the planning horizon.

Two natural heuristics for incremental network design problems are of interest. The *quickest-improvement* seeks to improve the value of the solution to the network optimization as quickly as possible, for instance by adding as few potential edges to the network as possible. The *quickest-to-ultimate* first finds an optimal solution to the network optimization on the complete network, referred to as an *ultimate solution*, and then seeks to improve the value of the solution to the network optimization as quickly as possible by choosing only potential edges that are part of the ultimate solution.

In Baxter et al. [2] the *incremental network design with shortest path* is described. The problem considers a graph $G = (V, A)$, a set of potential and existing arcs $A_p \in A$ and $A_e \in A$ respectively as well as a source node $s \in V$ and a sink node $t \in V$. Each arc is described by a length $l_a \geq 0$. In every time step there is the option to expand the usable network, which initially consists of only the existing arcs, by building a single potential arc which will be available in the following period. In every period the cost or length of a shortest $s-t$ path is incurred. The objective is to minimize the total cost over a planning horizon $T = |A_p| + 1$.

Authors investigate structural properties of optimal solutions and they propose a natural greedy solution together with a 4-approximation algorithm.

In Kalinowski et al. [9] authors present the *Incremental Network Design with Maximum Flows*, where in each time period of the planning horizon, an arc can be added to the network and a maximum flow problem is solved, in order to maximize the cumulative flow over the entire planning horizon. As in the previous problem, there is a a graph $G = (V; A)$, a set of potential and existing arcs $A_p \in A$ and $A_e \in A$ respectively as well as a source node $s \in V$ and a sink node $t \in V$. In this case each arc is described by an integer capacity $u_a \geq 0$ and every node $v \in V$ there is a set of arcs entering $v$ called $\delta^{in}(v)$ and a set of arcs leaving $v$ called $\delta^{out}(v)$. The length of the time horizon is defined as $T > |A_p|$. The network initially consists of only the existing arcs, and in every period there is the option to expand it by adding a single potential arc $a \in A_p$ which will be available for use in the following time period. In every period, the value of a maximum $s - t$ flow is recorded (using only existing arcs and potential arcs that have been added in previous periods). The objective is to maximize the total flow over the planning horizon.

Several heuristics are described for the solution of such problem whose MIP formulations are NP-complete. Computational experiments are presented to compare the performance of the MIP formulations as well as the heuristics.

The *incremental network design with minimum spanning tree* is described in Engel et al. [4]. The problem considers an edge-weighted graph $G = (V, A)$ and a set $A_0 \subset A$ with the objective to find a sequence of arcs $a'_1...a'_r \in A \setminus A_0$ minimizing $\sum_{t\in\{1...T\}} w(X_t)$ where $w(X_t)$ is the weight of a minimum spanning tree $X_t$ for the subgraph $(V, A_0 \cup \{a'_1...a'_t\})$ and $T = |A| \setminus A_0$.

Authors propose a greedy algorithm for the solution of such problem.

## 3.4 Network Flow Problems

This section is intended to give a brief introduction to the Network Flow Problems as they will be part of the topics of the present thesis. In particular we will find them in Part II where, together with the network design problem, we will have to take into account the thermal Energy flows along the district heating network; and in Part III where electrical Energy flows will be studied inside an off-grid network. In this section we will outline the main concepts on the *maximum flow problem*, the *minimum cost flows problem* and the *transportation problem* as they are the most important ones for the purpose of the present thesis. Besides the short introduction available in this thesis, it is possible to find more details on network flow in the comprehensive textbook by Ahuja et al. [1].

Network flow problems are related to the study of flows from a source node to a sink node, inside networks represented by graphs.

Given an oriented graph $G = (V, E)$, suppose that every arc $(i, j) \in E$ has a maximum capacity $q_{ij}$, that represents the maximum amount of units of product that can be sent from $i$ to $j$ in every time step. Let us define $s$ as a starting node and $t$ as a destination node. We call $f_{ij}$ the amount of units sent along the arc $(i, j) \in E$ and $v$ the amount of units that flow out the node source node or into the sink node.

The *maximum flow problem* asks for a flow of maximum value from a source to a sink without violating the given capacities of the arcs and in such a way that the value of $v$ is maximized. It is mathematically formulated as follow

$$\max v \tag{3.13}$$

$$0 \leq f_{ij} \leq q_{ij} \quad \forall v \geq 0 \tag{3.14}$$

$$\sum_{j:(i,j)\in E} f_{ij} - \sum_{k:(k,i)\in E} -f_{ki} = \begin{cases} v & \forall i = s \\ -v & \forall i = t \\ 0 & \forall i \neq s \neq t \end{cases} \tag{3.15}$$

where the constraint 3.14 imposes that the flow among every couple of nodes $i, j$ can't exceed the maximum capacity of the related arc $(i, j)$. Moreover, the constraint 3.15 imposes that for every node, the amount of flow into it must be equal to the amount of flow out of it., with the only exception of the source node $s$ from which the total amount $v$ must flow out, and the sink node $t$ for which the total amount $v$ must flow in.

Suppose now that every arc $(i, j) \in E$ is associated to a cost $c_{ij}$ and that $v$ is defined by a fixed value of product that must flow among $s$ and $t$.

The *minimum cost flow problem* aims at finding, among all the possible configurations that can guarantee a flow equal to $v$ from $s$ to $t$, the best configuration which correspond to the minimum cost. It is therefore mathematically formulated as follow

$$\min \sum_{i,j\in E} c_{ij} f_{ij} \tag{3.16}$$

$$0 \leq f_{ij} \leq q_{ij} \quad \forall v \geq 0 \tag{3.17}$$

$$\sum_{j:(i,j)\in E} f_{ij} - \sum_{k:(k,i)\in E} -f_{ki} = \begin{cases} v & \forall i = s \\ -v & \forall i = t \\ 0 & \forall i \neq s \neq t \end{cases} \tag{3.18}$$

A special case of the minimum cost flow problem is the *transportation problem* where the graph is a bipartite one, with different sources of capacity $s_i$ on one side and different sinks of capacity $t_j$ on the other side. It is formulated as follow

$$\min \sum_{i,j\in E} c_{ij} f_{ij} \tag{3.19}$$

$$\sum_{j:(i,j)\in E} f_{ij} = s_i \tag{3.20}$$

$$\sum_{i:(i,j)\in E} f_{ij} = t_j \tag{3.21}$$

$$\sum_{i:(i,j)\in E} s_i = \sum_{j:(i,j)\in E} t_j \tag{3.22}$$

The *maximum flow problem* and the *minimum cost flow problem* were extensively studied by Ford and Fulkerson who contributed with important concepts (i.e. residual networks, augmenting paths, max flow/min cut theorem) building the fundaments of the network flow theory. Therefore, for further readings it is possible to refer to Ford and Fulkerson [5] Ford and Fulkerson [6] Ford and Fulkerson [7].

# Bibliography


[1] R. K. Ahuja, T. L. Magnanti, and J. B. Orlin. Network flows: theory, algorithms, and applications. 1993.

[2] M. Baxter, T. Elgindy, A. T. Ernst, T. Kalinowski, and M. W. Savelsbergh. Incremental network design with shortest paths. *European Journal of Operational Research*, 238 (3):675–684, 2014.

[3] T. G. Crainic. Service network design in freight transportation. *European Journal of Operational Research*, 122(2):272–288, 2000.

[4] K. Engel, T. Kalinowski, and M. W. Savelsbergh. Incremental network design with minimum spanning trees. *arXiv preprint arXiv:1306.1926*, 2013.

[5] L. Ford and D. R. Fulkerson. *Flows in networks*, volume 1962. Princeton Princeton University Press, 1962.

[6] L. R. Ford and D. R. Fulkerson. *A simple algorithm for finding maximal network flows and an application to the Hitchcock problem.* Citeseer, 1955.

[7] L. R. Ford and D. R. Fulkerson. Maximal flow through a network. *Canadian journal of Mathematics*, 8(3):399–404, 1956.

[8] B. Gendron, T. G. Crainic, and A. Frangioni. *Multicommodity capacitated network design.* Springer, 1999.

[9] T. Kalinowski, D. Matsypura, and M. W. Savelsbergh. Incremental network design with maximum flows. *European Journal of Operational Research*, 242(1):51–62, 2015.

# Chapter 4

# Mathematical Modeling in the Energy Sector: a Literature Review

This chapter will present a literature review in the field of optimization and mathematical modeling applied to Energy problems. Section 4.1 will introduce the importance of Operational Research for the Energy field and will discuss the main classes of Energy problems that have been studied in literature, as well as the main mathematical approaches that have been used to solve such problems.

Then according to the proposed classification, the other sections will be organized as follow. In Section 4.2 we will introduce the most interesting papers in the field of district heating and cooling networks, in Section 4.3 we will introduce the main literature in terms of grid connected and off-grid systems optimization, while in Section 4.4 an overview on CHP and CHCP optimization problems will be presented. In every section we will further classify the proposed literature into the main groups of design problems, operational management problems and arbitrage/demand side problems and we will also assign papers to the main sets of deterministic approaches and heuristics/metaheuristics/machine learning approaches.

The last Section 4.5 will discuss some conclusions and will motivate the selected topics for the present Thesis, in light of the current available scientific production.

## 4.1 Introduction

The objective of this chapter is to make an overview of the main scientific literature in the field of Operational Research applied to the Energy field. We propose a literature classification in terms of main Energy topics and main mathematical techniques that has been used to study such topics.

As shown in Figure 4.1 the Energy topics that has been studied from an optimization point of view can be classified into two main groups, the *Thermal Energy side* and the *Electrical Energy side*.

The thermal Energy side can be split into two subsets that are the district heating networks for the distribution of thermal Energy and the district cooling networks for the distribution of cooled Energy. These problems are generally studied by focusing on two main aspects: the design of district heating/cooling networks and the operational

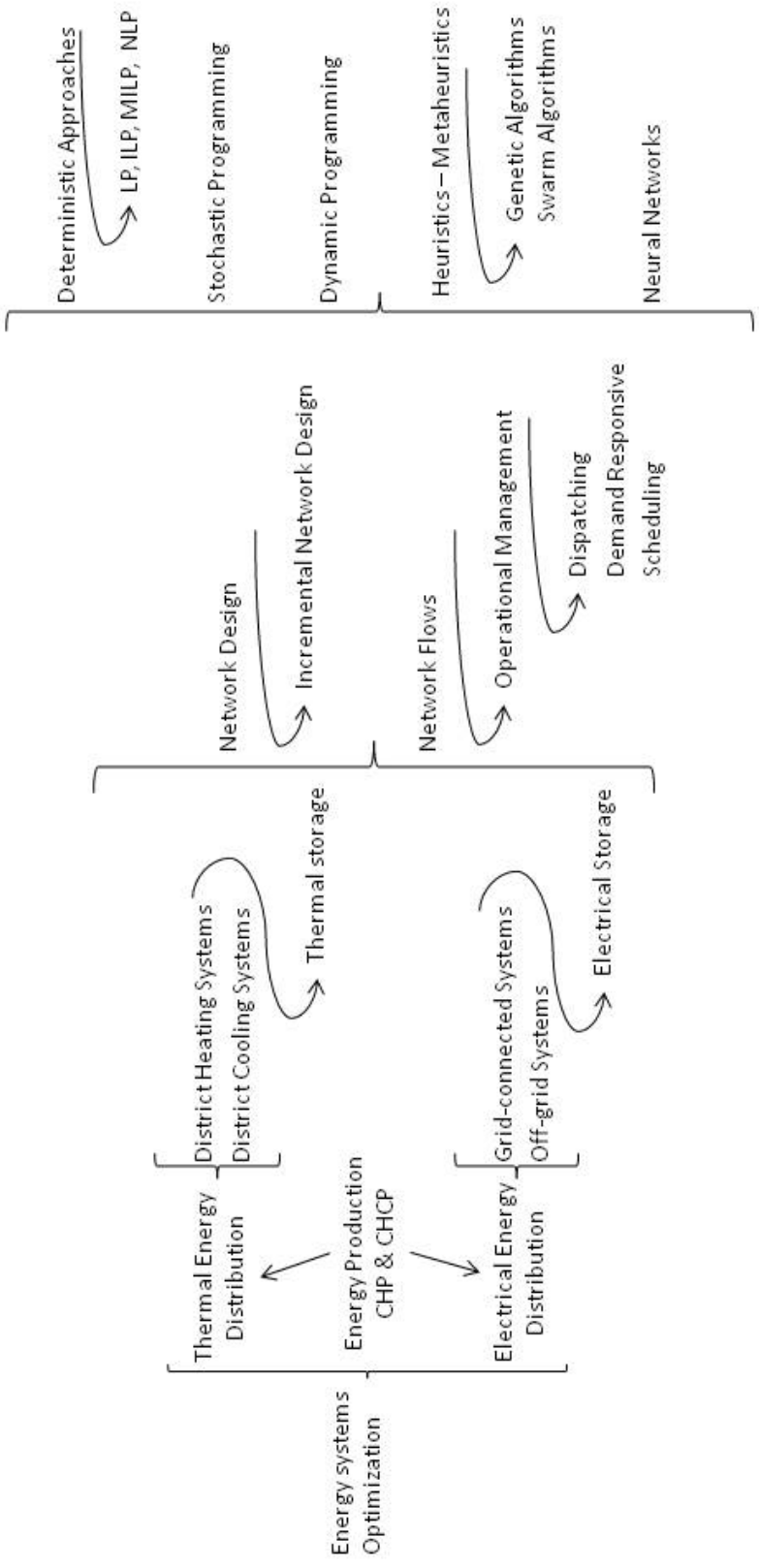


Figure 4.1: A classification criteria for the main Energy Optimization topics studied in literature

management of district heating/cooling networks. The first problem has a more strategic approach to optimize the investment for new networks or to optimize the incremental design and modification of existing networks; while the latter has a more management approach to optimize the hourly dispatching or scheduling of Energy in existing networks with a fixed specific design.

The electrical Energy side can be split into two main subsets that are the grid connected systems and the off-grid systems. Again these problems are mainly studied by focusing on two key aspects that are the network design problems and the operational management problems.

Inside the operational management problems we can find further subsets related to the optimal Energy distribution/dispatching, the optimal scheduling of the Energy systems resources and and demand side operational management problems. In particular demand responsive problems, with loads shifting and arbitrage techniques are widely studied in literature. These are particularly studied in the electrical field for grid connected systems, as the opportunity to exchange electrical Energy with the national grid, represents an important economical source for the electrical energy users. The arbitrage techniques represent the main motivation for users to shift their electrical loads along the day, taking advantage of different energy prices.

The electrical side and the thermal side are linked together as the thermal energy is often the "waste" product that originates from the main electrical energy production. This is the case of Combined Heat and Power Systems CHP, which refer to plants for the simultaneous production of heat and power, or Combined Heat Cooling and Power Systems CHCP characterized by the additional production of cool energy through the use of absorption chillers. A wide literature has been dedicated to optimal design, location, management and scheduling of such systems.

Both thermal and electrical side can be described by a further separate subset that is represented by the storage technologies. They are generally studied as part of Energy networks operational management problems, but they should be classified in a separate group as nowadays the Energy storage represents a key topic that is receiving an increasing particular attention by researchers.

As for the mathematical techniques, the main approaches through which the above Energy problems has been studied and solved, relate to deterministic methodologies, heuristic and metaheuristic algorithms. The main deterministic approaches refer to Linear Programming, Mixed Integer Linear Programming, Non-Linear Programming and Stochastic Programming. The latter is particularly appreciated to take into account the uncertainty of real world data.

For complex problems the main approaches are related to Dynamic Programming, Heuristics and Metaheuristics algorithms. Metaheuristics techniques are particularly appreciated as there is a quite wide literature related to such techniques applied to Energy problems. The most used are Genetic Algorithms and Particle Swarm optimization. Some machine learning techniques such as Neural Networks are appreciated as well.

## 4.2 Thermal Energy Distribution

This section will be dedicated to the presentation of the main scientific literature in the field of thermal energy distribution optimization, with regard to district heating systems and district cooling systems.

District heating (DH) concerns the centralized production of thermal and possibly electrical energy and its distribution to a set of users through an insulated network of pipes and a set of heat exchangers located at the users buildings. The thermal energy is generally produced through combined heat and power plants (CHP) where it is possible to recover the heat wasted during the electrical production. Such heat can be therefore used to feed networks and distribute thermal energy for heating and sanitary use.

District cooling (DC) is the opposite of District Heating and it is referred to as the technological concept of efficiently providing space cooling services to several customers of diverse nature (shopping malls, hospitals, sports facilities, airports, hotels, dwellings, various educational facilities, public administrations and industrial facilities). Broadly speaking, a District Cooling System (DCS) involves the centralized production of chilled water and its distribution to a network of users, thus obtaining much higher efficiency in production and maintenance costs as compared to the individual production of cooling services by end-users. The cold water pumped around the district cooling network is used to cool the air circulating in the properties ventilation systems. The same water is then fed back to the production plant to be cooled again. The temperature of the water fed to properties is around 6 degrees, while the return water is in excess of 16 degrees. Generally the cold water is provided by absorption cooling processes or heating pumps that are able to produce both heating and cooling at the same time. The most common plant for the cool production are combined heat and cooling power plants (CHCP).

### 4.2.1 District Heating

The scientific literature in the field of District Heating Optimization can be classified into some main topics that are: the optimal components selection and system configuration; the optimal network design; the optimal operational management along a representative period with some demand side models as well. Some models focus on very specific particular technical aspects optimization (i.e pumps, valves, temperature) while other are more related to investments decision making.

Deterministic approaches has been widely used for the optimal components selection and system configuration. In Mehleri et al. [57] a mixed-integer linear programming (MILP) super-structure model is presented where the objective is to find the optimal selection of the system components among several candidate technologies (micro combined heat and power units, photovoltaic arrays, boilers, central power grid), including the optimal design of a heating pipeline network, that allows heat exchange among the different nodes. A very little application for 10 buildings is discussed.

A similar work has been done in Ren and Gao [69] where the authors present a mathematical model that minimizes the overall energy cost for a test year by selecting the units to install and determining their operating schedules. Input data comprise the site's energy loads, local climate data, utility tariff structure, and technical and financial information on candidate technologies. A numerical study for an eco-campus in Kitakyushu (Japan) is presented.

In Sanaei and Nakata [77] a non-linear optimization is proposed to optimize the initial choice of the energy system components and the way they should interact. The optimum level of interaction between the energy system components has been identified by employing an optimization algorithm seeking to minimize the overall cost of the energy system.

The design of the energy production plant integrating cogeneration engines and renew-

able energy was recently examined by Reini et al. [68] who developed integer programming models capable of solving small-scale examples.

Beyond costs minimization, some authors propose more environmentally friendly models. For instance in Chinese and Meneghetti [21] a mixed integer linear-programming model is developed for a utility company profit maximization, together with a linear-programming model that aims at minimizing the balance of greenhouse-gas emissions related to the proposed energy system and the avoided emissions due to the substitution of current fossil-fuel boilers with district-heating connections.

The district heating network design problem has been widely studied through heuristics, metaheuristics and evolutionary models as well as non-linear models. In Craus et al. [26] the authors present a Genetic Algorithm to solve the problem of extending district heating networks by selecting the most profitable users and considering constraints on the optimal pipe path that has to follow the existing roads. Tests on a simple network of 50 individuals are presented.

A biologically inspired strategy of optimally building heating distribution network is presented in Shang and Zhao [78]. In this case an Ant Colony algorithm and a Genetic algorithm are used and compared.

A new method has been developed by Weber et al. [91] to design district energy systems by decomposing the multi-objective optimization problem in a way similar to the Bender's decomposition. In this case authors aims to solve two optimization problems: the minimization of costs and CO2 emissions and the optimal choice of heat pumps, temperature along the pipes, thickness of insulation. The objective is to find how shall a district energy system be designed to minimize the overall costs and the CO2 emissions while delivering the hourly energy services required by the customers. A multi objective evolutionary algorithm is presented for such purposes and tests on 12 buildings has been carried out.

Another multi-objective evolutionary algorithm is studied in Molyneaux et al. [58], to facilitate the design and planning of a district heating network based on a combination of centralized and decentralized heat pumps combined with on-site cogeneration. A Genetic Algorithm is selected to optimize pollution, costs and investments.

Examples of non-linear models for DH network design are presented by Bøhm et al. [9], Park et al. [64] and Bøhm et al. [8], while network aggregation techniques are discussed in Zhao [99], Zhao and Holst [100], Larsen et al. [48], Loewen et al. [51], Loewen et al. [52] and Larsen et al. [49].

The optimal operational management of District Heating Networks has been studied both through deterministic and heuristics approaches. An example of deterministic approach can be found in Dotzauer [28]. This study considers mid-term planning of the production of heat and power for periods of up to one month. The operation of fuel storage and the influence of the national tax system are considered. The major goal is to minimize the operation cost, subject to the condition of fulfilling heat demands. The main output results are the power produced and consumed each day of the planning horizon

An example of Heuristic approaches for the operational management problem can be found in Sakawa et al. [76] where Genetic algorithms are proposed to formulate the operation planning of a district heating and cooling plant as a mixed 0-1 linear programming problem. Authors consider the operation plan to minimize the cost of gas and electricity under the condition that the demand for cold water and steam must be supplied by running boilers and freezers.

Heuristics has been used also to model demand responsive systems. An example can

be found in the work published by Sipilä and Kärkkäinen [80], where authors describe a multiagent system that dynamically controls District Heating Systems (DHS) so that the load of the system is kept below certain threshold values without reducing the quality of service provided to the customers. It is important to underline that only peak cutting is considered in this work, while the demand shifting is not studied.

Other optimization studies in the field of District Heating has been carried out focusing on specific technical aspects of the system.

Deterministic approaches are used in Bojic and Trifunovic [10] and Bojic et al. [11]. The first work focuses on the evaluation of hydraulic resistance of valves that may be adjusted, and heat exchangers in substations that may be resized. Tests on three buildings present the computational results. The latter investigates an optimum strategy to mitigate the problem caused by changes of three of system characteristics: hydraulic resistance of secondary pipe network, heat transmittance of radiators inside buildings, and heat transmittance of building envelope.

Heat exchangers and pumps are considered in Xu and Chen [93] where an optimization model is developed based on the physical quantities, i.e. entransy, entransy dissipation and entransy dissipation-based thermal resistance. In particular, two complementary optimization problems are studied, the first one related to the minimization of the total thermal conductance of heat exchangers with total energy consumption of pumps given; and the second one related to the minimization of the total energy consumption of pumps with total thermal conductance of heat exchangers given. The final objective is to find the optimized configuration of all the structural and operating parameters.

An integer programming model for a different problem was defined by Aringhieri and Malucelli [4]. They considered the optimal selection of the type of heat exchangers to be installed at the users in order to optimize the return temperature at the plant and achieve good system efficiency at a reasonable cost.

Heuristics methods are used as well for such analyses. For instance in Kayfeci et al. [42] Artificial Neural Networks (ANNs) are implemented to predict insulation thickness and life cycle costs (LCCs) for pipe insulation applications. Artificial Neural Networks techniques are used in Keçebaş and Yabanova [44] as well, where authors deal with determination of the energy and exergy efficiencies and exergy destructions for thermal optimization of a geothermal district heating system.

Finally, some investments decision making are studied by deterministic methods, such as in Tveit et al. [86] where a MINLP model is presented. In this case the objective is the analysis of new investments and the long-term operation of CHP plants in a district heating network with long-term thermal storage. Authors created a decision making tool for investing either in a long-term thermal storage or for investments in a DH network with an existing long-term thermal storage.

A summary of the main scientific literature in the field of District Heating can be found in Table 4.1 where papers are classified according to different types of problems, together with the methodologies used to solve them. The word deterministic indicates all the exact methods of mathematical programming, LP, ILP and MILP techniques.

Table 4.1: District Heating literature summary

| TYPE OF PROBLEM | PAPERS | METHODOLOGY KEYWORDS |
|---|---|---|
| *UNITS SELECTION AND DESIGN* | | |
| Optimal components selection | Mehleri et al. [57] | Deterministic |
| | Ren and Gao [69] | Deterministic |
| | Sanaei and Nakata [77] | Non-linear optimization |
| Plant design integration | Reini et al. [68] | Deterministic |
| Environmental impact | Chinese and Meneghetti [21] | Deterministic |
| Components selection, evironmental impact | Weber et al. [91] | Bender's decomposition |
| | Molyneaux et al. [58] | Genetic Algorithm |
| Nework Design | Shang and Zhao [78] | Ant Colony |
| | Bøhm et al. [9] | Non-linear models |
| | Park et al. [64] | Non-linear models |
| | Bøhm et al. [8] | Non-linear models |
| | Zhao [99] | Network aggregation |
| | Zhao and Holst [100] | Network aggregation |
| | Larsen et al. [48] | Network aggregation |
| | Loewen et al. [51] | Network aggregation |
| | Loewen et al. [52] | Network aggregation |
| | Larsen et al. [49] | Network aggregation |
| Incremental Network Design | Craus et al. [26] | Genetic Algorithm |
| *MANAGEMENT* | | |
| Operational management | Dotzauer [28] | Deterministic |
| | Sakawa et al. [76] | Genetic Algorithm |
| Demand responsive | Sipilä and Kärkkäinen [80] | Heuristics, multi-agent |
| *TECHNICAL/ECONOMICAL ASPECTS* | | |
| Heat exchangers and valves | Bojic and Trifunovic [10] | Deterministic |
| | Bojic et al. [11] | Deterministic |
| Heat exchangers and pumps | Xu and Chen [93] | Deterministic |
| Heat exchangers and return temperature | Aringhieri and Malucelli [4] | ILP |
| Insulation thickness | Kayfeci et al. [42] | Artificial neural networks |
| Thermal optimization (energy-exergy efficiency) | Keçebaş and Yabanova [44] | Artificial neural networks |
| Investment decision making | Tveit et al. [86] | Deterministic |

### 4.2.2 District Cooling

The literature specialized in the District Cooling Systems optimization is slightly limited. The majority of works related to network design or operational management are in the field of District Heating and in such cases the Cooling problems are somehow complementary to the main Heating problems already studied. However, some papers specifically dedicated to District Cooling optimization can still be found in literature.

In Söderman [81] a Mixed Integer Linear Programming model is applied for the design and operational management of a District Cooling network in an urban region. On the network design side, the authors focus in particular on the structure of the district cooling system including the locations where cooling plants should be built, the cooling capacity of the plants, the cold media storage locations, the storage capacities and the routing of the distribution pipelines to individual consumers. On the operational management side the decisions are related to how the cooling generation plants will be run in different periods of the year, how the storages will be discharged and recharged and what will be the cold medium flow rates in the district cooling pipelines. Computational tests on a network of 53 users are presented.

Metaheuristics approaches have received a wider attention with particular regard to Genetic algorithms implemented to solve mainly design problems.

In Feng and Long [30] and Feng and Long [31] the design problem is related to the combined optimization of pipes layout, pipes size, water velocity and insulating layer thickness. The objective is finding the best combination with the minimum annual equivalent cost, which consists of the overall investment, annual operating cost, maintenance and amortization expense annual cooling loss cost. As for the constraints, hydraulic stability is also considered in this study besides the ordinary factors such as pipe diameter, flow velocity, flow needed by users, flow equilibrium and circuit pressure equilibrium. Computational experiments are presented with regard to 4 cooling plants and 7 nodes with 13 possible connection paths.

The pipe network design optimization is studied by Chan et al. [17] through a Genetic algorithm as well. The objective is to find the optimal/near optimal piping network configuration of a district cooling system that minimizes the infrastructure (piping) cost compatible with the minimum pumping energy cost.

Another Genetic algorithm is implemented in Chow et al. [23] to determine the desirable mix of building types, within the district of interest, to be served by the District Cooling System. Tests on very little networks of 5 buildings are presented as well.

Other studies are more focused on the chiller selection and management with some demand responsive formulations. In Powell et al. [65] a cooling network with multiple chillers is studied and an optimization model is presented to define which chillers should be used and their corresponding cooling loads. Thermal storage is considered to evaluate electrical loads shifting allowing the system to take advantage of less expensive off-peak rates.

Operational management problems are studied by Metaheuristics as well.

A Genetic algorithm is implemented in Sakawa et al. [75] to solve an operation planning problem of a district heating and cooling plant. The objective is to minimize the costs related to gas bills and electricity bills due to the Energy consumption of different components of the network (i.e. cooling towers, heat exchangers, freezers, storage, boilers). An interactive Fuzzy approach to the problem is proposed by the same Authors in Sakawa and Matsui [74].

Network design and operational management problems are combined with environmentally aware models in Burer et al. [14] where a clustering evolutionary multi-objective optimizer is used to carry thermo economic analyses. The objective in this case is the minimization of the overall internalized cost of an energy system, accounting for design, installation, operation but also pollution through the introduction of pollution cost factors.

Beyond deterministic and heuristics approaches, simulation is also used to study such systems. In Chow et al. [24] simulation is used to forecast the hourly energy consumption

of users and the optimal plant configuration to satisfy the users needs.

A summary of the main scientific literature in the field of District Cooling can be found in Table 4.2 where papers are classified according to different types of problems, together with the methodologies used to solve them. The word deterministic indicates all the exact methods of mathematical programming, LP, ILP and MILP techniques.

Table 4.2: District Cooling literature summary

| TYPE OF PROBLEM | PAPERS | METHODOLOGY KEYWORDS |
|---|---|---|
| Network design | Chan et al. [17] | Genetic Algorithm |
| Mix of building selection | Chow et al. [23] | Genetic Algorithm |
| Design and operational management | Söderman [81] | Deterministic |
| Design and technical aspects | Feng and Long [30] | Genetic Algorithm |
| | Feng and Long [31] | Genetic Algorithm |
| Design, management and environmnet impact | Burer et al. [14] | Evolutionary multi-objective optimizer |
| Chillers selection and demand response | Powell et al. [65] | Genetic Algorithm |
| Operational management | Sakawa et al. [75] | Genetic Algorithm |
| Consumptions forecast and plant configuration | Chow et al. [24] | Simulation |

## 4.3 Electrical Energy Distribution

This section will be dedicated to the presentation of the main scientific literature in the field of electrical energy distribution optimization, with regard to off-grid systems and grid connected systems.

In the Energy field, off-grid systems are systems that are not connected to the main or national electric grid. Off-grid can be stand-alone systems or mini-grids that provide electricity to small communities which are established in remote rural areas, locations that are not served by an electricity distribution system. But the term off-grid can also have a broader meaning, referring in general to a way of living in a self sufficient manner without any reliance on one or more public utilities.

A typical off-grid system includes one or more methods of electricity generation, storage devices and regulation devices. The electricity is typically generated by one or more methods among renewable and conventional resources. The most common renewable resources for the electricity production are solar panel (photovoltaic or PV systems) and wind turbines, followed by micro hydro and geothermal methods. The conventional generation of electricity can be related to conventional diesel generators (or biofuel generator for more environmentally friendly solutions) and micro combined heat and power plants (micro CHP).

The storage devices are typically represented by a battery bank (lead acid batteries are the most common for solar applications) but sometimes other solutions with fuel cells are implemented as well.

When the conventional generator is on it can send energy directly to the final users or to the storage units. Since the storage belongs to the DC side and the conventional generator

belongs to the AC side, converter units (rectifiers) are inserted. The final demand can be met also using the energy stored in the battery and the energy produced by the renewable resource, for instance a PV plant. In this case converter units (inverters) are inserted as well, since the demand belongs to the AC side and the storage and PV units belongs to the DC side. The renewable production can be sent to the storage units in those cases in which the energy produced by the renewable plant exceeds the final users Energy needs.

On the opposite, Grid Connected Systems are systems that are connected to the main national electric grid. A power system network integrates transmission grids, distribution grids, distributed generators and loads that have connection points called buses. Broadly speaking, transmission level is related to the transfer of electrical energy from generating power plants to electrical substations located near demand centers. Transmission lines, when interconnected with each other, become transmission networks. The distribution level represents the connection between high voltage substations and customers. Distribution substations connect to the transmission system and lower the transmission voltage to medium voltage with the use of transformers.

Renewable energy systems can provide electrical Energy to houses or small businesses without any connection to the electricity grid, but many economical advantages can be offered by a grid-connection. In fact a grid-connected system allows people to power their home or small business with renewable energy during those periods (daily as well as seasonally) when the sun is shining, the water is running, or the wind is blowing. Any excess electricity produced is fed back into the grid. When renewable resources are no available, electricity from the grid can supply people needs, eliminating the expense of electricity storage devices like batteries.

In addition, power providers (i.e. electric utilities) in most states allow net metering, an arrangement where the excess electricity generated by grid-connected renewable energy systems "turns back" people electricity meter as it is fed back into the grid. If a consumer unit uses more electricity than its system feeds into the grid during a given month, the consumer will pay its power provider only for the difference between what it used and what it produced. In such cases arbitrage plays an important role in optimizing the economic revenues that may come from the electricity exchange between the users and the main grid.

### 4.3.1 Off-Grid Systems

The scientific literature in the field of off-grid systems optimization can be classified into two main problems that are the optimal selection and sizing of components and the optimal operational management and dispatching of the electrical energy produced by the system. Components are generally storage devices (mainly batteries), conventional generators to cover peak demand and renewable resources, with particular regard to PV and wind plants.

These problems are studied both by deterministic and heuristics approaches.

Beyond such main wide topics, other studies take into account also environment and pollution issues and a separate part of literature is more dedicated to comparison between deterministic and heuristics approaches and existing design softwares analyses.

The optimal selection and sizing of components has been widely studied through deterministic approaches of Linear Programming and Mixed Integer Linear Programming.

In Zhang et al. [97] authors developed a deterministic approach for the optimum sizing of two hybrid power systems. One composed of PV, wind, battery and diesel and another one composed of just PV, wind and diesel. Optimum values are obtained with a time

horizon on 20 years, including the number of PV modules, the PV modules surface area, the number of wind turbines, the wind turbine installation height, the battery bank number and the diesel generator operating hours with their lowest system total investment costs.

The problem of sizing battery storage and renewable sources such as PV arrays and wind turbines at an off-grid facility has been studied by Linear Programming in Puri [67] as well.

The components sizing can be found also in Yu et al. [95] where authors developed a mixed integer linear programming algorithm to determine the optimal number of renewable energy and storage components in a microgrid given typical load profiles, local pricing regime, and capital costs. Case studies using solar panels and advanced lead acid battery modules are performed under residential, commercial, and off-grid sites.

In Huneke et al. [39] the optimal configuration of an electrical power supply system following characteristic restrictions as well as hourly weather and demand data is found. In particular, the optimal mix of solar and wind-based power generators combined with storage devices and a diesel generator set is formed.

A slightly different approach is used in Gupta et al. [35] where authors present a general methodological framework for the formulation of an action plan for a small-scale hybrid energy system for a remote area. The action plan is the output of a six stage procedure, where a deterministic approach for sizing and optimization takes place as well. The proposed procedure is made of selecting cluster of villages, demand assessment, resource assessment, estimation of unit cost of different resources, sizing and optimization, and model formulation.

The operational management problem of off-grid systems has been widely studied as well through deterministic approaches.

In Chen et al. [19] a mathematical programming approach is established for the analysis and design of an off-grid hybrid power system. In particular, the problem of allocating the power sources to demands as well as the storage of excess electricity for later use is solved.

An optimization framework for solving the scheduling and commitment problems of off-grid power systems is proposed by Zelazo et al. [96] as well. Authors propose a general optimization framework to manage load scheduling and utility maximization in the context of a self-contained power system.

In Bansal et al. [7] a linear programming mathematical model for the optimal daily scheduling of a solar-wind-diesel system with battery storages is presented. The objective, as usual, is profit maximization.

A linear mathematical program has been derived by Mustonen and Nanthavong [61] for an autonomous small scale village power system. The model considers a 24 hours operation period of a village power system. The peculiarity is that this study involves the linearization of cost functions for power load, generation, energy storage, and power distribution, taking into account that in reality, many components of a power system have non-linear characteristics.

Mixed integer linear programming is used in Dai and Mesbahi [27] where authors address the optimal power generation and load management problems in off-grid hybrid electric systems with renewable sources.

Slightly different off-grid systems has been studied by Morais et al. [60]. In this paper authors take into account a system with fuel cells, beyond the traditional components (wind, solar, batteries). A mixed-integer linear programming is developed to minimize the generation costs and optimize storage charging and discharging time subjected to all

the operation technical constraints

A more complex system with a greater amount of components can be found in Gupta et al. [36] where authors study the optimal configuration and operation of a hybrid energy generation system consisting of small/micro hydro based power generation, biogas based power generation, biomass (fuel wood) based power generation, photovoltaic array, a battery bank and a fossil fuel generator.

Heuristics approaches has been used both for the selection/sizing of off-grid systems components and for operational management problems.

The components selection and sizing has been studied in several papers by using heuristics and metaheuristics techniques.

The optimum mix of resources for a cost optimization has been studied in Sharma et al. [79] both through Genetic algorithms and Particle Swarm methods. Since standard Particle Swarm optimization algorithm suffers from premature convergence due to low diversity, and Genetic algorithm suffers from a low convergence speed, in this study authors propose some modification strategies in the two algorithms to achieve the properties of higher capacity of global convergence and a faster efficiency of searching.

Particle Swarm optimization is used in Boonbumroong et al. [12] as well for a design optimization problem. In particular, the objective is finding the optimal configuration of a stand alone hybrid power system composed of PV/wind/diesel.

In Gajbhiye and Suhane [32] the authors propose an optimization algorithm based on Ant Colony optimization to evaluate the optimal sizing and economic assessment of a Hybrid Energy System which combines PV, wind turbine, diesel and battery bank.

Several studies in the field of off-grid systems operational management has been carried through heuristics and metaheuristics as well.

The operational management problem is studied in Tutkun [85] through a Genetic algorithm and a Support Vector Machines method. The objective is to minimize the electricity cost of the renewable system by optimally scheduling generated and consumed powers.

Particle Swarm optimization is proposed in Amer et al. [2] for the optimization of the power generated from a Hybrid Renewable Energy Systems in order to achieve the load of a typical house as example of load demand.

Finally, in Priyadharshini and Chitra [66] an Ant Colony optimization based control strategy is proposed for self-tuning some control parameters related to voltage regulation and frequency regulation especially at the instant of shifting from grid tied mode to island mode of operation of the microgrid

Beyond the main classes of design/selection/sizing of components and operational management problems, there are other works in literature related to comparative analyses between heuristics, deterministic and simulation approaches.

In Upadhyay and Sharma [87] authors study the operational management problem by making a comparative analysis between a mathematical model developed in LINGO and a Genetic algorithm developed in MATLAB.

While in Whitefoot et al. [92] authors study the optimal system design problem by comparing results obtained through a deterministic linear programming model and results obtained using the publicly available rulebased dispatch strategy in HOMER Energy software. A case study of an islanded military base microgrid with renewable and non-renewable electricity generation, battery storage, and plug-in vehicles is presented.

Another group of papers use both deterministic and heuristics to study design and operational management problems with a more environmentally friendly approach that

takes into consideration environment issues and pollution emissions.

A deterministic approach is used in Kazemi and Rabbani [43] where authors takes into account greenhouse gas (GHG) emissions produced by utilization of renewable energies in decentralized energy planning optimization models with demand side management. A number of sustainability indicators are utilized upon which four renewable energy technologies are compared.

A binary evolutionary algorithm is used in Katsigiannis and Georgilakis [40] where an economic and environmental evaluation of an off-grid system is presented. The economic evaluation is referred to the minimization of the total net present cost, while the environmental objective refers to the minimization of the total CO2 equivalent emissions during the life cycle of system components (wind turbines, photovoltaics, diesel generator and batteries).

The environmental emissions and energy sustainability are considered also in Colson et al. [25] where an Ant Colony optimization method is proposed for the operational management problem related to dispatch control and power management of microgrid generation.

A summary of the main scientific literature in the field of off-grid systems can be found in Table 4.3 where papers are classified according to different types of problems, together with the methodologies used to solve them. The word deterministic indicates all the exact methods of mathematical programming, LP, ILP and MILP techniques.

Table 4.3: Off-grid systems literature summary

| TYPE OF PROBLEM | PAPERS | METHODOLOGY KEYWORDS |
|---|---|---|
| Components selection and sizing | Zhang et al. [97] | Determinisitc |
| | Puri [67] | Deterministic |
| | Yu et al. [95] | Deterministic |
| | Huneke et al. [39] | Deterministic |
| | Gupta et al. [35] | Deterministic, clusterization |
| | Sharma et al. [79] | Genetic, Particle Swarm |
| | Boonbumroong et al. [12] | Particle Swarm |
| | Gajbhiye and Suhane [32] | Ant Colony |
| Operational management | Chen et al. [19] | Deterministic |
| | Zelazo et al. [96] | Deterministic |
| | Bansal et al. [7] | Deterministic |
| | Mustonen and Nanthavong [61] | Deterministic |
| | Dai and Mesbahi [27] | Deterministic |
| | Morais et al. [60] | Deterministic |
| | Gupta et al. [36] | Deterministic |
| | Tutkun [85] | Genetic Algorithm |
| | Amer et al. [2] | Particle Swarm |
| | Priyadharshini and Chitra [66] | Ant Colony |
| Comparative analyses | Upadhyay and Sharma [87] | Deterministic vs Genetic |
| | Whitefoot et al. [92] | Deterministic vs simulation |
| Environmental impact | Kazemi and Rabbani [43] | Deterministic |
| | Katsigiannis and Georgilakis [40] | Binary Evolutionary Algorithm |
| | Colson et al. [25] | Ant Colony |

### 4.3.2 Grid Connected Systems

The field of Grid connected systems optimization has been mainly treated through deterministic linear programming and mixed integer linear programming approaches and heuristics approaches. It is possible to find simulation approaches as well as dynamic programming and quadratic programming methods.

The main type of problems are the components sizing/location/dimension and the operational management of the system along a defined time horizon. Generally the objective functions are related to profit maximization with particular regard to the possibility to sell the available Energy to the grid. The opportunity to play with arbitrage techniques (i.e. buying/selling Energy from/to the grid), is the main peculiarity that distinguish the grid connected studies from the off-grid studies.

Deterministic approaches has been used both for sizing, design problems and for operational management studies.

In Ren et al. [70] authors deal with the problem of the optimal size of a grid-connected photovoltaic (PV) system for residential applications. In particular, they propose a linear programming model that determines the economically optimal PV installation. The objective is to define the optimal PV capacity by minimizing the annual energy cost of a given customer, including PV investment cost, maintenance cost, utility electricity cost, subtracting the revenue from selling the excess electricity.

Another sizing problems more focused on storage devices is presented in Chen et al. [20]. In this case cost/benefit analyses for the optimal sizing of an energy storage system in a microgrid are presented. In particular authors propose a comparison between quantitative results obtained for an offgrid case and a grid connected case.

The optimal design of a hybrid wind-solar power system for either autonomous or grid-linked applications has been combined with a more environmentally friendly analysis in Chedid and Rahman [18]. The proposed analysis employs linear programming techniques to minimize the average production cost of electricity while meeting the load requirements in a reliable manner, and takes environmental factors into consideration as well.

The network design of the system through deterministic approaches and graph theory can be found in Paiva et al. [63]. The main purpose is the definition of the power flows in the branches and the convenience in the installation of each of the branches of the graph by minimizing costs and meeting restrictions imposed on the problem.

With regard to the operational management problem through deterministic approaches, the available literature makes use of Linear Programming and Mixed Integer Linear Programming.

In Kriett and Salani [46] a generic mixed integer linear programming model is proposed to minimize the operating cost of a residential grid-connected microgrid. Supply and demand of both electrical and thermal energy are modeled as decision variables. The micro grid covers solar energy, distributed generators, energy storages, loads and electric vehicle.

The electric vehicle management can be found in Stadler et al. [82] as well, where a mixed-integer linear program is proposed to examine and minimize the impact of electric vehicles on building energy costs and CO2 emissions.

An operational management problem with demand side applications can be found in Zhang et al. [98] where authors study the economic dispatch for a microgrid with high renewable energy penetration. In this case robust optimization is used to address the intrinsically stochastic availability of renewable energy sources.

A work more focused on storage management can be found in Lu and Shahidehpour [55]. The paper presents a short-term scheduling of battery and applies a Lagrangian relaxation-based optimization algorithm to determine the hourly charge/discharge commitment of battery in a utility grid. The main objective is to make analyses on the impact of grid-connected PV/battery system on locational pricing, peak load shaving, and transmission congestion management.

With regard to Heuristics approaches, Particle Swarm optimization has been used mainly for design problems.

Examples can be found in Kornelakis [45] where authors present an optimal design of photovoltaic grid-connected systems. The objective is to determine the optimal number of system devices and the optimal PV module installation details, in such a way that the economic and environmental benefits achieved during the system operational lifetime period are both maximized.

The optimal location and size of PV Grid-Connected Systems for distributed power generation is studied by Gómez et al. [34] through a Particle Swarm algorithm as well.

In Hassan and Abido [38] a slightly different problem is presented more focused on technical aspects of the operational management problem. In particular, Particle Swarm is used to find the optimal design of LC filter, controller parameters, and damping resistance for a grid-connected system.

Other approaches such as Dynamic Programming and Quadratic Programming has been used to study grid-connected optimization problems.

Dynamic Programming is used in Riffonneau et al. [71] to find an optimal power management mechanism for grid connected PV systems with storage.

While Quadratic Programming is used in Supriya and Siddarthan [83] to determine the optimal design of a hybrid wind-solar power system for either autonomous or grid-linked applications. The objective is to minimize the cost while meeting the load requirements in a reliable manner. The optimum number of PV modules and wind turbines subject to minimum cost can be obtained with good accuracy.

A probabilistic approach is used in Yokoyama et al. [94] to find the optimal unit sizing of a grid-connected photovoltaic system without storage batteries. In consideration of probabilistic characteristics of solar insolation and electricity demand, the surface area of photovoltaic array, capacity of receiving device, and electric contract demand are determined so as to minimize the expected values of annual total cost and annual energy consumption subject to the annual loss of power supply probability.

Other approaches more related to simulation procedures are available in literature.

In Liu et al. [50] authors investigate the economic, technical and environmental performance of residential PV system. The objective is to optimize the size and slope of PV array in the system by running simulations through a simulation software called Homer.

A simulation approach is proposed in Notton et al. [62] as well for a similar sizing problem. In this case the purpose is to calculate the optimal sizing of a grid-connected PV system under a wide variety of weather conditions and for four photovoltaic module technologies.

A summary of the main scientific literature in the field of grid-connected systems can be found in Table 4.4 where papers are classified according to different types of problems, together with the methodologies used to solve them. The word deterministic indicates all the exact methods of mathematical programming, LP, ILP and MILP techniques.

Table 4.4: Grid connected systems literature summary

| TYPE OF PROBLEM | PAPERS | METHODOLOGY KEYWORDS |
|---|---|---|
| Units selection, location and sizing | Ren et al. [70] | Deterministic |
| | Chen et al. [20] | Deterministic |
| | Gómez et al. [34] | Particle Swarm |
| | Supriya and Siddarthan [83] | Quadratic programming |
| | Yokoyama et al. [94] | Probabilistic approach |
| | Notton et al. [62] | Simulation |
| Design and environmental impact | Chedid and Rahman [18] | Deterministic |
| | Kornelakis [45] | Heuristic |
| | Liu et al. [50] | Simulation |
| Network design | Paiva et al. [63] | Deterministic |
| Operational management | Kriett and Salani [46] | Deterministic |
| | Hassan and Abido [38] | Particle Swarm |
| | Riffonneau et al. [71] | Dynamic programming |
| Op management, environmental impact | Stadler et al. [82] | Deterministic |
| Op management, demand response | Zhang et al. [98] | Deterministic |
| Op management of storage units | Lu and Shahidehpour [55] | Lagrangian-relaxation |

## 4.4 Heat and Power Production

This section will be dedicated to the presentation of the main scientific literature in the field of optimization applied to combined heat and power plants (CHP) and combined heat cooling and power plants (CHCP).

Combined heat and power production is commonly known as Cogeneration and it refers to the simultaneously production of electricity and useful heat. Cogeneration makes a thermodynamically efficient use of fuel. In fact in traditional electricity production, some energy has to be wasted as heat, as all thermal power plants emit heat during electricity generation. Such heat is generally released into the natural environment through cooling towers, or by other means. But through cogeneration plants such thermal energy can be recovered and put to use. One of the main example of heat recover is the use of such wasted thermal energy in District Heating networks.

Large cogeneration systems can provide heat and power for industrial sites or even whole towns.

On the other hand, micro-CHP, is used to provide Energy to houses or small business. Such installations are usually less than 5 $kW_e$. In this cases, instead of burning fuel to heat space and water, part of the energy is converted into electricity that can be used both for the home/business energy needs and, if possible, for energy exchange with the power grid.

Combined heat, cooling an power production is commonly known as Trigeneration and it refers to the simultaneous generation of electricity and useful heating and cooling. In trigeneration the waste heat can be used both for heating and cooling, gaining higher overall efficiencies than cogeneration or traditional power plants. The cooling production is typically obtained through an absorption refrigerator.

In both technologies (CHP and CHCP) the Energy production can come from the combustion of a fuel (diesel or biofuel) or a solar heat collector.

The main optimization problems studied in the field of CHP and CHCP systems are related to the scheduling and operational management of such plants, with profit maximiza-

tion objectives and sometimes additional environmental objectives related to emissions reduction. Part of the literature is also focused on the design of such plants and optimal dimension of technical components, although the design is always studied together with the hourly simulation of the system.

The main approaches for these optimization problems are deterministic approaches of linear programming and mixed integer linear programming and heuristic approaches with a wide use of Genetic algorithms in particular.

### 4.4.1 CHP Systems

The Combined Heat and Power (CHP) technology has been studied both through deterministic and heuristic approaches, with particular attention to deterministic methods.

The deterministic methods of linear programming and mixed integer linear programming has been used to solve pure applications related to optimal CHP plants management and optimized arbitrage techniques trying to take advantage of the electricity exchange with the main electrical network.

In Cho et al. [22] an energy dispatch algorithm is presented with the objective to minimize the cost of energy made of cost of electricity from the grid and cost of natural gas into the engine and boiler based on energy efficiency constrains for each component. A deterministic network flow model of a typical CHP system is developed as part of the algorithm.

A similar operational management study can be found in Gustafsson and Karlsson [37] where the objective is to find the best combination of electricity production, electricity purchase and heat production. In this case the CHP optimization is integrated with a district heating system where the heat can be further distributed. The optimal solution in the model is characterized by the lowest possible operating cost for one year.

Other works are still focused on operational management applications but with more attention to the benefits that thermal and electrical storage can bring inside the system. It is the case of Majic et al. [56] where authors present an optimization model for economical scheduling of a microgrid using linear programming. In this study two microgrid models are considered. The microgrid proposed in the first model consists of thermal and electrical loads and a CHP unit. The second model consists of the units considered in the first model with addition of thermal and electrical storage. Optimization results for the two cases are compared to determine the impact of energy storage on an optimal scheduling.

Beyond the pure applications, other works are more focused on mathematical tricks to improve the deterministic algorithms efficiency and robustness.

In Lahdelma and Hakonen [47] authors model the hourly CHP operation as an LP problem with a special structure and present the specialized Power Simplex algorithm that utilizes this structure efficiently. In this case the operational management problem of CHP is studied through a variant of the Revised Simplex algorithm, which is commonly used for solving LP problems.

Another mathematical study is proposed in Thorin et al. [84] where a tool for long-term optimization of CHP systems is developed that is based on mixed integer linear-programming and Lagrangian relaxation. Again the problem studied is the unit commitment and load dispatch problem and the possibility to buy and sell electric power at a spot market is considered as well as the possibility to provide secondary reserve. For larger and more complicated systems, a long optimization period has to be divided into shorter sub-periods. The main focus of this work is the improvement of the robustness of the

proposed algorithm. For that purpose Lagrangian relaxation is introduced, so that the solutions of the tool become more robust and near optimal solutions can be found also for more complicated situations.

Heuristic techniques are used to take into account more complex scenarios, for instance those whit uncertainty.

In Moradi et al. [59] Particle Swarm optimization is proposed to consider the CHP model under uncertainty. In this case the problem is a design one and the algorithm has been developed to determine the optimal capacities for the CHP and boiler such that thermal and electrical energy demands can be satisfied with high cost efficiency.

Finally other works consider the non-linearity of the CHP operational management problems. In Ashok and Banerjee [6] a Newton based algorithm for minimizing the total operating cost of a CHP plant is proposed to face the multiperiod and non-linear nature of the problem. The objective is to determine the optimal operating strategy of industrial cogeneration schemes. All types of cogeneration equipments, steam turbines, gas turbines, diesel generators, steam boilers, waste heat recovery boilers, and steam header configuration, with grid connection are separately represented in terms of their characteristics so that the model has the flexibility to be applicable for any industry.

A summary of the main scientific literature in the field of CHP systems can be found in Table 4.5 where papers are classified according to different types of problems, together with the methodologies used to solve them. The word deterministic indicates all the exact methods of mathematical programming, LP, ILP and MILP techniques.

Table 4.5: CHP systems literature summary

| TYPE OF PROBLEM | PAPERS | METHODOLOGY KEYWORDS |
|---|---|---|
| Design under uncertainty | Moradi et al. [59] | Particle Swarm |
| Operational management | Cho et al. [22] | Deterministic |
| | Gustafsson and Karlsson [37] | Deterministic |
| | Lahdelma and Hakonen [47] | Revised Simplex algorithm |
| | Thorin et al. [84] | Lagrangian relaxation |
| | Ashok and Banerjee [6] | Newton based Algorithm |
| Operational management storage units | Majic et al. [56] | Deterministic |

### 4.4.2 CHCP Systems

Optimization problems dedicated to CHCP systems are complementary to the ones dedicated to CHP as CHCP plants represent a further development of CHP by adding the opportunity to produce cool Energy beyond the electrical and heat Energy. Hence the problems studied in the field of CHCP belong to categories similar to the CHP ones described in previous section.

With regard to deterministic approaches, the main problems are related to optimal operational management of CHCP plants, with particular focus on applied problems and arbitrage. Some studies are focused also on environmental aspects and other studies are focused on mathematical improvement of traditional linear or mixed integer linear programming.

A simple operational management problem for a trigeneration plant can be found in Lozano et al. [53]. Arbitrage techniques are taken into consideration. The system is

interconnected to the electric utility grid, both to receive electricity and to deliver surplus electricity. A linear programming model provides the operational mode with the lowest variable cost. A thermoeconomic analysis, based on marginal production costs, is used to obtain unit costs for internal energy flows and final products as well as to explain the best operational strategy as a function of the demand for energy services and the prices of the resources consumed.

Another operational management problem can be found in Arosio et al. [5] where the operating policy of the plant is dynamically and automatically chosen by a mathematical model using linear optimization techniques. Such model is then used to make evaluations on the influence of each parameter on the performances of the whole system.

A slightly different study can be found in Arcuri et al. [3] where the operational management is studied together with the optimal investment decisions with regard to design issues as well. In particular, a procedure for optimizing the energy-management of a hospital complex is described, which derives from the optimal design. In this case the objective is the determination of the design and the running conditions of a trigeneration plant.

A thermoeconomic analysis of simple trigeneration systems is presented in Lozano et al. [54]. Different optimal operation conditions which combine the possibility of buying or selling electricity and/or wasting the excess of heat produced are considered. The aim is to determine the energy costs of final energy services and internal flows for such different operation conditions.

The operational management together with the optimal design/configuration and environmental issues has been studied in Carvalho et al. [15]. In this case the multiobjective optimization accounts for minimization of total annual costs and annual environmental loads in the design and operational stages. The environmental loads considered were the CO2 emissions released in the atmosphere. A set of Pareto solutions is obtained from the solution of a Mixed Integer Linear Programming (MILP) model, representing optimal trade-offs between the economic and environmental objectives.

A similar work can be found in Carvalho et al. [16] where the environmental information obtained through Life Cycle Analysis techniques has been incorporated into a Mixed Integer Linear Programming (MILP). The solution of the model provides the optimal configuration and operation of an energy supply system to be installed, minimizing the environmental burden associated with production of equipment and consumption of resources.

Other studies focus on mathematical tricks to improve the solution of operational management problems for CHCP systems.

The operational management problem together with the CO2 emission reduction and some mathematical tricks to improve the algorithm efficiency has been studied in Rong and Lahdelma [72]. Authors model the hourly trigeneration problem as a linear programming (LP) model with a joint characteristic for three energy components to minimize simultaneously the production and purchase costs of three energy components, as well as CO2 emissions costs. Then they explore the structure of the problem and propose the specialized Tri-Commodity Simplex (TCS) algorithm that employs this structure efficiently.

Another mathematical trick to better solve such problems can be found in Rong et al. [73] where authors present a Lagrangian relaxation based algorithm for trigeneration long-term planning with storages based on deflected subgradient optimization method. The trigeneration planning problem is modeled as a linear programming (LP) problem.

As for heuristic approaches in the field of CHCP, they have been widely used with particular regard to Genetic algorithms and some Particle Swarm Optimization as well.

The optimal design of CHCP has been studied in Ghaebi et al. [33] where an exergoeconomic optimization is carried on through a Genetic algorithm. The design parameters of this study are selected as: air compressor pressure ratio, gas turbine inlet temperature, pinch point temperatures in dual pressure heat recovery steam generator, pressure of steam that enters the generator of absorption chiller, process steam pressure and evaporator of the absorption chiller chilled water outlet temperature.

A Genetic algorithm to determine the best design parameters for a CHCP plant has been used in Ahmadi et al. [1] as well. In this case two objective functions are considered: the total cost rate of the system, which is the cost associated with fuel, component purchasing and environmental impact, and the system exergy.

A more comprehensive work can be found in Kavvadias and Maroulis [41] where a Genetic algorithm has been implemented for the design of trigeneration plants. In this case the optimization is carried out on technical, economical, energetic and environmental performance indicators in a multi-objective optimization framework. Both construction (equipment sizes) and discrete operational (pricing tariff schemes and operational strategy) variables are optimized based on realistic conditions.

The operational management problem has been studied in Wang et al. [90] through a Genetic algorithm. The paper analyses the energy flow of a CHCP system and deduces the primary energy consumption following the thermal demand of building. Three criteria, primary energy saving, annual total cost saving, and carbon dioxide emission reduction are selected to evaluate the performance of CHCP system. The objective is to maximize the technical, economical and environmental benefits achieved by CHCP system in comparison to separation production system.

A model more focused on environmental impact has been proposed in Wang et al. [88]. The algorithm is still a Genetic one, but the objective is the construction of environmental impact models for CHCP systems compared to conventional separation production (SP) systems.

The same authors propose a different heuristic algorithm in Wang et al. [89]. In particular, Particle Swarm optimization is used to optimize the design and the operation strategy of a CHCP system. Four decision variables are considered: the capacity of power generation unit (PGU), the capacity of heat storage tank, the on-off coefficient of PGU and the ratio of electric cooling to cool load. The objective function simultaneously measures the energetic, economical and environmental benefits achieved by CHCP system. Three energy-related environmental issues, global warming, acid precipitation and stratospheric ozone depletion, are assessed in the proposed emission model. The objective is the maximization of the benefits (energy-saving and emission-reducing).

Finally, some studies are focused on the introduction of storage systems for CHCP plants, as the introduction and the correct management of energy storage systems is a key point for such plants. In fact, energy storage brings on the one side advantages as for the reduced components sizes, but more importantly allows for a substantial decoupling of the thermal and electrical demands, making load following less of a stringent requirement.

A heuristic approach has been used in Bruno et al. [13] where the focus is to find the best cooling energy storage solution for a real site served by a trigeneration system. In particular the authors developed a two-step multiperiod algorithm based on two subproblems to explore the opportunities given by the exploitation of different technologies for energy storage in the development of a trigeneration and district energy project.

The analysis of thermal storage in trigeneration plants is proposed also in Facci et al. [29] where an optimization methodology, based on energy fluxes simulation and on the

application of the graph theory, has been used. The optimization algorithm searches for the plant management envelope that minimizes a prescribed objective function. Specifically, two different optimization criteria are considered: the economic optimization that minimizes the total daily operating cost and the primary energy use optimization, that minimizes the total daily amount of primary energy used by the plant.

A summary of the main scientific literature in the field of CHCP systems can be found in Table 4.6 where papers are classified according to different types of problems, together with the methodologies used to solve them. The word deterministic indicates all the exact methods of mathematical programming, LP, ILP and MILP techniques.

Table 4.6: CHCP systems literature summary

| TYPE OF PROBLEM | PAPERS | METHODOLOGY KEYWORDS |
|---|---|---|
| Design | Ghaebi et al. [33] | Genetic algorithm |
| Design, environmental impact | Ahmadi et al. [1] | Genetic algorithm |
| | Kavvadias and Maroulis [41] | Genetic algorithm |
| Design, operation strategy | Wang et al. [89] | Particle swarm |
| Environmental impact | Wang et al. [88] | Genetic algorithm |
| Operational management | Lozano et al. [53] | Deterministic |
| | Arosio et al. [5] | Deterministic |
| | Wang et al. [90] | Genetic algorithm |
| Op management and investment | Arcuri et al. [3] | Deterministic |
| Op management and storage | Rong et al. [73] | Lagrangian relaxation |
| Op management, design and environment | Carvalho et al. [15] | Deterministic |
| | Carvalho et al. [16] | Deterministic |
| | Rong and Lahdelma [72] | Tri-Commodity Simplex |
| | Wang et al. [90] | Genetic algorithm |
| Storage selection and management | Bruno et al. [13] | Heuristic |
| | Facci et al. [29] | Energy fluxes simulation |
| Thermoeconomic analysis | Lozano et al. [54] | Deterministic |

## 4.5 Conclusions

The previous sections showed an overview of the main literature in the field of Energy optimization, by focusing on the main class of topics described in the introduction and represented in Figure 4.1. The scientific areas that are still quite uncovered can be identified as follow.

On the thermal side, the district heating strategic design and incremental design has received a very little attention, especially with regard to deterministic approaches applied to large scale problems. The majority of the available literature is focused on very small instances and many design problems are studied by heuristic and metaheuristic techniques rather than deterministic methods.

On the electrical side, there is a wide literature in the field of off-grid systems but very little attention is given to optimal storage operational management with regard to degradation issues that may be involved in the batteries use for hybrid systems.

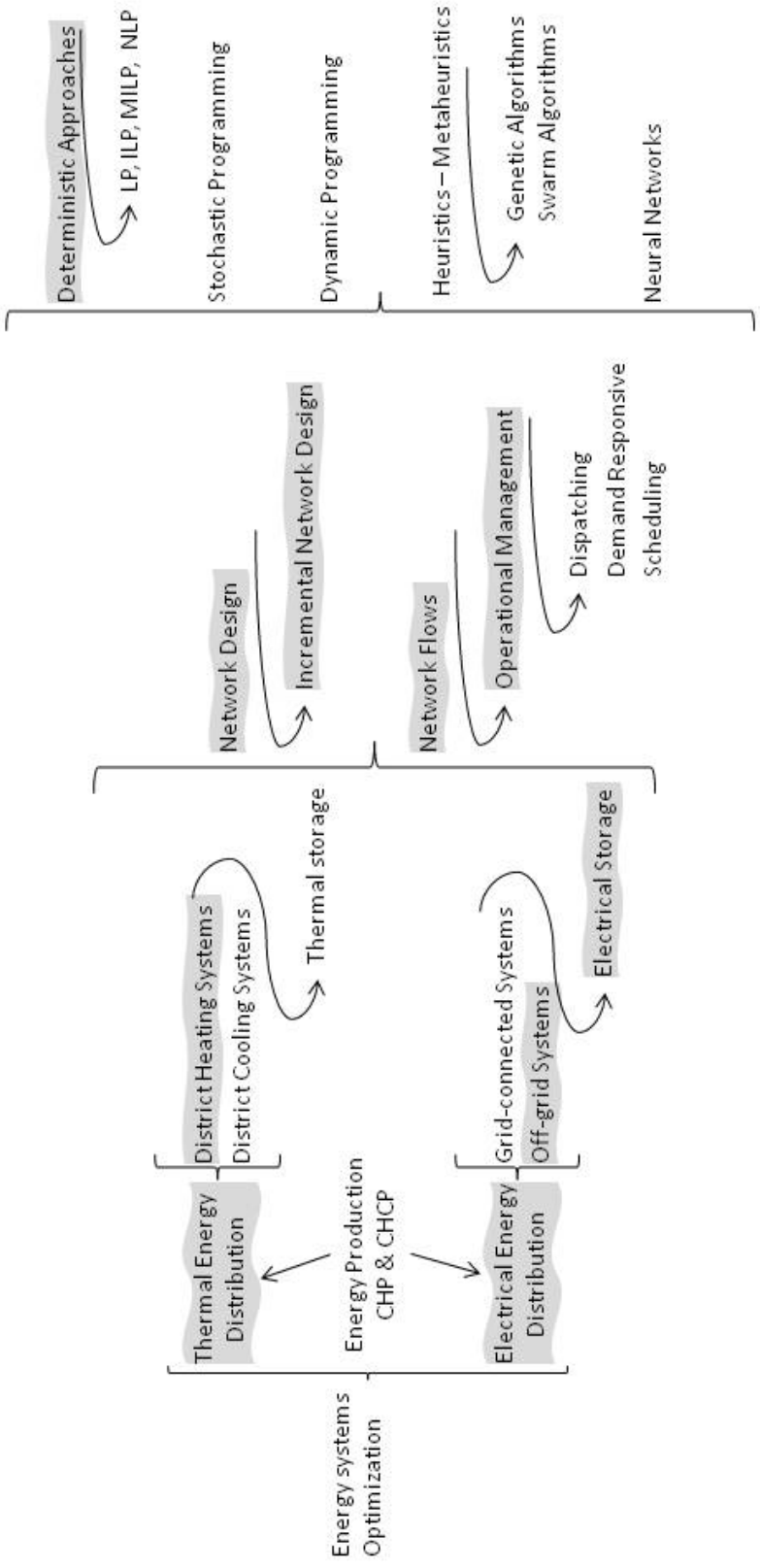


Figure 4.2: Selected Energy Optimization topics and methodology for the present Thesis

Hence, the most interesting topics that will be covered in this Thesis are related to the district heating strategic incremental network design and to the battery optimal management in off-grid power systems with renewable integration, with particular focus on battery degradation issues.

Figure 4.2 highlights the selected topics and the mathematical techniques through which such topics will be studied. In particular we will focus on deterministic approaches and graph theory, both for the network design of district heating systems and the hourly operational management of off-grid power systems.

# Bibliography


[1] P. Ahmadi, M. A. Rosen, and I. Dincer. Multi-objective exergy-based optimization of a polygeneration energy system using an evolutionary algorithm. *Energy*, 46(1): 21–31, 2012.

[2] M. Amer, A. Namaane, and N. M'Sirdi. Optimization of hybrid renewable energy systems (hres) using pso for cost reduction. *Energy Procedia*, 42:318–327, 2013.

[3] P. Arcuri, G. Florio, and P. Fragiacomo. A mixed integer programming model for optimal design of trigeneration in a hospital complex. *Energy*, 32(8):1430–1447, 2007.

[4] R. Aringhieri and F. Malucelli. Optimal operations management and network planning of a district heating system with a combined heat and power plant. *Annals OR*, 120(1–4):173–199, 2003.

[5] S. Arosio, M. Guilizzoni, and F. Pravettoni. A model for micro-trigeneration systems based on linear optimization and the italian tariff policy. *Applied Thermal Engineering*, 31(14):2292–2300, 2011.

[6] S. Ashok and R. Banerjee. Optimal operation of industrial cogeneration for load management. *Power Systems, IEEE Transactions on*, 18(2):931–937, 2003.

[7] M. Bansal, R. Saini, and D. Khatod. An off-grid hybrid system scheduling for a remote area. In *Electrical, Electronics and Computer Science (SCEECS), 2012 IEEE Students' Conference on*, pages 1–4. IEEE, 2012.

[8] B. Bøhm, M. Lucht, Y. Park, K. Sipil, S. Ha, K. Won-tae, K. Bong-kyun, T. Koljonen, H. Larsen, M. Wigbels, and M. Wistbacka. Simple models for operational optimization. *Contract*, 524110:0010, 2002.

[9] B. Bøhm, H. Pálsson, H. V. Larsen, and H. F. Ravn. Equivalent models for district heating systems. In *7th International Symposium on District Heating and Cooling*, pages 1–16, 2008.

[10] M. Bojic and N. Trifunovic. Linear programming optimization of heat distribution in a district-heating system by valve adjustments and substation retrofit. *Building and Environment*, 35(2):151–159, 2000.

[11] M. Bojic, N. Trifunovic, and S. Gustafsson. Mixed 0–1 sequential linear programming optimization of heat distribution in a district-heating system. *Energy and Buildings*, 32(3):309–317, 2000.

[12] U. Boonbumroong, N. Pratinthong, S. Thepa, C. Jivacate, and W. Pridasawas. Particle swarm optimization for ac-coupling stand alone hybrid power systems. *Solar Energy*, 85(3):560–569, 2011.

[13] S. Bruno, S. Lamonaca, M. La Scala, and U. Stecchi. Optimal design of trigeneration and district energy in the presence of energy storage. In *International Conference on Renewable Energies and Power Quality (ICREPQ10), Granada (Spain), 23th to 25th March*, 2010.

[14] M. Burer, K. Tanaka, D. Favrat, and K. Yamada. Multi-criteria optimization of a district cogeneration plant integrating a solid oxide fuel cell–gas turbine combined cycle, heat pumps and chillers. *Energy*, 28(6):497–518, 2003.

[15] M. Carvalho, M. A. Lozano, and L. M. Serra. Multiobjective optimization of trigeneration systems considering economic and environmental aspects. In *2nd European Conference on Polygeneration*, 2011.

[16] M. Carvalho, L. M. Serra, and M. A. Lozano. Optimal synthesis of trigeneration systems subject to environmental constraints. *Energy*, 36(6):3779–3790, 2011.

[17] A. L. Chan, V. I. Hanby, and T.-T. Chow. Optimization of distribution piping network in district cooling system using genetic algorithm with local search. *Energy Conversion and Management*, 48(10):2622–2629, 2007.

[18] R. Chedid and S. Rahman. Unit sizing and control of hybrid wind-solar power systems. *Energy Conversion, IEEE Transactions on*, 12(1):79–85, 1997.

[19] C.-L. Chen, C.-T. Lai, and J.-Y. Lee. A process integration technique for targeting and design of off-grid hybrid power networks. *Chemical Engineering*, 35, 2013.

[20] S. Chen, H. B. Gooi, and M. Wang. Sizing of energy storage for microgrids. *Smart Grid, IEEE Transactions on*, 3(1):142–151, 2012.

[21] D. Chinese and A. Meneghetti. Optimisation models for decision support in the development of biomass-based industrial district-heating networks in italy. *Applied energy*, 82(3):228–254, 2005.

[22] H. Cho, R. Luck, S. D. Eksioglu, and L. M. Chamra. Cost-optimized real-time operation of chp systems. *Energy and Buildings*, 41(4):445–451, 2009.

[23] T. Chow, A. L. Chan, and C. Song. Building-mix optimization in district cooling system implementation. *Applied Energy*, 77(1):1–13, 2004.

[24] T. Chow, K. Fong, A. Chan, R. Yau, W. Au, and V. Cheng. Energy modelling of district cooling system for new urban development. *Energy and Buildings*, 36(11): 1153–1162, 2004.

[25] C. Colson, M. Nehrir, and C. Wang. Ant colony optimization for microgrid multi-objective power management. In *Power Systems Conference and Exposition, 2009. PSCE'09. IEEE/PES*, pages 1–7. IEEE, 2009.

[26] M. Craus, F. Leon, and D. Arotăriţei. A new hybrid genetic algorithm for the district heating network problem. *Development and Application Systems*, page 84, 2010.

[27] R. Dai and M. Mesbahi. Optimal power generation and load management for off-grid hybrid power systems with renewable sources via mixed-integer programming. *Energy Conversion and Management*, 73:234–244, 2013.

[28] E. Dotzauer. Experiences in mid-term planning of district heating systems. *Energy*, 28(15):1545–1555, 2003.

[29] A. L. Facci, L. Andreassi, S. Ubertini, and E. Sciubba. Analysis of the influence of thermal energy storage on the optimal management of a trigeneration plant. *Energy Procedia*, 45:1295–1304, 2014.

[30] X. Feng and W. Long. Applying single parent genetic algorithm to optimize piping network layout of district cooling system. In *Natural Computation, 2008. ICNC'08. Fourth International Conference on*, volume 1, pages 176–180. IEEE, 2008.

[31] X. Feng and W. Long. Optimal design of pipe network of district cooling system based on genetic algorithm. In *Natural Computation (ICNC), 2010 Sixth International Conference on*, volume 5, pages 2415–2418. IEEE, 2010.

[32] P. Gajbhiye and P. Suhane. Methodology for optimal sizing & power management of hybrid energy system.

[33] H. Ghaebi, M. Saidi, and P. Ahmadi. Exergoeconomic optimization of a trigeneration system for heating, cooling and power production purpose based on trr method and using evolutionary algorithm. *Applied Thermal Engineering*, 36:113–125, 2012.

[34] M. Gómez, A. López, and F. Jurado. Optimal placement and sizing from standpoint of the investor of photovoltaics grid-connected systems using binary particle swarm optimization. *Applied Energy*, 87(6):1911–1918, 2010.

[35] A. Gupta, R. Saini, and M. Sharma. Hybrid energy system for remote area-an action plan for cost effective power generation. In *Industrial and Information Systems, 2008. ICIIS 2008. IEEE Region 10 and the Third international Conference on*, pages 1–6. IEEE, 2008.

[36] A. Gupta, R. Saini, and M. Sharma. Steady-state modelling of hybrid energy system for off grid electrification of cluster of villages. *Renewable Energy*, 35(2):520–535, 2010.

[37] S.-I. Gustafsson and B. G. Karlsson. Linear programming optimization in chp networks. *Heat Recovery Systems and CHP*, 11(4):231–238, 1991.

[38] M. Hassan and M. Abido. Optimal design of microgrids in autonomous and grid-connected modes using particle swarm optimization. *Power Electronics, IEEE Transactions on*, 26(3):755–769, 2011.

[39] F. Huneke, J. Henkel, J. A. B. González, and G. Erdmann. Optimisation of hybrid off-grid energy systems by linear programming. *Energy, Sustainability and Society*, 2(1):1–19, 2012.

[40] Y. Katsigiannis and P. Georgilakis. A multiobjective evolutionary algorithm approach for the optimum economic and environmental performance of an off-grid power system containing renewable energy sources. *Journal of optoelectronics and advanced materials*, 10(5):1233, 2008.

[41] K. Kavvadias and Z. Maroulis. Multi-objective optimization of a trigeneration plant. *Energy Policy*, 38(2):945–954, 2010.

[42] M. Kayfeci, İ. Yabanova, and A. Keçebaş. The use of artificial neural network to evaluate insulation thickness and life cycle costs: Pipe insulation application. *Applied Thermal Engineering*, 63(1):370–378, 2014.

[43] S. M. Kazemi and M. Rabbani. An integrated decentralized energy planning model considering demand-side management and environmental measures. *Journal of Energy*, 2013, 2013.

[44] A. Keçebaş and İ. Yabanova. Thermal monitoring and optimization of geothermal district heating systems using artificial neural network: A case study. *Energy and Buildings*, 50:339–346, 2012.

[45] A. Kornelakis. Multiobjective particle swarm optimization for the optimal design of photovoltaic grid-connected systems. *Solar Energy*, 84(12):2022–2033, 2010.

[46] P. O. Kriett and M. Salani. Optimal control of a residential microgrid. *Energy*, 42 (1):321–330, 2012.

[47] R. Lahdelma and H. Hakonen. An efficient linear programming algorithm for combined heat and power production. *European Journal of Operational Research*, 148 (1):141–151, 2003.

[48] H. V. Larsen, H. Palsson, B. Bøhm, and H. F. Ravn. An aggregated dynamic simulation model of district heating networks. *Energy Conversion and Management*, 43(8):995–1019, 2002.

[49] H. V. Larsen, B. Bøhm, and M. Wigbels. A comparison of aggregated models for simulation and operational optimisation of district heating networks. *Energy Conversion and Management*, 46(7–8):1119–1139, 2004.

[50] G. Liu, M. Rasul, M. Amanullah, and M. M. K. Khan. Techno-economic simulation and optimization of residential grid-connected pv system for the queensland climate. *Renewable Energy*, 45:146–155, 2012.

[51] A. Loewen, M. Wigbels, W. Althaus, A. Augusiak, and A. Renski. Structural simplification of complex DH networks-part 1 (in german). *Euroheat and Power*, 30(5): 42–44, 2001.

[52] A. Loewen, M. Wigbels, W. Althaus, A. Augusiak, and A. Renski. Structural simplification of complex DH networks-part 2 (in german). *Euroheat and Power*, 30(6): 46–51, 2001.

[53] M. Lozano, M. Carvalho, and L. Serra. Operational strategy and marginal costs in simple trigeneration systems. *Energy*, 34(11):2001–2008, 2009.

[54] M. A. Lozano, L. Serra, and M. Carvalho. Energy cost analysis of simple trigeneration systems under variable operation conditions. In *22nd International Conference on Efficiency, Cost, Optimization, Simulation and Environmental Impact of Energy Systems*, page 44, 2009.

[55] B. Lu and M. Shahidehpour. Short-term scheduling of battery in a grid-connected pv/battery system. *Power Systems, IEEE Transactions on*, 20(2):1053–1061, 2005.

[56] L. Majic, I. Krzelj, and M. Delimar. Optimal scheduling of a chp system with energy storage. In *Information & Communication Technology Electronics & Microelectronics (MIPRO), 2013 36th International Convention on*, pages 1253–1257. IEEE, 2013.

[57] E. D. Mehleri, H. Sarimveis, N. C. Markatos, and L. G. Papageorgiou. A mathematical programming approach for optimal design of distributed energy systems at the neighbourhood level. *Energy*, 44(1):96–104, 2012.

[58] A. Molyneaux, G. Leyland, and D. Favrat. Environomic multi-objective optimisation of a district heating network considering centralized and decentralized heat pumps. *Energy*, 35(2):751–758, 2010.

[59] M. H. Moradi, M. Hajinazari, S. Jamasb, and M. Paripour. An energy management system (ems) strategy for combined heat and power (chp) systems based on a hybrid optimization method employing fuzzy programming. *Energy*, 49:86–101, 2013.

[60] H. Morais, P. Kádár, P. Faria, Z. A. Vale, and H. Khodr. Optimal scheduling of a renewable micro-grid in an isolated load area using mixed-integer linear programming. *Renewable Energy*, 35(1):151–156, 2010.

[61] S. Mustonen and K. Nanthavong. Modeling of autonomous power systems-a mathematical model of a hybrid power system. In *Proceedings of the 2nd Joint International Conference on" Sustainable Energy and Environment (SEE 2006)" 21-23 November, 2006, Bangkok, Thailand*, 2006.

[62] G. Notton, V. Lazarov, and L. Stoyanov. Optimal sizing of a grid-connected pv system for various pv module technologies and inclinations, inverter efficiency characteristics and locations. *Renewable Energy*, 35(2):541–554, 2010.

[63] P. Paiva, H. Khodr, J. Domínguez-Navarro, J. Yusta, and A. Urdaneta. Integral planning of primary-secondary distribution systems using mixed integer linear programming. *Power Systems, IEEE Transactions on*, 20(2):1134–1143, 2005.

[64] Y. S. Park, W. T. Kim, and B. K. Kim. State of the art report of Denmark, Germany and Finland. Simple models for operational optimization. Technical report, Department of Mechanical Engineering, Technical University of Denmark, 2000.

[65] K. M. Powell, W. J. Cole, U. F. Ekarika, and T. F. Edgar. Optimal chiller loading in a district cooling system with thermal energy storage. *Energy*, 50:445–453, 2013.

[66] P. Priyadharshini and N. Chitra. Power quality improvement using ant colony optimization based control strategy in an islanded microgrid.

[67] A. Puri. Optimally sizing battery storage and renewable energy sources on an off-grid facility. In *Power and Energy Society General Meeting (PES), 2013 IEEE*, pages 1–5. IEEE, 2013.

[68] M. Reini, D. Buoro, C. Covassin, A. De Nardi, and P. Pinamonti. Optimization of a distributed trigeneration system with heating micro-grids for an industrial area. *Distributed Generation and Alternative Energy Journal*, 26(2):7–34, 2011.

[69] H. Ren and W. Gao. A milp model for integrated plan and evaluation of distributed energy systems. *Applied Energy*, 87(3):1001–1014, 2010.

[70] H. Ren, W. Gao, and Y. Ruan. Economic optimization and sensitivity analysis of photovoltaic system in residential buildings. *Renewable energy*, 34(3):883–889, 2009.

[71] Y. Riffonneau, S. Bacha, F. Barruel, and S. Ploix. Optimal power flow management for grid connected pv systems with batteries. *Sustainable Energy, IEEE Transactions on*, 2(3):309–320, 2011.

[72] A. Rong and R. Lahdelma. An efficient linear programming model and optimization algorithm for trigeneration. *Applied energy*, 82(1):40–63, 2005.

[73] A. Rong, R. Lahdelma, and P. B. Luh. Lagrangian relaxation based algorithm for trigeneration planning with storages. *European Journal of Operational Research*, 188(1):240–257, 2008.

[74] M. Sakawa and T. Matsui. Fuzzy multiobjective nonlinear operation planning in district heating and cooling plants. *Fuzzy Sets and Systems*, 231:58–69, 2013.

[75] M. Sakawa, K. Kato, and S. Ushiro. Operation planning of district heating and cooling plants through genetic algorithms for nonlinear 0–1 programming. *Computers & Mathematics with Applications*, 42(10):1365–1378, 2001.

[76] M. Sakawa, K. Kato, S. Ushiro, and M. Inaoka. Operation planning of district heating and cooling plants using genetic algorithms for mixed integer programming. *Applied Soft Computing*, 1(2):139–150, 2001.

[77] S. M. Sanaei and T. Nakata. Optimum design of district heating: Application of a novel methodology for improved design of community scale integrated energy systems. *Energy*, 38(1):190–204, 2012.

[78] L. Shang and X. Zhao. Biologically inspired optimization of building district heating networks. *TELKOMNIKA Indonesian Journal of Electrical Engineering*, 11(12): 7769–7772, 2013.

[79] D. Sharma, P. Gaur, and A. Mittal. Comparative analysis of hybrid gapso optimization technique with ga and pso methods for cost optimization of an off-grid hybrid energy system. *Energy Technology & Policy*, 1(1):106–114, 2014.

[80] K. Sipilä and S. Kärkkäinen. Demand side management in district heating systems. *Euroheat and Power*, 29(3):36–45, 2000.

[81] J. Söderman. Optimisation of structure and operation of district cooling networks in urban regions. *Applied thermal engineering*, 27(16):2665–2676, 2007.

[82] M. Stadler, C. Marnay, M. Kloess, G. Cardoso, G. Mendes, A. Siddiqui, R. Sharma, O. Mégel, and J. Lai. Optimal planning and operation of smart grids with electric vehicle interconnection. *Journal of Energy Engineering*, 138(2):95–108, 2012.

[83] C. Supriya and M. Siddarthan. Optimization and sizing of a grid-connected hybrid pv-wind energy system. *International Journal of Engineering Science and Technology*, 3(5), 2011.

[84] E. Thorin, H. Brand, and C. Weber. Long-term optimization of cogeneration systems in a competitive market environment. *Applied Energy*, 81(2):152–169, 2005.

[85] N. Tutkun. Minimization of operational cost for an off-grid renewable hybrid system to generate electricity in residential buildings through the svm and the bcga methods. *Energy and Buildings*, 76:470–475, 2014.

[86] T.-M. Tveit, T. Savola, A. Gebremedhin, and C.-J. Fogelholm. Multi-period minlp model for optimising operation and structural changes to chp plants in district heating networks with long-term thermal storage. *Energy Conversion and Management*, 50(3):639–647, 2009.

[87] S. Upadhyay and M. Sharma. Optimization of hybrid energy system for off-grid application. In *Energy Efficient Technologies for Sustainability (ICEETS), 2013 International Conference on*, pages 343–348. IEEE, 2013.

[88] J. Wang, Z. J. Zhai, Y. Jing, and C. Zhang. Optimization design of bchp system to maximize to save energy and reduce environmental impact. *Energy*, 35(8):3388–3398, 2010.

[89] J. Wang, Z. J. Zhai, Y. Jing, and C. Zhang. Particle swarm optimization for redundant building cooling heating and power system. *Applied Energy*, 87(12):3668–3679, 2010.

[90] J.-J. Wang, Y.-Y. Jing, and C.-F. Zhang. Optimization of capacity and operation for cchp system by genetic algorithm. *Applied Energy*, 87(4):1325–1335, 2010.

[91] C. Weber, F. Maréchal, and D. Favrat. Design and optimization of district energy systems. *Computer Aided Chemical Engineering*, 24:1127–1132, 2007.

[92] J. W. Whitefoot, A. R. Mechtenberg, D. L. Peters, and P. Y. Papalambros. Optimal component sizing and forward-looking dispatch of an electrical microgrid for energy storage planning. In *Proc. ASME Int. Design Eng. Tech. Conf. Comput. Inf. Eng. Conf.(IDETC/CIE)*, 2011.

[93] Y.-C. Xu and Q. Chen. An entransy dissipation-based method for global optimization of district heating networks. *Energy and Buildings*, 48:50–60, 2012.

[94] R. Yokoyama, K. Ito, M. Sakashita, Y. Matsumoto, and Y. Yuasa. Multiobjective optimal unit sizing of a grid-connected photovoltaic system in consideration of its probabilistic characteristics. *Journal of solar energy engineering*, 119(2):134–140, 1997.

[95] X. E. Yu, P. Malysz, S. Sirouspour, and A. Emadi. Optimal microgrid component sizing using mixed integer linear programming. In *Transportation Electrification Conference and Expo (ITEC), 2014 IEEE*, pages 1–6. IEEE, 2014.

[96] D. Zelazo, R. Dai, and M. Mesbahi. An energy management system for off-grid power systems. *Energy Systems*, 3(2):153–179, 2012.

[97] L. Zhang, G. Barakat, and A. Yassine. Deterministic optimization and cost analysis of hybrid pv/wind/battery/diesel power system. *International Journal of Renewable Energy Research (IJRER)*, 2(4):686–696, 2012.

[98] Y. Zhang, N. Gatsis, and G. B. Giannakis. Robust energy management for microgrids with high-penetration renewables. *Sustainable Energy, IEEE Transactions on*, 4(4):944–953, 2013.

[99] H. Zhao. *Analysis, modelling and operational optimization of district heating systems*. Centre for District Heating Technology, Laboratory of Heating and Air Conditioning, Technical University of Denmark, DK-2800 Lyngby, Denmark, 1995.

[100] H. Zhao and J. Holst. Study on a network aggregation model in dh systems. *Euroheat and Power*, 27(4-5):38–44, 1998.

# Part II

# Thermal Energy Side Mathematical Programming Applications

# Chapter 5

# Thermal Energy Distribution and District Heating Systems Theory

In this chapter we will discuss the main theory in the field of District Heating and thermal Energy distribution, by introducing the most important hydraulic and thermodynamics concepts that represent the fundamental skills for the mathematical model building. A brief introduction to illustrate the general aspects and state of the art of District Heating Systems will be presented in Section 5.1 followed by a general description of the most important technical aspects in Section 5.2. Section 5.3 will discuss in deep the different network structures and the graph representation of such systems. Then the concept of substation together with the most important thermodynamic theory will be introduced in Section 5.4, while the most important hydraulic theory will be discussed in Section 5.5. Further important concepts that need to be considered when modeling such networks, such as concurrent factor, vertical quota and temperature drops, will be introduced in the last Sections, 5.6, 5.7 and 5.8 respectively.

## 5.1 Introduction

A good energy policy should be focused on two main aspects: the reduction of energy consumption and a better use of the available sources. From this point of view, District Heating (DH) is an important resource to reach environmental sustainability and energy efficiency of modern cities. Broadly speaking, DH is an energy service based on moving heat from available heat sources to immediate use directly by customers. It concerns the centralized production of thermal and possibly electrical energy and its distribution to a network of users, thus obtaining much higher efficiency in the production and maintenance costs with respect to the individual production by the end-users (see, e.g., Gustavsson [3] and Nitsch et al. [6]). It was introduced commercially in the United States in the late nineteenth century and in Europe in the early twentieth century. During the last decades DH has reached a considerable diffusion not only in northern Europe, but also in central and southern European countries, North America and Japan. Just to give an example of the steep trend line of DH systems implementation, in Italy from 2000 to 2010 the number of towns having DH networks increased from 27 to 104, the Km of pipe raised from 1000 to about 3000 and the thermal and electric capacity produced more than doubled reaching 7700 GWh (see EuroHeat and Power [1]). This also correspond to a yearly saving of 1.3 millions of $CO_2$ tons. A similar growing trend can be found in other European nations

(see Table 5.1) and also in other countries such as China - with 147000 Km of pipes and 338 GWth - and Canada, where Dalkia company feeds 19 towns with a total DH extension of 320 millions of $ft^2$ and the Enwave company feeds the city of Toronto with a total DH extension of 40M $ft^2$. For more information about the DH infrastructures diffusion the reader is referred to the survey EuroHeat and Power [1] performed by EuroHeat&Power, the European association of district heating and cooling.

Table 5.1: Development of DH infrastructures in some European countries (source EuroHeat&Power, 2013 survey EuroHeat and Power [1]).

| Country | Served Citizens (%) | Pipelines ($Km$) | Heated Surface ($10^6 m^2$) | Heating Capacity ($MWth$) | Cooling Capacity ($MWth$) |
|---|---|---|---|---|---|
| Austria | 21 | 4,376 | 57 | 9,500 | 35 |
| Denmark | 61 | 30,288 | n.a. | | |
| France | 7 | 3,644 | n.a. | 16,293 | 668 |
| Germany | 12 | 20,151 | 438 | 49,931 | 161 |
| Italy | 5 | 2,951 | 96 | 2,556 | |
| Poland | 5 | 19,286 | 472 | 59,790 | |
| Sweden | 42 | 21,100 | 678 | 15,000 | 650 |

Starting from early infrastructures fed by traditional boilers, the DH networks saw a progressive increase in the complexity of the energy production system, which today are mainly based on modern Combined Heat and Power (CHP) systems with co-generation engines, and in many cases integrate renewable energy sources such as Waste-to-Energy, Solar, Geothermal and Biofuel engines.

The most important physics equations required for the description of the DH network are discussed in the following. For a general introduction to the engineering physics see, e.g., Khare and Swarup [5], while for details on the DH specific characteristics see, e.g., Phetteplace [7].

## 5.2 District Heating Fundamentals

Today the fundamental idea of district heating is to use local fuel or heat resources that would otherwise be wasted, in order to satisfy local customer demands for heating, by using a heat distribution network of pipes as a local market place. Hence, a DH network is made up by three main elements that are, one or more energy production plants that provide cheap heat, a heat market that is represented by a group of final users with heat needs and a network of insulated pipes through which the heat produced in the power plant can be transported to the consumers in the form of hot water or steam. The plants produce hot water at a temperature of 90°C (or even overheated water at the temperature of 120°C). When the hot fluid reaches a user, its heat is transferred to a heat exchanger. The fluid cools down (until a temperature of 60°C) and can flow back to the production plant. The plant then provide warming up the cold water again, so that the cycle can restart. The heat exchanger is a substitute of the classic domestic boiler and it can also produce water for sanitary use. Typically it is assumed that heat exchangers can provide the consumers with hot water at 40°C.

Summarizing, the main elements of a DH system are (see Figure 6.1 for an example):

- One or more plants, where heat energy is produced in order to warm up a heating fluid.
- A group of users, which can be represented by the associated heat exchanger. Each such user $v$ has a power requirement $PI_v$ (expressed in kW). Suitable heating demands are space heating and domestic hot water for residential, public and commercial buildings as well as low temperature industrial heating demands.
- A set of insulated pipes which distribute the heating fluid from the plants towards the users.

These elements should be local in order to minimize the capital investment in the distribution network through the use of short pipes. As explained in Frederiksen and Werner [2], the five current most strategic local heat and fuel resources for district heating are:

- excess heat from thermal power stations (co-trigeneration plants)
- heat obtained from waste incineration
- excess heat from industrial processes and fuel refineries
- fuels that are difficult to handle and manage in small boilers, including most combustible renewables such as wood waste, straw, or olive residues
- geothermal heat sources

The thermal station can be made of simple boilers to produce just heat (see Figure 5.1), or combined plants where the heat production is the waste of the main electrical production (see Figure 5.2). In large district heating networks a common solution is to install a main central plant for the combined production of heat and electricity and some smaller sparse boilers for the heat production in order to cover peak loads. Indicatively we can say that a plant that produces just electrical energy has an efficiency of 35-40%, a thermal power station for the combined production of heat and electricity has an efficiency of 60-70% and a thermal power station that produces both electricity and heat and at the same time can feed up a district heating network has an efficiency greater than or equal to 90%.

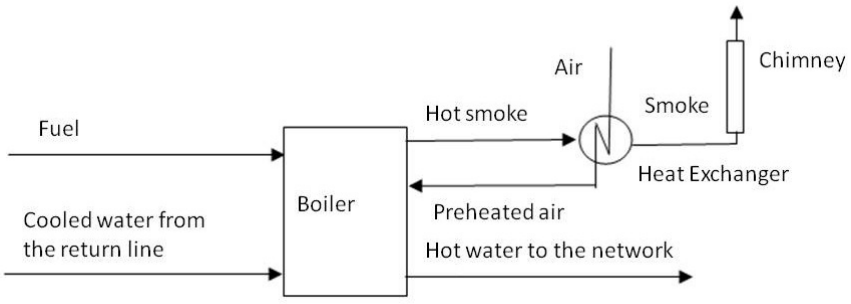


Figure 5.1: Diagram of a simple plant dedicated just to heat production. Adapted from Tarenzi and Ceré [9]

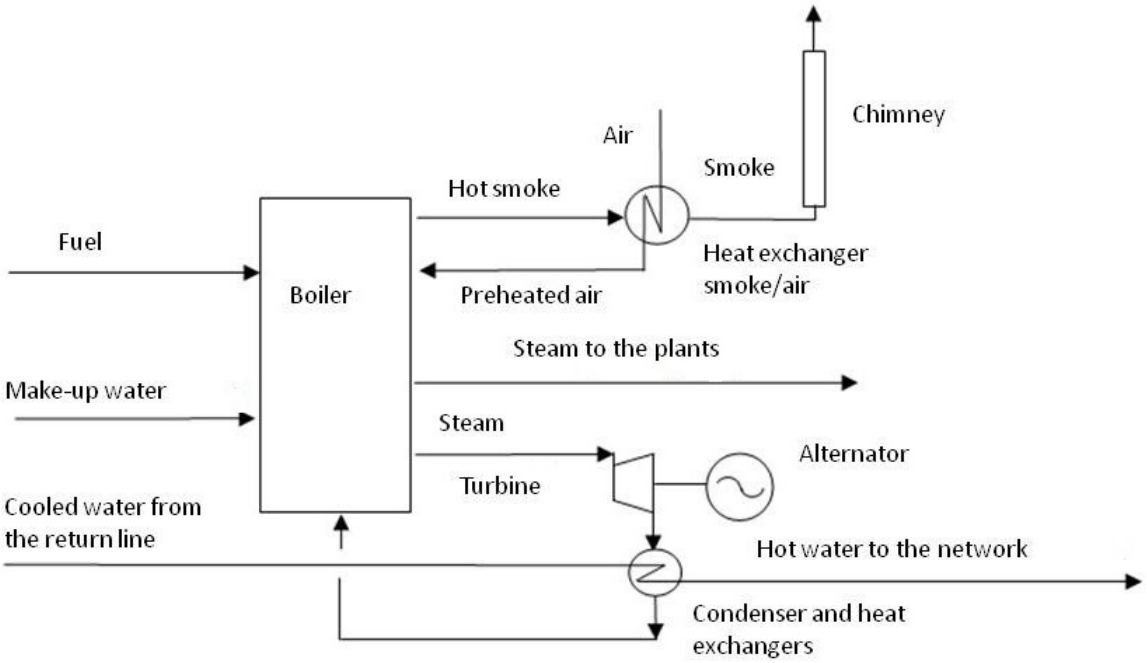


Figure 5.2: Diagram of a CHP plant. Adapted from Tarenzi and Ceré [9]

The heat demands are geographically distributed in an area and their location can be illustrated by a *heat density map* where the heat density is the total heat demand divided by the land area being considered. In such documents the average annual heat density in $kWh/m^2$ for each part of a city is indicated by different colors. The information required are generally obtained through a *Geographical Information System - GIS* which contains detailed information about the heat demands for each building in a urban area. The basic information about the current heat supply contained in a heat density map, can be used to plan and design a district heating network and evaluate the related investment costs. Priority areas for possible district heating delivery are areas that have a heat density over a certain threshold value. A typical threshold value for a feasible district heating is $40 - 50kWh/m^2$.

## 5.3 Networks Structures, Growth Structures and Maps

A network is a set of elements and devices through which the water can be transported among the heating plants and the consumers. It is important to note that the network can be split into two separate parts: the first one is the so-called *feed line*, which contains the set of pipes bringing hot fluid from the plants to the users. The second part is called the *return line*, which includes the pipes bringing cooled down fluid from the users back to the plants. These pipes are usually laid down in pairs, with one feed and the corresponding return pipes, and they share physical properties (such as insulation) and geometric properties (such as diameters and length). Furthermore, the nodes of the network, representing both users' exchangers and points in which the pipes bifurcate or merge, called *tees*, are also considered in couple. In fact, as the pipes, the nodes are strictly connected both from a thermal and from a hydraulic point of view. As a consequence, a topological representation

of a DH network can be obtained by mapping just the feed line.

As shown in Figure 5.3 - 5.6 a district heating network can be described by an oriented graph were arcs represent the network pipes oriented in the flow direction and nodes represent plants, final users and ramification tees. Arcs and nodes of the oriented graph can be associate to the most relevant thermal and hydraulic conditions of the network, in such a way that:

- every node is associate to a temperature (in $^{\circ}K$) and a pressure (in $bar$)
- every arc is associate to a flow mass in the flow direction (in Kg/s), a drop of pressure in the flow direction (in $bar$) and a drop of temperature (in $^{\circ}K$)

It is important to remember that these variables are required both for the feed line and for the returns line.

Every existing network structure is the result of a growth process. Four main stages of growth can be identified in the development from small to large systems.

A single grid with a tree structure is initially established (Figure 5.3). The tree structure implies that only one line can be drawn to anyone of the connected buildings from a heat supply plant. The flow direction is unique, from the main heat supply plant (black pentagon) to the final users connected. Generally after the first stage, few additional smaller independent grids provided with smaller boilers (gray pentagons) can start to develop in other parts of the city, initially to serve just small groups of similar buildings.

The second stage (Figure 5.4) is the one in which one or more of the smaller grids of the first stage will be interconnected to the central grid, which has a base load plant. The structure is still a tree one, even though larger and more complex. In this case the flow direction isn't unique anymore, as the presence of more than one plant in different nodes of the graph can create different operational conditions with different flows along the network.

At a third stage (Figure 5.5) of development certain pairs of feed and return pipes will be interconnected, initially between two of the largest branches, to form a ring. The pure tree-structure is abandoned and more ends are connected establishing a ring of significant diameter. In this case flow direction along pipes can vary as well.

The last stage (Figure 5.6) is the one in which the structure design grows further and the network complexity becomes higher as more branch ends will become interconnected creating a meshed structure feed up by multiple heat supply plants. Distribution pipes will generally follow the street map, although the street map will remain more fully meshed.

With respect to the size and local conditions there are five typical network structures as described in Frederiksen and Werner [2]. As depicted in Figure 5.7, smaller systems are generally based on a network with one central location where all heat supply units are concentrated at one site (network A). In this case the distance between the heat supply plant and each substation is short. In medium sized systems decentralized peak load plants can complement the central base load plant, allowing the reduction of the pipe diameters from the base load plant (network B). At lower heat loads the whole network is supplied from the central base load plant, while at higher heat loads the peak plants will handle the peripheral parts of the city and the base load plant will only supply its own local neighbourhood. Sometimes large CHP plants are situated at a significant distance from the central parts of a city for many reasons (i.e. minimize the environmental impact) while the peak load plants are located in the city area. In this case a transmission pipeline is required to connect the base load with the general grid (network C). Other types of

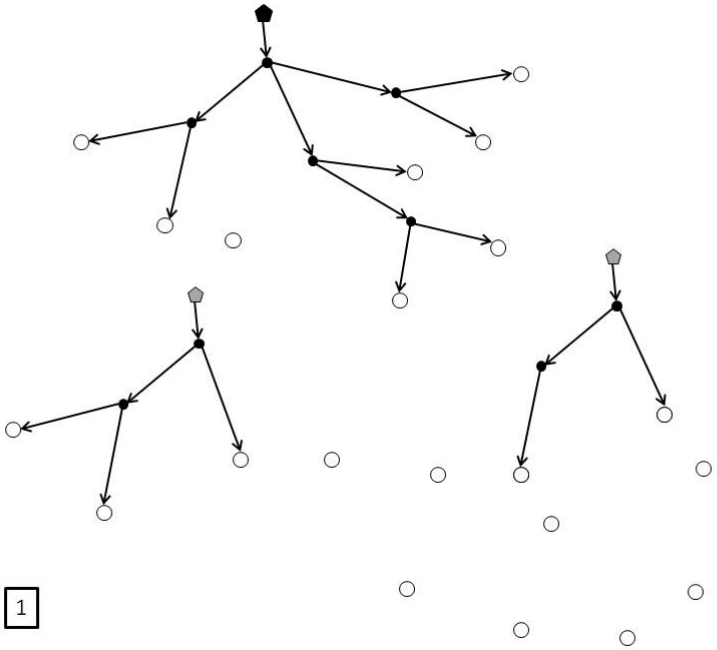


Figure 5.3: First stage of development for a district heating network with a basic tree structure for smaller areas. Adapted from Frederiksen and Werner [2]

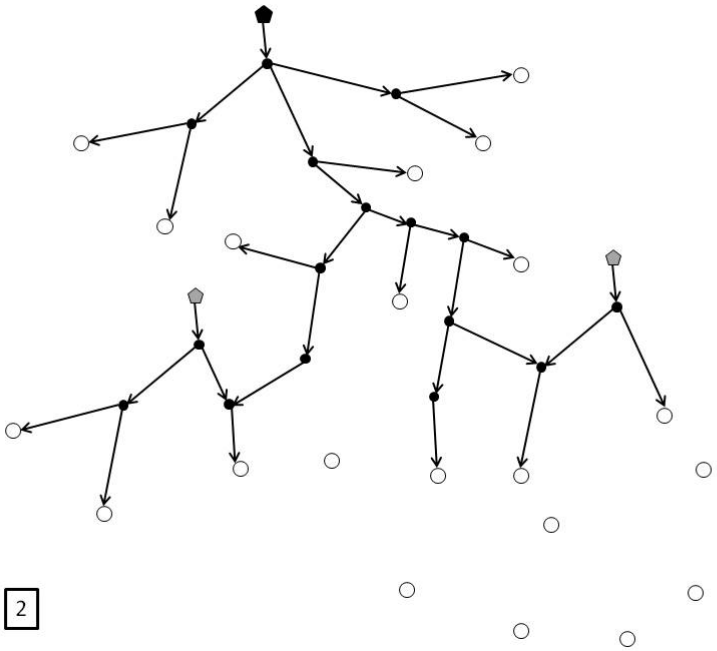


Figure 5.4: Second stage of development for a district heating network with an extended tree structure. Adapted from Frederiksen and Werner [2]

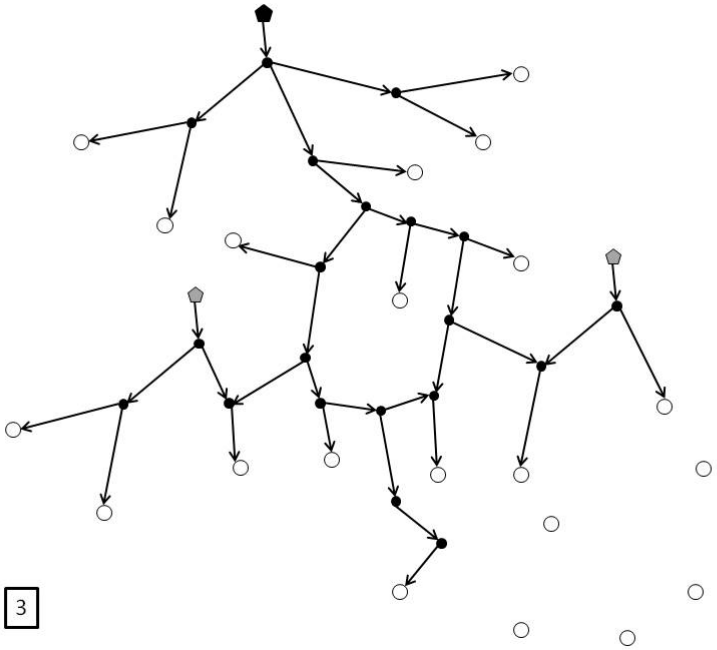


Figure 5.5: Third stage of development for a district heating network with ring formation. Adapted from Frederiksen and Werner [2]

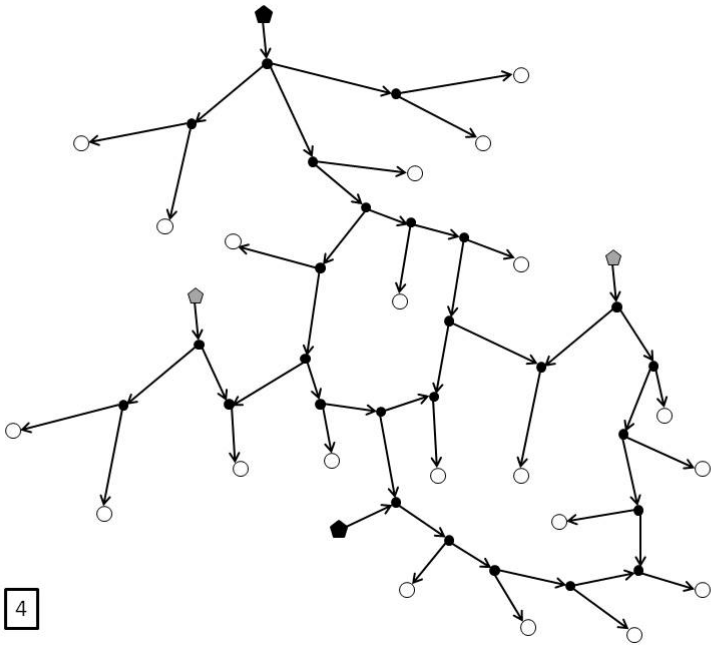


Figure 5.6: Fourth stage of development for a district heating network with meshed structure. Adapted from Frederiksen and Werner [2]

networks contain several base load plants. These plants can be connected to one central heat transmission pipe maintaining a tree structure (network D) or, in cities with more than one million inhabitants there can be large integrated networks where each major part of the city has its own base load plant and creating a fully meshed structure as depicted in Figure 5.6.

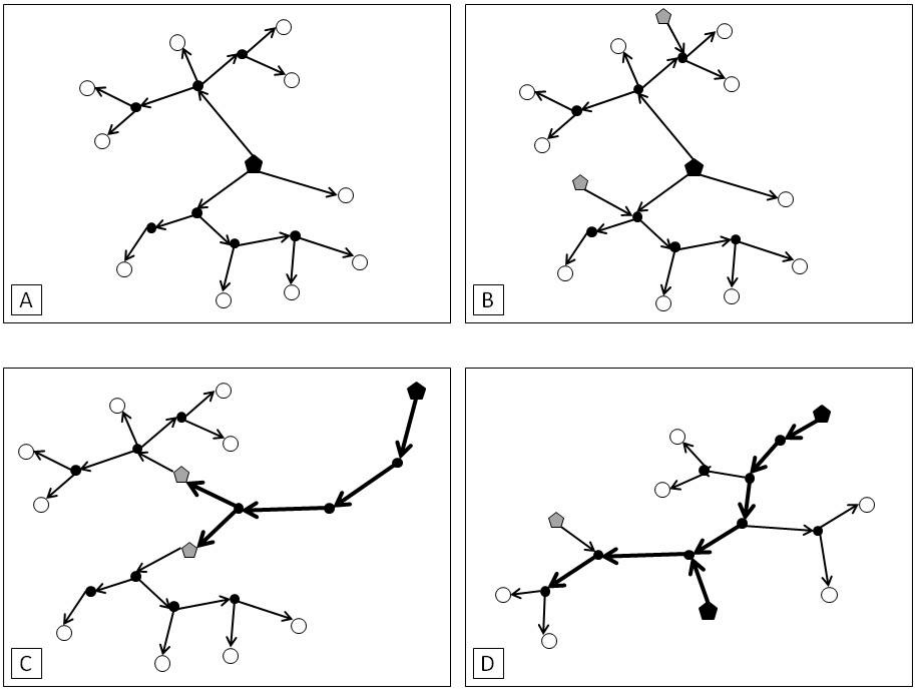


Figure 5.7: Different typical network structures. One central base load (A), one central based load with peripheral base loads (B), one common transmission pipe (c) and peripheral decentralized base loads (D). The black and gray pentagons represent the base load plant and a peak load plant respectively. Adapted from Frederiksen and Werner [2]

## 5.4 Substations

In district heating the concept of substation is similar to the same concept adopted in electrical power engineering. A substation can be defined as a unit in which the type of energy being distributed is transformed from a higher to a lower level, in terms of one or more characteristic energy-related parameters. In electric power substations the voltage level is lowered, while in district heating substation temperature and pressures are lowered, in order to permit the use of less expensive equipment within buildings without risking malfunctions or accidents. Hence, through the substation the energy transfer can be interrupted in case of a disturbance or repair. Most of district heating substations are specific to each building being served and are usually placed inside of these buildings (i.e. house substations). Sometimes lowering of temperature and pressure is carried out also in area substations within a network, to serve a local distribution network. At the other extreme there are flat substations or apartment substations, one for each flat.

In district heating substations, the key elements are heat exchangers, equipments through which it is possible to exchange thermal energy between fluids at different temperatures. Broadly speaking, in a district heating system, the heat exchangers are made of a primary circuit through which the hot fluid from the district heating network feed line flows, and a secondary circuit through which a cooler fluid from the connected users flows. The circuits are close each other so that when the two fluids with different temperatures flows along them, they can exchange their thermal energy. This way the cool fluid from the users will heat up taking the heat from the hot fluid that comes from the feed line of the district heating network. Hence the hot fluid will cool down and will come back to the heat plant through a return line to be heated again and restart the cycle. Figure 5.8 shows a schematic representation of a final user substation.

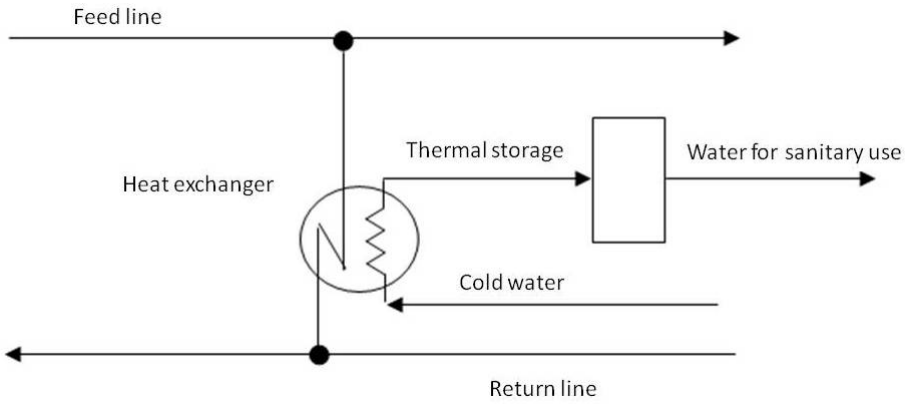


Figure 5.8: Schematic representation of a final user substation with heat exchanger

The heat exchanger work can be mathematically described by two main thermodynamics equations.

The first equation relates the final user heat loads, the fluid flow rate and the temperature gradient as follows:

$$Q = \dot{m} * c_p * \Delta T \tag{5.1}$$

where $Q$ is the heat (W), $\dot{m}$ is the fluid flow rate along the primary circuit of a heat exchanger, (kg $s^{-1}$), $c_p$ is the water specific heat evaluated in constant pressure conditions (kJ $kg^{-1}$ $K^{-1}$ or kcal $kg^{-1}$ $C^{-1}$ where $1kcal = 4,18kJ$) and $\Delta T$ is the thermal gradient defined among feed line and returns line (K)
The equation (5.1) is a general one and derives directly from the first law of thermodynamics, which is usually formulated by stating that the change in the internal energy of a closed system is equal to the amount of heat supplied to the system, minus the amount of work performed by the system on its surroundings.

The water specific heat is a function of the temperature and the pressure. As the pressure dependence is very limited, it is generally defined in constant pressure conditions. As for the temperature relationship, an example of this is given by Figure 5.9. In district heating systems planning and operational management it can be assumed that the water specific heat is a constant value. In particular, in our study we will assume $c_p = 4,18$ kJ $kg^{-1}$ $K^{-1}$

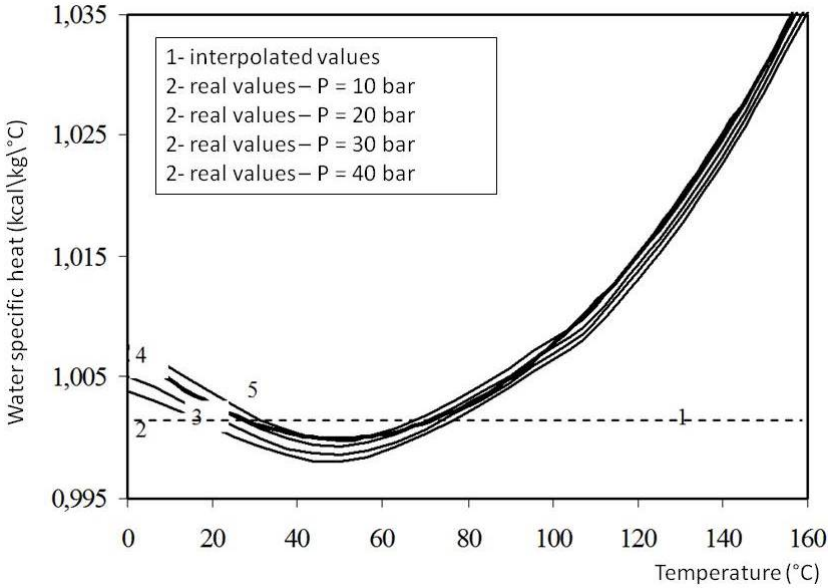


Figure 5.9: Water specific heat trends as a function of the temperature and pressures.

The behavior of a generic heat exchanger is instead described by the following relation that relates the technical properties of the particular heat exchanger that is being inserted:

$$Q = U * A * \Delta T_{ml} \tag{5.2}$$

where $U$ is the overall heat transfer coefficient (in W/(m$^2$* K)), $A$ is the heat transfer surface area (m$^2$) and $\Delta T_{ml}$ is the log mean temperature difference (in $^\circ K$). The equation (5.2) is a specific one and defines a generic heat exchanger, whose heat transfer rate is equal to the product of an overall heat transfer coefficient (that characterizes a particular heat exchanger), a heat transfer surface area and the log mean temperature difference of the heat exchanger itself. As previously outlined, inside the heat exchanger, there are two different flows: one is the heat transfer fluid which flows along a hydraulic circuit called the *primary circuit*; the other one is the cooled down water which flows along another circuit called the *secondary circuit*. This second type of flow has to be warmed up by the hottest fluid of the primary circuit. The log mean temperature difference factor $\Delta T_{ml}$ includes both the input temperature of the hottest flow (flowing along the primary circuit) and the input temperature of the warmest flow (flowing along the secondary circuit) together with the relative output temperatures.

## 5.5 Pumps and Flow Distribution

In addition to the relations introduced before, it is also important to consider friction losses along the pipes and flow rate constraints, defined by the water requirement of the users. As can be seen in the following equations 5.3 and 5.5 the pressure drop is proportional to the square of the water speed $v$. At the same time the water speed is proportional to the square root of the pressure difference. Hence, in order to get a double water flow in a pipe, it is necessary to provide a pressure difference that is four times as great as the current

pressure difference between the inlet and the outlet of the pipe. This pressure difference is provided by circulations pumps positioned in the closed circuit of feed and return pipes. Figures 5.10 and 5.11 show examples of different pressure drop trends for different pipes inner diameter as a function of the water flow rate. According to the UK/US notation, in the figures pressure drops are defined in *pound per square inch* (*psi*) that corresponds to 0.0689 bar, while the flow rate is expressed in *gallons per minute* (*gpm*) that corresponds to 0.063 $kg/sec$ and the pipe diameters are expressed in inch that corresponds to 2.54 cm. These are examples of diagrams provided by manufacturers to assist technicians in the network design of district heating networks.

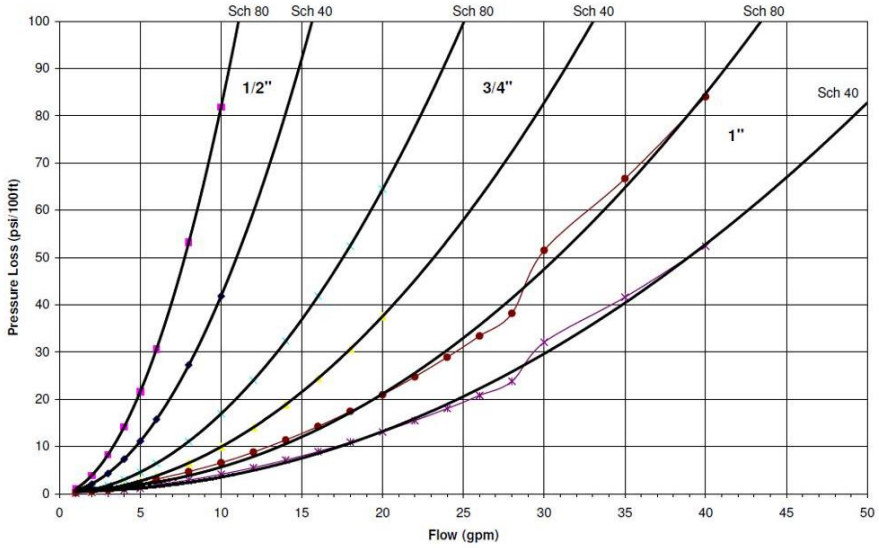


Figure 5.10: Steel Pipe Pressure Loss: 1/2" to 1" Chart - Information chart assists in determining pressure loss (psi per 100 LF) for 1/2", 3/4" and 1" diameter steel pipes at flows from 0 to 50 gpm. Data distributed online by Industrial Equipment *www.industrial-equipment.biz*

According to basic fluid mechanics, the pressure losses in turbulent flow conditions, in the flow direction in a circular pipe, can be formulated as a sum of two terms: *localized pressure losses* $\Delta P_c$ and *distributed pressure losses* $\Delta P_d$.

$$\Delta P = \Delta P_c + \Delta P_d \tag{5.3}$$

Distributed pressure losses $\Delta P_d$ are due to the viscous friction in turbulent flow conditions. Broadly speaking, the flow along a pipe can be of two types, laminar flow and turbulent flow. Laminar flow occurs when a fluid flows in parallel layers, with no disruption between the layers, while turbulent flow is a chaotic flow regime that is charachterised by eddies or small packets of fluid particles which result in lateral mixing. In the first case the fluid speed is very low and the viscous force prevail on the inertia force. In the second case the fluid speed is very high with an inertia force that prevails on the viscous one. In a standard operational regime a district heating network is characterised by turbulent flows. If a pipe has a laminar flow that means the pipe has been over sized for that particular operational conditions.

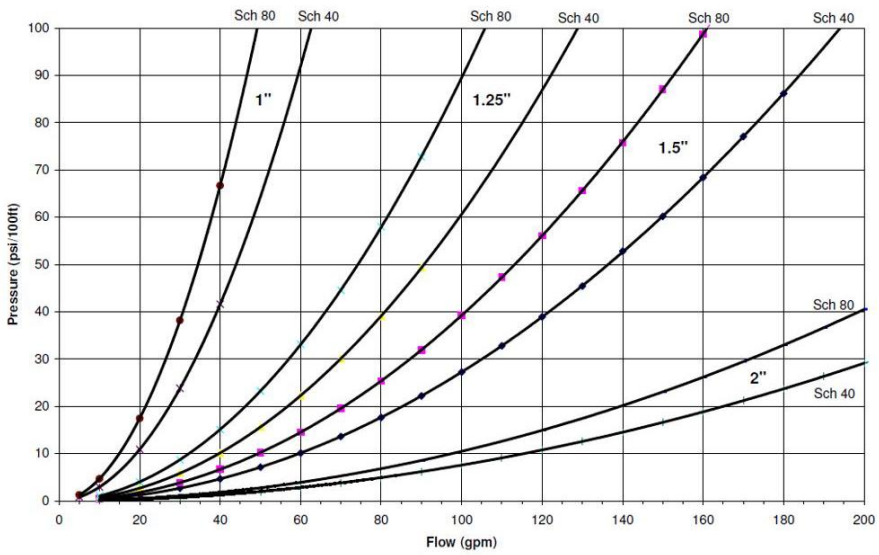


Figure 5.11: Steel Pipe Pressure Loss: 1" to 2" Chart - Information chart assists in determining pressure loss (psi per 100 LF) for 1" , 1-1/4", 1-1/2" and 2" diameter steel pipes at flows from 0 to 200 gpm. Data distributed online by Industrial Equipment *www.industrial-equipment.biz*

Localized pressure losses $\Delta P_c$ are due to the presence of junction elements and devices along the network such as angle pipes, T-joints, increasing or decreasing pipe dimensions, filter, valves etc. It is generally very difficult to determine such losses in an experimental way, however, localized pressure losses are considerably lower than the distributed ones, hence, also an approximation of the 20% can be enough. A localized losses coefficient is generally defined for every particular type of element of the network. Figures 5.12, 5.13, 5.13 and 5.14 shows example of such junction elements.

In particular, the values of localized and distributed pressure losses can be derived by fluid dynamics formulations as follows:

$$\Delta P_c = 0.5 * \xi * \rho * v^2 \tag{5.4}$$

$$\Delta P_d = 0.5 * f * L * \rho * v^2 * D^{-1} \tag{5.5}$$

where:
$\xi$ is the localized losses coefficient ($dimensionless$)
$\rho$ is the water density ($kg/m^3$)
$v$ is the water speed ($m/s$)
$f$ is the friction factor ($dimensionless$)
$D$ is the pipe inner diameter ( $m$)
$L$ is the pipe length ($m$)
The water speed $v$ is defined as $v = \dot{m} * (\rho * a)^{-1}$ where $\dot{m}$ is the water flow rate in $kg/s^{-1}$ and $a$ is the circular pipe area $\pi * (D/2)^2$. Hence, the equation 5.5 can be rewritten as:

$$\Delta P_d = 8 * f * L * D^{-5} * \pi^{-2} * \rho^{-1} * \dot{m}^2 \tag{5.6}$$

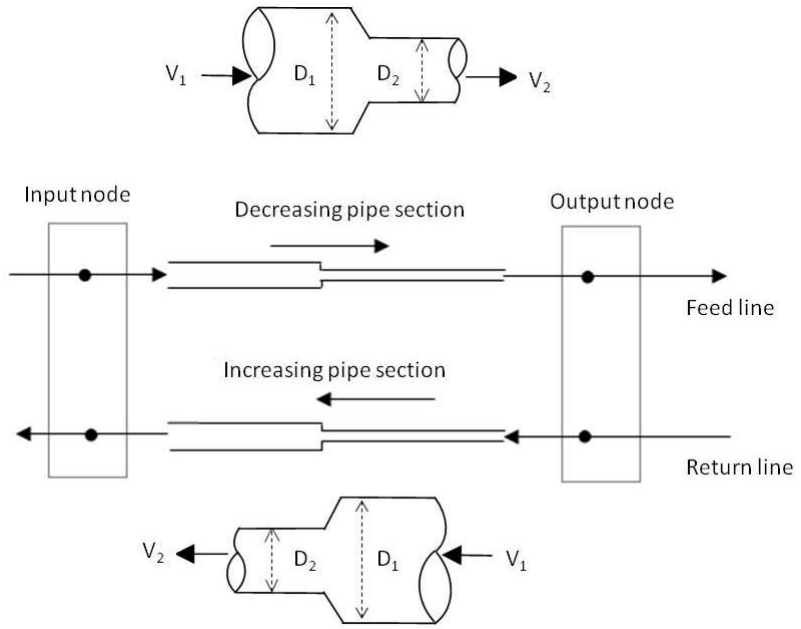


Figure 5.12: Schematic representation of increasing and decreasing pipe sections and their symmetrical integration both in the feed and return line. A decreasing pipe section in the feed line has an equal decreasing section in the return line with the opposite flow direction. Adapted from Tarenzi and Ceré [9]

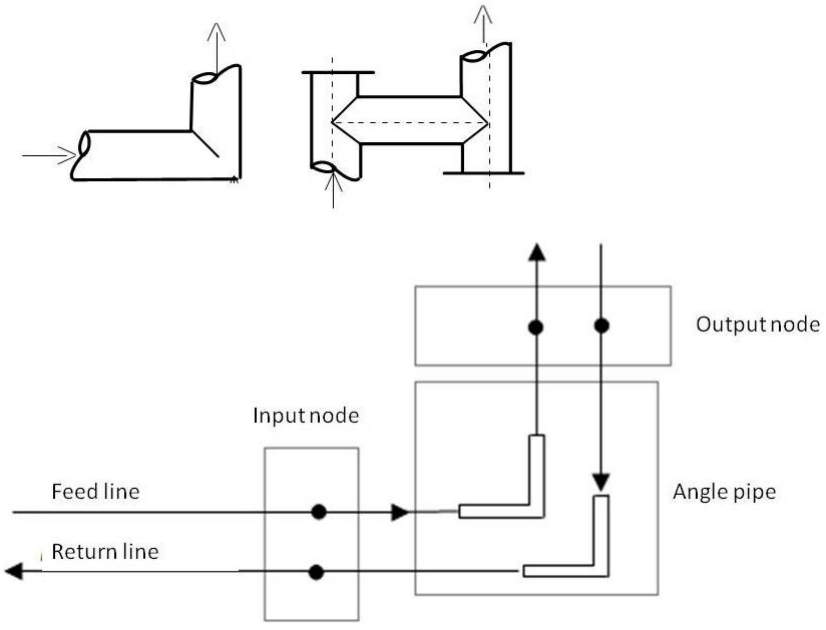


Figure 5.13: Schematic representation of an angle joint and its symmetrical integration both in the feed and return line. Adapted from Tarenzi and Ceré [9]

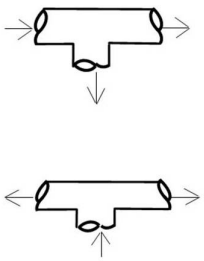

Figure 5.14: Schematic representation of a T joint and possible flows throughout it

The equation 5.5 is the Darcy Weisbach law, which refers to the distributed pressure losses due to viscous friction in turbulent flow conditions. The expression contains the geometric properties of the pipe, the physical properties of the fluid and the Darcy friction factor. There are different formulation of the Darcy friction coefficient, obtained in an experimental way in different conditions, however every formulation is always related to the inner pipe diameter, the inner pipe surface roughness and the Reynolds number (which is a dimensionless number used to define the flow motion). In particular, the friction factor increases with the increasing roughness of the inner pipe surface. The Moody diagram presented in Figure 5.15 shows the dependence of the friction factor on the Reynolds number and the pipe roughness. Fortunately friction factor values do not increase dramatically with surface roughness, hence in practice, there is no need to use detailed friction factors in the pressure drops calculations. Generally system friction factors are defined through a comparison between a computerized simulation and an actual measured pressure drop in an entire system. The system friction factor is identified as the friction factor in the calculation that gives the same pressure drop as that being measured.

In our study we will refer to the following definition of the friction coefficient $f$:

$$f = 0.07 * Re^{-0.13} * D^{-0.14} \tag{5.7}$$

where $Re$ is the Reynolds number and $D$ is the pipe inner diameter.

Through proper algebraic manipulation we can approximate the pressure loss as a function of the fluid flow rate as follows

$$\Delta P = \Delta P_c + \Delta P_d = K_1 \cdot \dot{m}^2 + K_2 \cdot \dot{m}^{1.87} \tag{5.8}$$

where $K_1$ and $K_2$ are empirical coefficients derived by the hydraulic equations discussed above. They depends on the specific characteristics of the pipe, such as its diameter and length, and properties of the fluid as previously described.

As the equation 5.6 shows, the pressure drop is inversely proportional to the fifth of the power of the pipe diameter. That means the pressure drop increases significantly when the next narrower pipe dimension is chosen. This makes the incremental network design of a district heating network a true challenge, as the final users to be connected to an existing network have to be chosen very carefully, taking into consideration not only the economical aspects, but also the more important hydraulic constraints due to pressure drops issues.

In fact one of the main issues of companies involved in the district heating management, is related to the incremental network design. The commercial department can make deep analyses to define the optimal set of new users from an economic point of view (profit

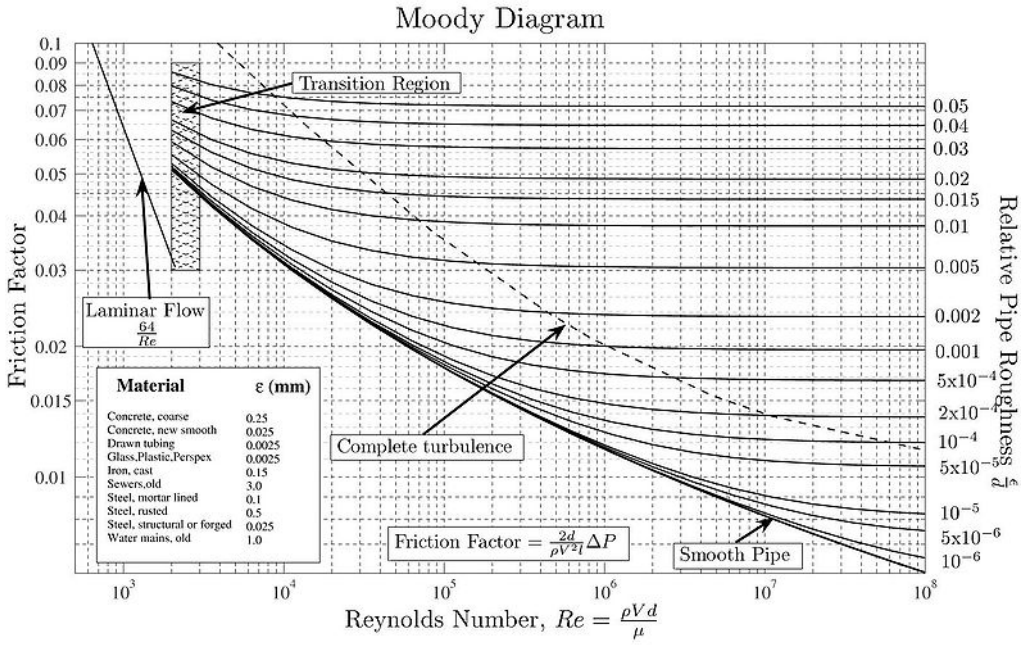


Figure 5.15: Friction factor as a function of the Reynolds number and the inner pipe surface roughness in a circular pipe

maximization), but it can happen that the suggested connections will not be practically feasible from a physical point of view, or they will require important improvement and modifications of the existing network in order to be realized. In such cases the company is going to face very high unexpected expenses. From that point of view the operational research techniques can offer a holistic approach to the problem, more suitable to better integrate the economical and technical requirements of such analyses.

Since the heat-transfer fluid loses pressure along the pipes because of the above mentioned localized and distributed pressure drops, the fluid pressure decreases gradually from the plants towards the users and from the users back to the plant. That means that such networks always present at least one point in the feed line corresponding to the minimum value of pressure and this point is typically associated with a user. The fluid flow along the return line has an opposite direction but same value of flow rate, while the pressure drop along the return line has an opposite sign and slightly larger value due to the lower temperature of the fluid that increases its kinematic viscosity.

Furthermore, note that when we have a single plant serving the network, it is clear that at the plant connection with the feed line we have the highest pressure in the network, while at the connection of the plant node on the return line with have the lowest pressure. As a consequence, the plant is the point with the highest pressure drop between feed and return lines and these consideration can be extended also in the case where we have multiple plants. Pressure at the plants has to be monitored and kept within specific ranges so as to permit the fluid flow and be compatible with the required pumping system.

## 5.6 Concurrent Factor

The final user demand, especially the residential users one, is extremely discontinuous. The higher the number of consumers is, the lower is the probability that all the users requirements will be simultaneously at the maximum value. If the network is planned supposing that every user consumption will be equal to the medium value of all users' needs, then the network will be undersized. That means that in this case the network will not be able to guarantee the amount of heated water corresponding to a peak request. On the other hand, if the network is planned to satisfy the maximum contemporary request of all users', then the network will be extremely over sized. Hence, one of the most common tricks used in such systems is the concepts of *concurrent factor*. The *concurrent factor* can be defined as the ratio between the actual maximum number of users and the theoretical maximum number of users. The latter is defined as the summation of the maximum heat requirements of all the currently connected users (or alternatively, in incremental network design, the maximum heat requirements of all the users that will be presumably connected to the grid is considered). The *concurrent factor* is a function of the type and number of consumers and it decreases as the the number of consumers increases. It is used to reduce the peak demand of each user. Such a reduction of the demand is practically used to reproduce the fact that not all users are actually requesting the heat concurrently and, as a consequence, it is feasible to define the network capacity taking into account just a fraction of the total demand of the users.

## 5.7 Vertical Quota

There are some implications related with the unevenness of the vertical quota of the pipes that need to be briefly outlined for further information.

Let us consider an ideal fluid that moves along a pipe represented in Figure 5.16.

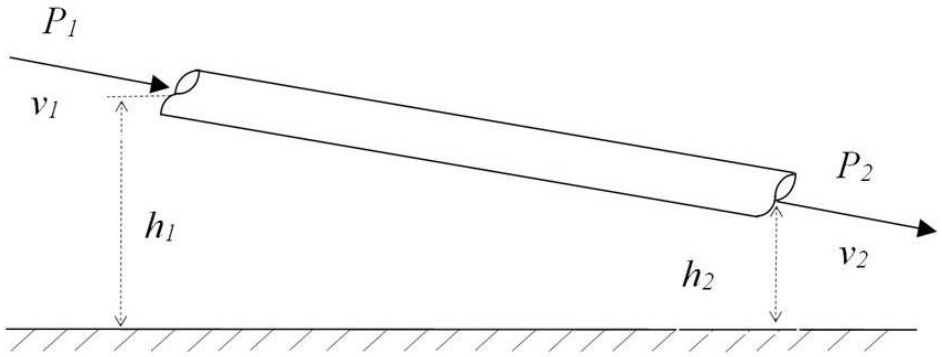


Figure 5.16: Pipe and vertical quota representation. Source Tarenzi and Ceré [9]

Under the ideal fluid assumptions, the specific volume of the fluid is constant and there no frictions inside it or between it and the pipe layer. If the pipe diameter is constant, then the fluid speed in input is equal to fluid speed in output $v_1 = v_2$

The Bernoulli equation (Schaschke [8]) applied to the pipe ends can be therefore written as follow

$$\frac{P_1}{g * \rho} + h_1 = \frac{P_2}{g * \rho} + h_2 \tag{5.9}$$

Let us define the parameters as follow
$h_1$, $h_2$ are the vertical quota $(m)$
$P_1$, $P_2$ are the pressures $(kg/cm^2)$
$g * \rho$ is the specific weight $(kg/m^3)$

Then the equation becomes

$$h_1 + 10000 * \frac{P_1}{\gamma} = h_2 + 10000 * \frac{P_2}{\gamma} \tag{5.10}$$

In the case of a real fluid it is necessary to take into consideration the friction losses due to the fluid viscosity, hence the hydraulic load will drop in the flow direction.

The equation 5.9 for a real fluid becomes

$$h_1 + 10000 * \frac{P_1}{\rho} = h_2 + 10000 * \frac{P_2}{\rho} + \sum \lambda \tag{5.11}$$

where $\sum \lambda$ represents the summation of the overall losses due to frictions.

$\sum \lambda$ is generally defined as $J * L$ where $J$ is the energy lost per every unit of length and $L$ is the length of the pipe.

Broadly speaking, the effect of different vertical quotas at the ends of the pipe involves changes in the pressures behavior. If the pipe rise then the pressure value tends to decrease of 0,0980665 bar.

## 5.8 Pipes Insulation and Temperature Drops

District heating pipes are always insulated and often underground. This section will briefly introduce the most important concepts and formulas with regard to insulation and temperature drops. Figure 5.17 shows the main mathematical notation for an insulated pipe (above) and for the pipe itself underground (below).

The overall *thermal resistance* of a pipe is the summation of four different kinds of thermal resistance: water/pipe thermal resistance, pipe thermal resistance, insulation layer thermal resistance and insulation/air thermal resistance.

It is important to note that the pipe thermal resistance and the water/pipe thermal resistance are quite small and can be overlooked while the insulated layer thermal resistance is definitely prevalent. As for the insulation/air resistance due to the convection phenomenas, this is smaller than the latter one, but there are cases in which it can't be overlooked. With such assumptions, the overall thermal resistance $R_{tot}$ $(m\ ^\circ C\ h\ /\ kcal)$ can be written as follow:

$$R_{tot} = R_{is} + R_{conv} \tag{5.12}$$

The values of $R_{is}$ and $R_{conv}$ come from the fundamentals of thermal and fluid engineering that can be found in many books such as Kaminski and Jensen [4].

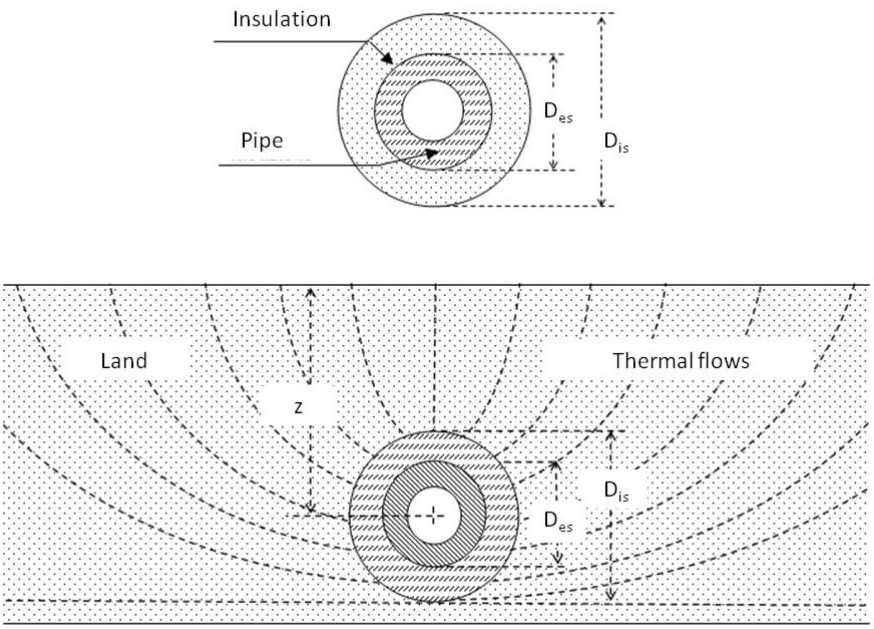


Figure 5.17: Insulation of a pipe (above) and insulation of an underground pipe (below). Source Tarenzi and Ceré [9]

In particular the insulation thermal resistance $R_{is}$ is defined as follow

$$R_{is} = \frac{1}{2 * \pi * \lambda_{is}} * ln\left(\frac{D_{is}}{D_{est}}\right) \tag{5.13}$$

The insulation/air thermal resistance $R_{conv}$ due to convection phenomenas is instead defined as follow

$$R_{conv} = \frac{1}{\pi * D_{is} * k_{is-air}} \tag{5.14}$$

where
$\lambda_{is}$ is the insulation thermal conductivity ($kcal$ / $m$ $h$ $°C$)
$k_{is-air}$ is the heat transfer coefficient insulation/air ($kcal$ / $m^2$ $h$ $°C$)
$D_{est}$ is the outer diameter of the pipe ($m$)
$D_{in}$ is the inner diameter of the insulation layer ($m$)

With regard to the underground pipes, they are both insulated and protected by a further cover to be positioned underground. The overall thermal resistance is the summation of five thermal resistances: the water/pipe thermal resistance, the pipe thermal resistance, the insulation layer thermal resistance, the soil thermal resistance and the soil/air thermal resistance.

It can be assumed that the insulation layer thermal resistance and the soil thermal resistance are definitely prevalent.

Hence in this case the overall thermal resistance $R_{tot}$ ($m\ °C\ h\ /\ kcal$) can be defined as follow

$$R_{tot} = R_{is} + R_{terr} \tag{5.15}$$

The insulation layer thermal resistance $R_{is}$ has been already defined in formula 5.13. The soil thermal resistance $R_{terr}$ comes from the fundamentals of thermal and fluid engineering as well (i.e. Kaminski and Jensen [4]) and is defined in $m\ °C\ h\ /\ kcal$ as follow

$$R_{terr} = \frac{1}{2 * \pi * \lambda_{soil}} * ln\left(\frac{2 * z}{D_{is}} + \sqrt{\left(\frac{2 * z}{D_{is}}\right)^2 - 1}\right) \tag{5.16}$$

where
$\lambda_{soil}$ is the soil thermal conductivity ($kcal/\ m\ h\ °C$)
$z$ is the pipe depth ($m$)

We can finally define the most important equations for the calculation of the water temperature right outside a pipe. Let us consider a pipe fragment of $dx$ lenght as depicted in Figure 5.18

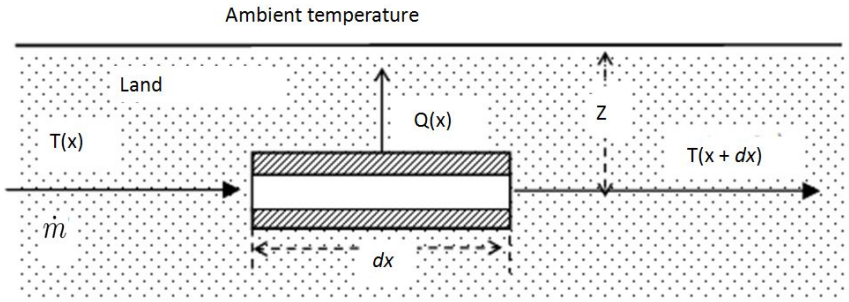


Figure 5.18: Water temperature outside a pipe. Source Tarenzi and Ceré [9]

In perfect thermal equilibrium conditions the heat losses along a pipe fragment can be defined in $kcal/m/h$ as follow

$$Q(x) = \frac{T(x) - T_{amb}}{R_{tot}} \tag{5.17}$$

where
$Q(x)$ is the heat exchanged for every unit of length and for every unit of time ($kcal/m/h$)
$T(x)$ is the pipe temperature on the $x$ coordinate ($°C$)
$T_{amb}$ is the ambient temperature ($°C$)
$R_{tot}$ is the pipe/soil thermal resistance per every unit of length ($°C\ m\ h\ /kcal$)

The enthalpy balance along the fragment $dx$ is defined as follow

$$3600 * \dot{m} * c_p * \frac{dT(x)}{dx} = -Q(x) \tag{5.18}$$

where $c_p$ is the water specific heat in $kcal/\ kg\ ^\circ C$ and $\dot{m}$ is the water flow rate.

It is then possible to insert in the 5.18 the value of $Q(x)$ found in 5.17 and make the integral for $x$ getting the following formulation

$$T(x) = T_{amb} + (T_{in} - (T_{amb}) * e^{-\frac{x}{3600 * \dot{m} * c_p * R_{tot}}} \tag{5.19}$$

By imposing $x = L$ it is possible to get the water temperature outside the pipe fragment of length $L$

$$T_{out} = T(L) \tag{5.20}$$

where

$T_{in}$ is the water temperature in input ($^\circ C$)

$T_{out}$ is the water temperature in output ($^\circ C$)

# Bibliography


[1] EuroHeat and Power. District heating and cooling country by country survey 2013, 2013. available at www.euroheat.org.

[2] S. Frederiksen and S. Werner. *District heating and cooling.* Studentlitteratur, 2013.

[3] L. Gustavsson. Biomass and district-heating systems. *Renewable Energy*, 5(5–8):838–840, 1994.

[4] D. A. Kaminski and M. K. Jensen. *Introduction to thermal and fluids engineering.* Wiley New York, 2005.

[5] P. Khare and A. Swarup. *Engineering Physics, Fundamentals and Modern Applications.* Jones & Bartlett Learning, 5 Wall Street, Burlington, MA 01803, 2009.

[6] J. Nitsch, W. Krewitt, and O. Langniss. Renewable energy in europe. In *Encyclopedia of Energy*, chapter 4, pages 313–331. Elsevier, 2004.

[7] G. Phetteplace. Optimal design of piping systems for district heating. Technical report, DTIC Document, 1995.

[8] C. Schaschke. *Fluid mechanics: worked examples for engineers.* IChemE, 2005.

[9] V. Tarenzi and A. Ceré. *Calcolo del regime stazionario di una rete di teleriscaldamento.*

# Chapter 6

# MILP models for the District Heating Incremental Network Design

This chapter will focus on mathematical modeling formulations for the District Heating design and incremental design problems, with particular regard to instances characterized by big networks dimensions. The chapter is organized as follows. A brief introduction to the problem and research motivation will be presented in Section 6.1. In Section 6.2 we discuss a brief literature review about optimization techniques applied to the District Heating (DH) Network Design field. Section 6.3 will present the main assumptions used to build an optimization model for the DH incremental network design problem. The mathematical model developed for supporting DH system optimal planning is described in Section 6.4. The computational testing of the model on large-scale randomly generated networks is presented in Section 6.6, while Section 6.7 draws some conclusions and illustrates possible future developments of the model.

## 6.1 Introduction

The main aim of this chapter is to show how mathematical optimization techniques developed within operations research may offer appropriate methods to support planning and management activities in the DH field. In particular, we focus our research on finding a viable quantitative methodology to support strategic decisions and commercial policies related to the connection of new users to an existing DH network. The resulting optimization problem is modeled through the application of graph theory and integer linear programming paradigms.

To better explain the problem we study, let us consider Figure 6.1 which depicts a simple DH network whose nodes and links are associated with the following elements: one plant (represented by node 1), a set of existing users already connected to the network (i.e., nodes 4, 7 and 13), a set of potential users that can be connected to the network in the future (i.e., nodes 10, 11 and 12), a set of pipes which connect the existing users (i.e., the links in solid lines) and a set of potential pipes (i.e., the links in dashed lines) which might be lied down when potential users are connected to the network.

Our strategic network design problem aims at deciding which potential users can be connected to the network in order to maximize the overall profit for the energy provider,

while respecting the physics and hydraulic operational conditions of the system. The optimal solution of such a problem is then obtained by constructing a graph representation of the DH network and considering an integer linear programming model which is then solved through a commercial solver.

Our research was motivated by the *Innovami* project financed within the regional program *PRRIITT*, activated by Emilia-Romagna regional authority to promote and support industrial research, innovation and technology transfer. During the project a prototype of the model presented hereafter was developed in collaboration with a local utility company and tested on a small-scale realistic network. Following the positive evalutation by practitioners the model was further extended in partnership with Optit, a spinoff company of the University of Bologna, making it possible to solve large-scale networks. The model represents the main hydraulic constraints of the real-world networks and constitutes an effective compromise between the accuracy of representation of physical behaviour and the capability of handling realistic instances of the problem.

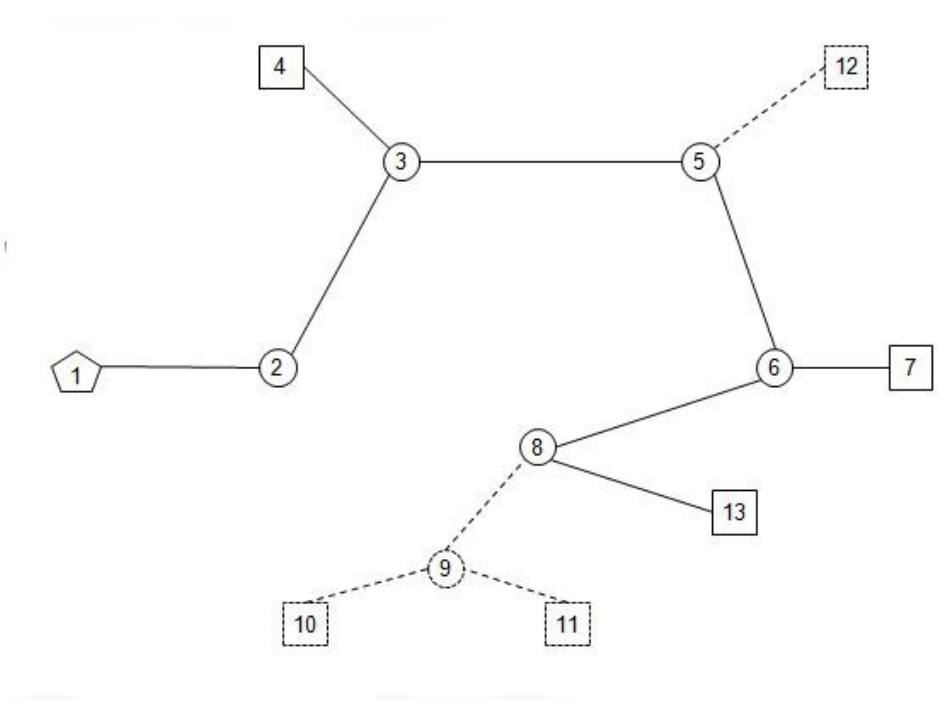


Figure 6.1: An example of a generic district heating network. The pentagon represent the plant, squares represent existing or potential users, circles are tees and other junctions in the pipe networks, solid lines are existing pipes and hashed lines are potential ones.

## 6.2 Literature Review

The optimization of DH networks has received relatively little attention in the literature. A first type of modeling approaches aims at representing in detail the network physics through sets of non-linear equations derived from the thermo and fluid dynamic theories. In this way one generally obtains a very good precision of the representation of fluid distribution and thermal gradients along the different network components.

However, the algorithmic difficulty of the solution of the required non-linear relations makes such approaches not adequate to model large networks those found in real-world applications where hundreds of users are served by the DH system. In this case, aggregation techniques of the network elements are often used to reduce the size enough to permit the numerical solution of the model at the expense of the accuracy of the network representation.

Examples of non-linear models for DH network design are presented by Bøhm et al. [4], Park et al. [11] Bøhm et al. [3], while network aggregation techniques are discussed in Zhao [14], Zhao and Holst [15], Larsen et al. [6], Loewen et al. [8], Loewen et al. [9] and Larsen et al. [7].

An alternative modeling of the DH networks is based on their empirical simulation starting from observation of temperature and pressure distributions of the real system (see, e.g., Benonysson et al. [2] and Pálsson [10]). Such approaches require long observations of the system to get sufficient accuracy and are not suited to study different system configurations with respect to the observed ones. Network simulation was also used by Wernstedt et al. [13] to study the performance of different real-time control strategies for DH network management.

An integer programming model for a different network design problem was defined by Aringhieri and Malucelli [1]. They considered the optimal selection of the type of heat exchangers to be installed at the users in order to optimize the return temperature at the plant and achieve good system efficiency at a reasonable cost. Finally, the design of the energy production plant integrating cogeneration engines and renewable energy was recently examined by Reini et al. [12] who developed integer programming models capable of solving small-scale examples.

## 6.3 Assumptions

The problem is modeled considering stationary peak conditions. As generally done in practice the peak demand requirements of downstream users is reduced to take into account that not all are active simultaneously. To this end, a so-called *concurrent factor*, for example equal to 60-70% is used to reduce the peak demand of each user.

Because of the thermal insulation of the pipes, the temperature losses in the DH system are mainly localized at the user's heat exchangers. Moreover, the temperature drop at the exchanger is generally assumed to be constant. Such an assumption is clearly very strong when the dynamic behavior of the system has to be analyzed (e.g., to derive operational models) but is acceptable for the purposes of network planning where stationary peak conditions are considered. Note that the main consequence of assuming constant the temperature drop $\Delta T$ at the heat exchangers is that formula (5.2) permits to express the heat power as proportional to the flow rate $\dot{m}$ of the fluid.

Note also that, because pipes bifurcates and merge at tees the overall network may contains loops. However, in our study we will simplify both the notation and the model description and we will limit ourselves to networks having a tree configuration and with a single plant. This is not limiting since all models and experiments we performed can be extended to the case where loops and multiple plants are present in the network.

In addition, for the sake of simplicity we assume that the network lies on a plane, i.e., we do not consider the implications related with the unevenness of the vertical quota of the pipes.

## 6.4 A Mathematical Model for District Heating Network Design Problem

In this section we introduce a mathematical formulation of the District Heating Network Design Problem (DHNDP) as previously defined. The model is based on a graph representation of the the DH network where nodes and arcs of the graph corresponds to the relevant elements of the network. As an example, Figure 6.2 depicts a graph representation of the simple DH network shown in Figure 6.1. Each node of the original network is represented by a pair of nodes: one, with positive identifier, associated with the feed network and the second, with negative identifier, with the return network. It is possible to identify plant node, user nodes and tee nodes as described in Section 5.1. The links in the graph represent pipes either of the feed or of the return circuits, and heat exchangers at user nodes. The orientation of the links is compatible with the flow of the heating fluid and it is possible to distinguish between existing pipes, represented by solid arcs and potential ones, represented by hashed arcs.

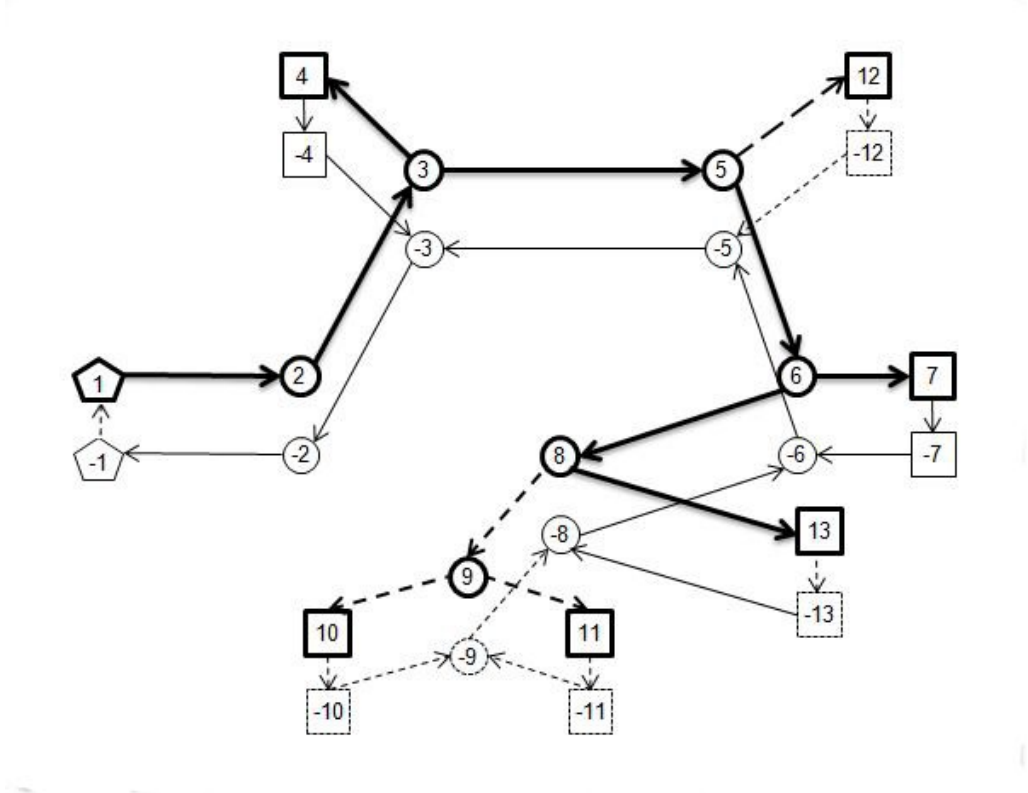


Figure 6.2: The graph representation of the simple DH system of Figure 6.1. Feed pipes are represented by solid lines and hashed lines are associated with potential parts of the network.

Figure 6.3 focuses on the representation of user links and illustrates how such user is inserted into the network, i.e., through a heat exchanger and a parallel configuration between feed line and return line. Note that user arcs are the only connections between feed and return networks because are the only portions of the network where heat exchange is assumed to take place.

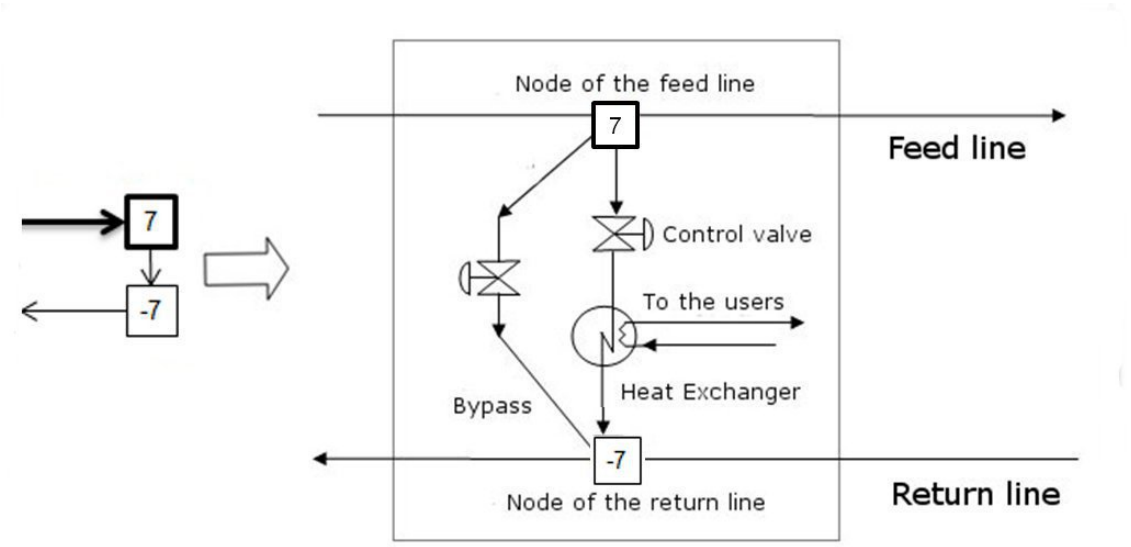


Figure 6.3: Schematic representation of feed and return line connected through a heat exchanger at a user's site.

As previously mentioned, in a DHNDP the DH network includes both *existing* and *potential* elements. The existing elements are associated with the initial network configuration made up by one or more plants and a set of pipes connecting the existing users. The potential elements of the network are instead:

- A set of potential users, each with an associated thermal demand.
- A set of potential pipes and tees that may be connected to the existing ones to reach the potential users.

More precisely, we are given a directed graph $G = (V, A)$, where $V$ is the set of nodes, $A$ is the set of arcs. Node set $V$ includes both nodes $v$, with $v > 0$, belonging to the feed line and the corresponding nodes $-v$ belonging to the return line. Set $V$ is also partitioned into some relevant subsets. Namely, $V_I$ is the subset of plant nodes, $V_S$ is that of existing user nodes, $V_P$ is the set of potential users nodes, $V_T = V_{TE} \cup V_{TP}$ is the set of tee nodes, which is further split in subset $V_{TE}$ of existing tees and subset $V_{TP}$ of potential tees. Finally, we denote by $V_E = V_S \cup V_{TE}$ the set of all the existing nodes, i.e., that of existing users and tees.

The set of arcs $A$ is, in turn, partitioned into five subsets, namely $A = A_F \cup A_R \cup A_S \cup A_P \cup A_I$. Set $A_F = A_{FE} \cup A_{FP}$ includes all feed line pipes, i.e., both the existing and potential ones (i.e., sets $A_{FE}$ and $A_{FP}$, respectively). Similarly, $A_R = A_{RE} \cup A_{RP}$ is the set of all returns line pipes, including both existing and potential ones (i.e., sets $A_{RE}$ and $A_{RP}$, respectively). Finally, $A_S$ and $A_P$ represent the existing and potential user heat exchangers, and $A_I$ are the plant arcs.

The demand of each user $v \in V_S \cup V_P$ is represented by the required flow $\mu_e$ of heat fluid in the corresponding user arc $e = (v, -v) \in (A_S \cup A_P)$.

The generic feed line arc is denoted as $e = (i, j) \in A_F$, while the corresponding return line arc is denoted as $r(e) = (-j, -i) \in A_R$. Similarly, user arcs are indicated

as $(v, -v)$ where $v$ belongs to $V_S$, $V_P$, and plant arcs are represented as $(-v, v)$ with $v \in V_I$, respectively. For each pipe arc $e = (i, j) \in (A_F \cup A_R)$, we define a *conventional orientation* from node $i$ to node $j$ with $i < j$. Since we consider here only networks with a tree configuration and with a single plant (i.e., $|V_I| = |A_I| = 1$), the flow direction along pipes is defined a-priori as the water will flow from the plant node to the users nodes and there are no loops which may change the conventional direction. However, as will be discussed in Section 6.5, the model described here can be easily extended to consider more general network structures including loops and multiple plants.

By considering the sample network depicted in Figure 6.2 the nodes and arcs sets are defined as follows.

$V_I = \{1, -1\}$,
$V_S = \{4, 7, 13, -4, -7, -13\}$,
$V_P = \{10, -10, 11, -11, 12, -12\}$,
$V_{TE} = \{2, -2, 3, -3, 5, -5, 6, -6, 8, -8\}$,
$V_{TP} = \{9, -9\}$,
$A_{FE} = \{(1, 2), (2, 3), (3, 4), (3, 5), (5, 6), (6, 7), (6, 8), (8, 13)\}$,
$A_{FP} = \{(5, 12), (8, 9), (9, 10), (9, 11)\}$,
$A_{RE} = \{(-1, -2), (-2, -3), (-3, -4), (-3, -5), (-5, -6), (-6, -7), (-6, -8), (-8, -13)\}$,
$A_{RP} = \{(-5, -12), (-8, -9), (-9, -10), (-9, -11)\}$,
$A_S = \{(4, -4), (7, -7), (13, -13)\}$,
$A_P = \{(10, -10), (11 - 11), (12 - 12)\}$
$A_I = \{(-1, 1)\}$.

All the non-linear relations in the network will be approximated by piecewise-linear functions. In particular, such a linear approximation is used to express the pressure drop $\Delta P = f(\dot{m})$ given in (5.8) as a piecewise-linear function $f_L(\dot{m})$.

The economic parameters of the model are the profits associated with the connection of potential users and the costs for the network setup. In particular, for each arc corresponding to the heat exchanger at a potential users (i.e., arcs $e = (v - v) \in A_P$) the parameter $R_e$ denotes the net profit of connecting it to the network. Such a profit is the difference between the net present value of the income associated with the energy sold to the user during the time horizon $T$ (generally between ten and thirty years), minus the costs of user connection, such as, for example, the cost of the exchanger and those of the commercial activities related to the contract setup. Furthermore, for each potential pipe (i.e., arcs $e = (i, j) \in A_{FP}$), cost $C_e$ represents the global cost of the installation of the required pipes. For the sake of simplicity we only associate cost to potential pipes of the feed line and we include into them also those of the corresponding return pipes.

The physical characteristics of the network are described through several parameters. The pressure in each node of the network must be larger than a minimum value $P^{\min}$, whereas at each plant node $v \in V_I$ must not exceed a maximum feed line pressure limit $P_v^{\max}$. Each pipe arc $e = (i, j) \in (A_F \cup A_R)$ is associated with a maximum capacity $\mu_e^{\max}$ for the heat fluid, that depends on the diameter of the pipe and on the given maximum speed of the fluid. Finally, each arc $e = (v, -v) \in (A_E \cup A_P)$ associated with a user exchanger must have a pressure drop larger than a prescribed minimum value $\Delta P^{\min}$.

The objective of the problem is to find the subset potential users that can be connected to the network, trying to both maximizing the overall net profit and to respect the main physical and logical constraints imposed by the configuration of the network.

As previously discussed, the network is designed by considering stationary peak conditions. The formulation uses two main sets of decision variables. The binary variables $x_e$, $e = (v, -v) \in A_P$ define connection the state of a potential user and take value 1 if the user $v \in V_P$ is connected to the network, and 0 otherwise. Furthermore, binary variables $y_e$, $e = (i, j) \in A_{FP}$ defines the use of a potential feed line pipe and take 1 if the pipe is used in the optimal solution, and 0 otherwise. In addition to the main decision variables, the model uses continuous variables to represent the hydraulic conditions of the network. In particular, we introduce specific variables for the node pressure $P_v, v \in V$, for the pressure drop and flow rate along the pipes, $\Delta P_e$ and $\dot{m}_e$, $e \in A$, respectively. The resulting mathematical model follows.

$$\max \sum_{e \in A_P} R_e x_e - \sum_{e \in A_{FP}} C_e y_e \tag{6.1}$$

subject to

$$\dot{m}_e = \mu_e \qquad \forall e \in A_S \tag{6.2}$$
$$\dot{m}_e = \mu_e x_e \qquad \forall e \in A_P \tag{6.3}$$
$$\dot{m}_e \leq \mu_e^{\max} \qquad \forall e \in A_{FE} \tag{6.4}$$
$$\dot{m}_e \leq \mu_e^{\max} y_e \qquad \forall e \in A_{FP} \tag{6.5}$$
$$\dot{m}_{r(e)} = \dot{m}_e \qquad \forall e \in A_F \tag{6.6}$$
$$\sum_{e=\langle i,v\rangle \in A} \dot{m}_e - \sum_{e=\langle v,j\rangle \in A} \dot{m}_e = 0 \qquad \forall v \in V \tag{6.7}$$
$$P_v \leq P_v^{\max} \qquad \forall v \in V_I \tag{6.8}$$
$$P_v \geq P^{\min} \qquad \forall v \in V \tag{6.9}$$
$$\Delta P_e \leq \Delta P^{\max} \qquad \forall e \in A_I \tag{6.10}$$
$$\Delta P_e \geq \Delta P^{\min} \qquad \forall e \in A_S \tag{6.11}$$
$$\Delta P_e \geq \Delta P^{\min} x_e \qquad \forall e \in A_P \tag{6.12}$$
$$\Delta P_e = f_L(\dot{m}_e) \qquad \forall e \in A_F \cup A_R \tag{6.13}$$
$$\dot{m}_e \geq 0 \qquad \forall e \in A_F \cup A_R \tag{6.14}$$
$$P_v \geq 0 \qquad \forall v \in V \tag{6.15}$$
$$\Delta P_e \geq 0 \qquad \forall e \in A \tag{6.16}$$
$$x_e \in \{0, 1\} \qquad \forall e \in A_P \tag{6.17}$$
$$y_e \in \{0, 1\} \qquad \forall e \in A_{FP} \tag{6.18}$$

The objective function (6.1) of the problem maximizes the net profit of the optimal network, which is defined as the difference between the net present value of the revenues associated with the connection of potential users and the costs required to setup the potential pipes to join them to the network. The total revenues derive from the summation of fixed revenues due to potential users connection, revenues due to an annual consume, that represents a fix booked power and revenues due to an annual real consume,which comes from bills. As for costs there are fix costs of connections and variable pipes installation costs.

The constraints of the model can be grouped into four categories. In the first one, we have the relations that refer to the flows of the heating fluid in the pipes. In particular, constraints (6.2) and (6.3) define the flow $\dot{m}_e$ in the user's pipes. Namely, existing users ones have their flow imposed by the users' heat demand, while in pipes corresponding to potential users the flow is non-zero only if the user is connected to the network, i.e. when $x_e = 1$. Similarly, inequalities (6.4) and (6.5) impose an upper bound on the flow of the other forward pipes of the network, where such upper bound is zero if a potential pipe is not used, i.e. when $y_e = 1$. The flow on each return pipe $r(e)$ is set equal to that of the corresponding forward pipe $e$ by equalities (6.6).

The second group of constraints are related with the nodes of the network, corresponding to tees and connections of users and plants to the pipes. First of all, equalities (6.7) impose the balance of the flows entering and leaving each such node. Then, a lower bound for the pressure in all the nodes is set by (6.9), while for plant nodes of the feed line is an upper bound for the pressure is also imposed in (6.8).

The third set of constraints refer to the pressure drops along the pipes. More precisely, the maximum pressure drop at the plant, and the minimum drop on existing and potential users' pipes are set by inequalities (6.10), (6.11) and (6.12), respectively. As to the remaining pipes of the network, the linearized relation between flow and pressure is synthetically expressed by inequalities (6.13). Note that, because of the convex nature of the non-linear relation between pressure drop and flow, in the actual implementation of the model for a specific solver such inequalities need be transformed into a set of linear relations, possibly involving auxiliary binary variables.

Finally, constraints (6.14) to (6.16) set the lower bounds for the continuous variables, while (6.17) and (6.18) define the binary variables.

## 6.5 Model Extensions and Solution

The proposed model can be nimbly extended to represent additional technical aspects of the network such as the possibility to include loops and multiple plants and to consider the cost of different pipe connections, as well as economic and practical aspects such as the possibility to change the client contracts or to incorporate deeper pressures control. A brief discussion of such features follows.

### 6.5.1 Networks With Loops

As previously discussed, the above model can be easily extended to represent networks including loops and multiple plants. We note, however, that in such cases the direction of the flow along forward and return pipes is not implicitly defined. As a consequence, an appropriate binary variable should be used to define the flow direction on the non-user pipes of the network and the existing pressure related variables and flow related variables should be split into two to take into consideration the flow direction and the drop of pressure direction. Note that a generic arc $e = \langle i, j \rangle$ connecting nodes $i$ and $j$, corresponds to the pipe connecting the same real point $i$ and $j$. That means that arcs must be oriented according to the direction of the water flow along the pipes. It's always used the following rule:

$(\forall e = \langle i, j \rangle \in A_F \cup A_R)\ i \leq j$

The above rule defines the conventional direction of every arc $e$ in such a way that node $i$ is always before node $j$. Note that such rule is not valid in the case of user's arcs and plant's arcs since they connect feed line and return line and they present a positive node and a negative node.

We define conventional positive direction the direction of a fluid which moves from $i$ to $j$. Otherwise we have a negative direction. The definition of a conventional direction of the arcs, introduces a new binary variable $dir_e$ which will be equal to 1 if flow direction along the pipe is equal to the conventional direction (positive direction), and 0 otherwise. Flow rate continuous variables and drop of pressures continuous variables will be split as follow: $\dot{m}_e^+$ is the flow rate along a pipe in a positive direction (conventional direction) and $\dot{m}_e^-$ is the flow rate along a pipe in a negative direction (opposite to the conventional direction); $\Delta P_e^+$ is the drop of pressure along a pipe in a positive direction (conventional direction) and $\Delta P_e^-$ is the drop of pressure along a pipe in a negative direction (opposite to the conventional one).

The set of constraints should be then integrated as follow

$$\Delta P_e^+ = f_L(\dot{m}_e^+) \quad \forall e \in A_F \cup A_R \tag{6.19}$$
$$\Delta P_e^- = f_L(\dot{m}_e^-) \quad \forall e \in A_F \cup A_R \tag{6.20}$$
$$\dot{m}_e^+ \leq dir_e \mu_e^{max} \quad \forall e \in A_F \cup A_R \tag{6.21}$$
$$\dot{m}_e^- \leq (1 - dir_e)\mu_e^{max} \quad \forall e \in A_F \cup A_R \tag{6.22}$$
$$\Delta P_e^+ \leq dir_e big\dot{m} \quad \forall e \in A_F \cup A_R \tag{6.23}$$
$$\Delta P_e^- \leq (1 - dir_e) big\dot{m} \quad \forall e \in A_F \cup A_R \tag{6.24}$$
$$\Delta P_e = \Delta P_e^+ - \Delta P_e^- \quad \forall e \in A_F \cup A_R \tag{6.25}$$
$$\dot{m}_e = \dot{m}_e^+ - \dot{m}_e^- \quad \forall e \in A_F \cup A_R \tag{6.26}$$

In constraints (6.19) and (6.20) the linearized relation between flow and pressure is split into the positive and negative direction of the continuous variables $\Delta P_e$ and $\dot{m}_e$.

The constraints (6.21) and (6.22) imposes that the flow rate along the pipes must be minus than or equal to the maximum acceptable value $\mu_e^{max}$. The boolean variable $dir_e$ imposes that, once the direction is defined, one of the two flow rate (among the positive flow $\dot{m}_e^+$ and the negative flow $\dot{m}_e^-$ ) must be equal to zero. That means that the direction of the flow along a pipe must be univocal. Since $dir_e$ is a boolean variable, one of the two constraints is always neutralized so that the remaining flow has its defined direction.

The multiplicative factor $big\dot{m}$ in constraints (6.23) and (6.24) represents a very big value of pressure. It is used to neutralize one of the constraints (6.23) and (6.24) when the related binary variable $dir_e$ is equal to zero. That means that the only active constraints will be related to the drop of pressure along those pipes where fluid direction is the one corresponding to the value of $dir_e$.

Constraints (6.25) and (6.26) define the positive (conventional) or negative (non conventional) direction of drop of pressures $\Delta P_e$ and flow rate $\dot{m}_e$ for every pipe $e$. It is important to remember that the binary variable $dir_e$ allows only one univocal direction for every pipe $e$.

### 6.5.2 Cost of Pipe Connections and Degree Rules for Nodes

The proposed model can be further developed by adding the cost of different types of pipe connection. In real applications there are three levels of joints, schematically represented in Figure 6.4. The different levels represent the way through which pipes are connected each other. Level 1 is related to nodes with just one ingoing pipe (i.e. users nodes) or just one outgoing pipe (i.e. plant nodes); level 2 is related to tee nodes with a total of two pipes among ingoing and outgoing pipess; level 3 is related to tee nodes with a total of three pipes among ingoing and outgoing pipes. Generally the cost tends to become higher as the level grows from 1 to 3 as different joints are required to build up the practical connection.

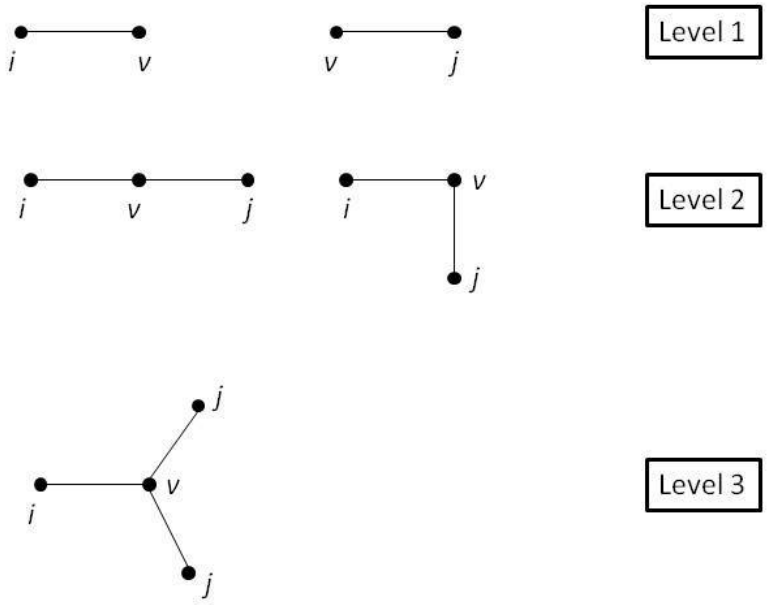


Figure 6.4: Different pipe connections

Therefore it is possible to add a new term of cost inside the objective function, so that the model will be able to choose the best configuration, considering that, different ramifications of the network, may cause different global costs of connection. This feature becomes very useful when a complete potential network has to be created. This is, for example, the case of a new district where there is no district heating at all and where it is necessary to plan the whole grid, by choosing the optimal pipe paths to reach the optimal subset of potential users.

For that purpose it is necessary to define a new binary variable $g_{vh}$ that will be equal to 1 if node $v$ is associated to level $h$, and 0 otherwise. Then we need to define two new parameters: $C_h$ which represents the cost of configuration $h$ and $\varepsilon_h$ which will indicate the type of configuration: $\varepsilon_h = 1$ for configurations of type 1, $\varepsilon_h = 2$ for configurations of type 2, $\varepsilon_h = 3$ for configurations of type 3.

The model can be modified by adding the configuration cost $C_h$ multiplied by the new binary variable $g_{vh}$ in the objective function as showed in formula (6.27)

$$- \sum_{v \in V} \sum_{h} C_h * g_{vh} \tag{6.27}$$

While the set of constraints has to be integrated as follow

$$\sum_{e=\langle i,v\rangle \cup e=\langle v,j\rangle \in A} 1 + \sum_{e=\langle i,v\rangle \cup e=\langle v,j\rangle \in A} y_e \leq \sum_{h} g_{vh} * \varepsilon_h \quad \forall v \in V \tag{6.28}$$

$$\sum_{h} g_{vh} \leq 1 \quad \forall v \in V \tag{6.29}$$

Constraint (6.28) creates a mathematical relation between the new decision variable $g_{vh}$ and the existing variable $y_e$. The term $\sum_{e=\langle i,v\rangle \cup e=\langle v,j\rangle \in A} 1$ relates to all the existing arcs connected to the node $v$ (both ingoing and outgoing arcs), while the term $\sum_{e=\langle i,v\rangle \cup e=\langle v,j\rangle \in A} y_e$ relates to all the potential arcs that will be connected to node $v$ (both ingoing and outgoing potential arcs). The meaning of constraint (6.28) is to ensure that the total number of arcs connected to every node will be equal to the related level defined by the binary variable $g_{vh}$ and the parameter $\varepsilon_h$.

Constraint (6.29) means that every node $v$ can be associated to at most one type of connection $h$.

In real world problems it is also important to impose the following degree rules for nodes:

- Every plant node must have one outgoing arc and no ingoing arcs (0in / 1out)
- Every user node must have one ingoing arc and no outgoing arcs (1in / 0out)
- Every tee node can have at most three arcs among ingoing and outgoing arcs, through the following combinations:
  - One ingoing arc and two outgoing arcs (1in / 2out)
  - Two ingoing arcs and one outgoing arc (2in / 1out)
  - One ingoing arc and no outgoing arcs (1in / 0out)

The last rule in particular describes very well a realistic district heating constraint, as the available joints for pipe connections allow at most three ramifications.

The above rules can be expressed by the following additional constraints:

$$\sum_{e=\langle i,v\rangle \in A} 1 + \sum_{e=\langle i,v\rangle \in A} y_e = 0 \quad \forall v \in V_I \tag{6.30}$$

$$\sum_{e=\langle v,j\rangle \in A} 1 + \sum_{e=\langle v,j\rangle \in A} y_e = 1 \quad \forall v \in V_I \tag{6.31}$$

$$\sum_{e=\langle i,v\rangle \in A} 1 + \sum_{e=\langle i,v\rangle \in A} y_e = 1 \quad \forall v \in V_S \cup V_P \tag{6.32}$$

$$\sum_{e=\langle v,j\rangle \in A} 1 + \sum_{e=\langle v,j\rangle \in A} y_e = 0 \quad \forall v \in V_S \cup V_P \tag{6.33}$$

$$\sum_{e=\langle i,v\rangle \cup e=\langle v,j\rangle \in A} 1 + \sum_{e=\langle i,v\rangle \cup e=\langle v,j\rangle \in A} y_e \leq 3 \quad \forall v \in V_T \tag{6.34}$$

### 6.5.3 Client Contract Change

The set of existing users can be described by an additional parameter, that is the effective consumption $CE$ (kWh / year). This value can be deduced by the user absorption of thermal energy along the period after the user connection to the grid.

Let us define *convertible users* $CR$ the existing users that have an effective consumption $CE$ much smaller than the historical consumption $C_{Sto}$.

$C_{Sto}$ represents the average absorption of thermal energy in the period before the user connection to the grid; its value is used to determine the initial installation power $PI$.

If the real consumption is smaller than the installed power, it might be possible to reduce the original power PI to a new smaller value of power $PI^{''}$.

Since the plant is able to supply a power $PI$, if the original power $PI$ of a user is reduced to a new smaller value $PI^{''}$, the result is a power availability equal to $PI - PI^{''}$ which could be used to feed up new potential users.

Generally Energy Societies define a particular limit below which it is worthy to evaluate the client contract change. If the ratio $CE/C_{Sto}$ is smaller than 70-80%, then the existing user wil be considered as a *convertible user* whose power might be reduced as a function of the actual consumption.

In this new feature, the objective is to find which potential users can be connected to the grid, by using the exceeding power that derives from the reduction of some existing users power (users with an actual consumption smaller than the installed power). As usual, that must be done together with the overall net profit maximization and by fulfilling physics and logical constraints imposed by the configuration of the network.

The model can be modified by adding a new binary variable $s_e \in A_S$ in order to define the contract conditions of an existing user. In particular $s_e = 1$ if the existing user is going to become a convertible user, while $s_e = 0$ otherwise.

We need to define a new parameter $\Delta\dot{m}_e^S$ that is the amount of flow rate that could be distributed to other users. As shown in formula 6.35 this is calculated through the difference between the flow rate defined by the existing contract $\dot{m}_e^{max}$ (which is supposed before the connection) and the actual flow rate $\dot{m}_e^{min}$.

$$\Delta\dot{m}_e^S = \dot{m}_e^{max} - \dot{m}_e^{min} \quad \forall e \in A_S \tag{6.35}$$

It's necessary to add a new term of cost inside the objective function as shown in 6.36. This is related to the costs associated to the convertible users. These costs are obtained from the summation of a fixed penalty cost $C_S$ related to the convertible users plus the missed actualized revenue $R_e\Delta\dot{m}_e^S$. The latter is due to the reduction of the power previously assigned to those existing users with an actual consumption less than the forecasted consumption.

$$\sum_{e} s_e(C_S + R_e \Delta \dot{m}_e^S) \quad \forall e \in A_S \tag{6.36}$$

Finally the flow rate constraint has to be modified as follow

$$\dot{m}_e = \dot{m}_e^{max} - \Delta \dot{m}_e^S s_e \quad \forall e \in A_S \tag{6.37}$$

In constraint (6.37) if the service delivered to an existing user $e \in A_S$ is going to remain unchanged ($s_e = 0$), then the forecasted flow rate previously defined will remain the same (equal to $\dot{m}_e^{max}$). Otherwise, if the the service delivered to an existing user $e \in A_S$ is going to be reduced, then total flow rate will be reduced to a smaller value equal to the actual consumption, that is $\dot{m}_e^{min}$.

### 6.5.4 Other Practical and Economic Features

Several other practical requirements may be easily incorporated in the proposed model. A common example is represented by the need to limit the maximum pressure values in specific parts of the network, which may be imposed by adding constraints similar to (6.8) or (6.10) for specific nodes or pipes subsets. Similarly, either to take into account pumping costs or to favor solution that have a lower values of pressures or flows in presence of additional features such as loops, one can add suitable penalties or costs to the objective function. More precisely, let $\varepsilon_1, \ldots, \varepsilon_3$ be the unit penalties (or costs) associated with the node pressures, the pressure drops and the fluid flow along the pipes, respectively. Then a more general objective function can be written as:

$$\max \sum_{e \in A_P} R_e x_e - \sum_{e \in A_{FP}} C_e y_e - \sum_{v \in V} \varepsilon_1 * P_v - \sum_{e \in A_F \cup A_R} (\varepsilon_2 \Delta P_e + \varepsilon_3 \dot{m}_e) \tag{6.38}$$

Whenever for a given user there exist alternative ways of connecting it to the network or alternative levels of demand, hence of required exchanger, it is possible to consider all of them and let the model chose the optimal one. This is simple done by adding constraints which impose that at most one among a subset of binary variables corresponding to the alternatives is selected.

Economic features of the real-world problem may be also added to the model. For example, generalized budget constraints may limit the total investment costs. In addition, it may be desirable to favor solutions that or favoring solutions that connect users, (e.g. buildings or shops) with a common administrator since this will reduce the administrative cost of setting up the contract.

Model (6.1)-(6.18) belongs to the class of Mixed-Integer Linear Programming models which are notoriously difficult to solve computationally. However, as we will discuss in the following sections we found that realistically-sized models of this type, i.e. with hundreds of potential users, can be solved to optimality or near-optimality within reasonable computing time by a commercial solver. The possibility of directly solving DHNDP does not come as a surprise, since current solvers incorporate very sophisticate solution strategies capable of successfully attacking several classes of important problems similar to the DHNDP (see, e.g., Fischetti, Lodi and Salvagnin Fischetti et al. [5]). However, specifically designed heuristic algorithms may be required to solve large-scale instances of DHNDP or some variants involving additional real-world constraints as those described above.

## 6.6 Computational Testing of the DHNDP Model

In this section we describe the results we obtained during the computational testing of the DHNDP model on a set of test networks. First of all we consider a small real-world network defined within the Innovami project and used to validate a preliminary version of the model described in previous sections.

To provide a more extensive and detailed analysis of the model potentialities we next examined a set of 100 large-scale DHNDP instances with up to 1000 potential and 500 existing users. The data for the cost and demand used in such instances are derived from real-world information obtained from Italian multi-utility companies, and the random layout of the network is designed through a procedure that tries to reproduce the characteristics of real-world urban DH networks.

### 6.6.1 Testing on a Real-World Urban Network

We describe here the testing of the model conducted on a small real-world instance representing a portion of the DH network in a town of Emilia-Romagna, in northern Italy. The instance, defined during the Innovami project funded by the Emilia-Romagna Region in 2009-10, includes 33 users in total of which 20 are existing and 13 potential. The structure of the network is depicted in Figure 6.5, where the plant is represented by the square node, existing and potential users are identified by solid and empty large circles, respectively. Similarly, the existing and potential intermediate tee nodes are shown as solid and empty small circles, respectively. Finally, existing (forward) pipes are drawn as solid directed lines, while potential pipes are represented by hashed ones. The type of each user (indicated as E or P) and the corresponding thermal demand in kW are reported in Table 6.1 (note that the reported data are slightly altered to preserve the confidentiality). The existing network is about 4.3 km long and the total length of the potential pipes is slightly less than 1.9 km.

Specific data are also defined for the cost of the heat exchangers, depending on the users' demand class, for the potential pipes depending on their diameter and length and for the revenues of the sale of energy. In addition, the maximum pressure at the plant is 9 bar, the minimum pressure at each node is 2 bar and the minimum pressure drop at a user' pipes is equal to 0.5 bar.

Two different scenarios are considered, the first one considers a time horizon of 10 years for the computation of net present value of the network. The second considers a reduced time horizon of 5 years only in which pipes costs are reduced by 10% and the user's fee for the connection to the network are increased by 50%. The results of the model for the two scenarios are shown in Figure 6.6 where the connected potential users are identified by gray circles and the potential pipes which must be used are now drawn with a thick solid line. In particular, in Scenario 1 the potential users 4, 6, 7, 9, 27, 29, 32, 35 and 37 are selected, while in Scenario 2 the optimal set of potential users to be connected includes 4, 7, 9, 27 and 29.

By comparing the two solutions we may observe that some users, such as 11 or 20, are not compatible with the connection in both scenarios. This is either due to the relatively small demand compared to the length of the pipe required to connect them that may make them unprofitable, or to the insufficient capacity of the network due to the limits of the pressure at the plant that does not allow to connect all potential users even when they are profitable (as, for example, user 33). Some other users, such as 6 and 32, which turn out

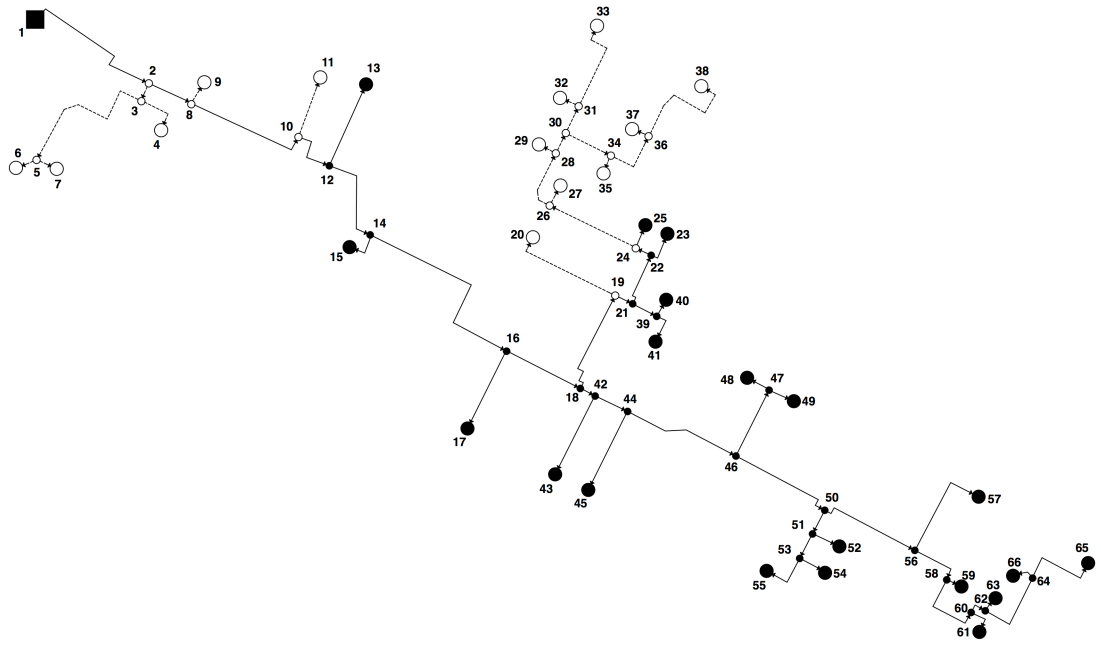


Figure 6.5: The real-world network used within Innovami project.

Table 6.1: The existing (left) and potential (right) users of the real world instance.

| User id | Type | Demand (kW) |
|---|---|---|
| 13 | E | 1400 |
| 15 | E | 400 |
| 17 | E | 1050 |
| 23 | E | 250 |
| 25 | E | 150 |
| 40 | E | 200 |
| 41 | E | 350 |
| 43 | E | 1050 |
| 45 | E | 1050 |
| 48 | E | 300 |
| 49 | E | 300 |
| 52 | E | 400 |
| 54 | E | 400 |
| 55 | E | 400 |
| 57 | E | 500 |
| 59 | E | 250 |
| 61 | E | 400 |
| 63 | E | 350 |
| 65 | E | 400 |
| 66 | E | 500 |

| User id | Type | Demand (kW) |
|---|---|---|
| 4 | P | 1200 |
| 6 | P | 300 |
| 7 | P | 450 |
| 9 | P | 100 |
| 11 | P | 100 |
| 20 | P | 250 |
| 27 | P | 150 |
| 29 | P | 200 |
| 32 | P | 650 |
| 33 | P | 450 |
| 35 | P | 300 |
| 37 | P | 50 |
| 38 | P | 100 |

to be selected with the longer time horizon are instead no longer profitable in the second scenario even if the capacity of the network would allow to connect them.

Since the optimal solutions for this network can be obtained in few seconds of computation by using IBM Cplex solver, it is evident the great value for decision makers of the model we propose for the evaluation of several alternative scenarios to support the decision process.

### 6.6.2 Testing on Randomly Generated Networks

To analyze the performance of the model on large-scale instances we randomly generated a set of 100 instances. The generation procedure is designed so as to create realistic network, inspired by those found in the real-world. We generated five classes of networks, each characterized by a different size of the network in terms of existing nodes $V_E$, i.e. existing tees and users. In particular, we considered $V_E \in \{100, 200, 300, 400, 500\}$. Furthermore, for each size of network, we considered four different number of potential users $V_P$ defined proportionally $V_E$, namely: $V_P = V_E/2$; $V_P = V_E$; $V_P = V_E + V_E/2$; $V_P = 2 \cdot V_E$. Finally, for each pair of $V_E$ and $V_P$ we randomly generated five different test instances.

Given the value of $V_E$ we define a circle with a diameter of $D$ Km. In particular, we used $D = 5$ if $V_E \leq 200$ and $D = 10$ otherwise. Random coordinates within such circle are associated with each existing node. Then a shortest spanning tree for the complete graph including all existing nodes and with arc cost equal to the Euclidean distance between the endpoints. Such shortest spanning tree represents the existing network. The plant is defined as the node with smaller *abscissa* coordinate value. In addition, all leave nodes of

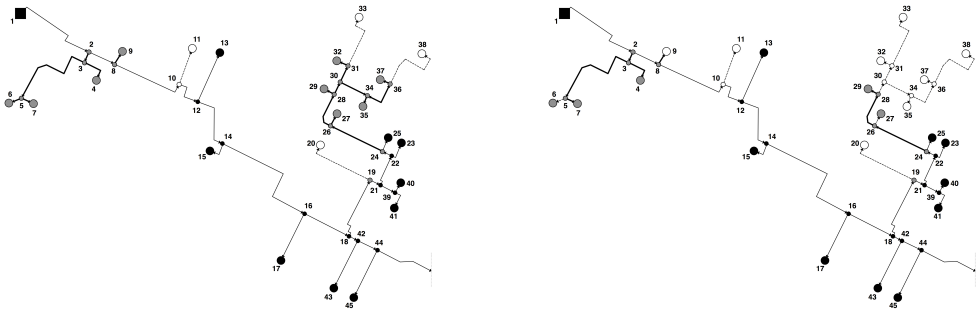

Figure 6.6: The potential users which are connected to the network in the two scenarios examined. The left solution is relative to a 10 years time horizon with original costs and revenues, the right one is relative to a reduced time horizon of 5 years but with reduced construction costs. Connected users are grey circles and potential pipes installed are identified by thick solid lines.

the tree are defined as existing users.

We next randomly generate the points corresponding to the potential users so that their coordinates are close to the arcs of the existing network. The potential users nodes are connected to the existing network through potential arcs ending at the closest point of the existing network. If such point is along a link a potential tee is added and the existing arc is split in that point.

Each existing and potential user is associated with a random value for the thermal demand $PI_e$ drawn from a T-Gamma distribution with an average value of 75 kW. Note that such demand is already reduced taking into account a concurrent factor of 60% with respect to the typical original demand. Then, the required flow rate along existing user's arcs is computed through the relation $\mu_e = PI_e/(\Delta T * c_p)$, where $\Delta T = 27°K$ and $c_p = 4.18$.

Given the flow rates on the existing users arcs flow rate, the flow rate on the remaining existing arcs is computed by recursively adding the flow of the outgoing arcs starting from the leaves of the network. The flow rate along the potential pipes is instead simply equal to the flow rate required by the potential user at its endpoint.

Then the diameter, in centimeters, of the pipe required for each existing and potential arc is determined through standard hydraulic equations and the value is rounded up to the next existing pipe value chosen between the set {25, 32, 40, 50, 65, 80, 100, 125, 150, 200, 250, 300, 350, 400, 500, 600}. In particular, given the water speed as shown in Table 6.2 the diameter $D$ of a pipe is given by

$$D = \sqrt{(\dot{m}/v) * (4/\pi) * (1/\rho)} \tag{6.39}$$

where $\dot{m}$ is the water flow rate $(kg/s)$, $v$ is the water speed $(m/s)$ and $\rho$ is the water density $(kg/m^3)$.

In fact the water flow rate can be defined both through the water volume (volumetric flow $\dot{m}_v$ in $m^3/s$) and through the water mass (mass flow rate $\dot{m}_m$ in $kg/s$).

The relationship between the two can be expressed as $\dot{m}_m = \dot{m}_v * \rho$ where $\rho$ is the water density.

The water speed $v$ in $m/s$ is linked to the water volumetric flow through the relationship $\dot{m}_v = A * v$ where $A$ is the circle area of a pipe in $m^2$ ($A = \pi * (D/2)^2$).

Through proper algebraic manipulation of the above formulas it is possible to derive the equation 6.39 for the diameter definition.

Once such diameter is known, we can compute the cost of the pipe by multiplying its unit cost (see table 6.2) times the length of the pipe and we can determine the coefficients $K_1$ and $K_2$ to be used in formula (5.8) to compute the pressure drop along the pipe.

All data of the generated instances are available on request from the authors.

Table 6.2: Prices and water speed for different pipe dimensions

| Pipe nominal diameter ($mm$) | Pipe price ($Euro/m$) | Water speed ($m/sec$) |
|---|---|---|
| DN25 | 455 | 1.5 |
| DN32 | 467 | 1.5 |
| DN40 | 487 | 1.5 |
| DN50 | 550 | 1.5 |
| DN65 | 569 | 1.5 |
| DN80 | 617 | 1.5 |
| DN100 | 648 | 1.5 |
| DN125 | 751 | 1.5 |
| DN150 | 800 | 1.5 |
| DN200 | 886 | 1.5 |
| DN250 | 1017 | 2 |
| DN300 | 1111 | 2 |
| DN350 | 1205 | 2 |
| DN400 | 1386 | 2 |
| DN500 | 2036 | 2 |
| DN600 | 2378 | 2.5 |
| DN700 | 2774 | 2.5 |
| DN800 | 3054 | 2.5 |

The computational testing has been performed using an Intel Pentium processor SU4100 1.30 GHz PC, with 4GB of memory and the MILP models are solved through the branch-and-cut algorithm implemented in the IBM Cplex 12.2 solver.

Three different scenarios have been considered corresponding to different values of the plant capacity and of the maximum number of potential nodes that can be connected.

The tables including the results includes several information and report the average values over the five instances for each value of $V_E$ and $V_P$. In particular, the tables report:

"$|V_P|/|V_E|$" is the ratio between $V_P$, the number of potential users and $V_E$, the number of nodes of the existing network;

"$|V_S|$" is the average number of existing users;

"$V_S$ pow" is the average total power (in kW) required by existing users;

"$V_P$ pow" is the average total power (in kW) required by potential users;

"Conn. $V_P$" is the average number and percentage of connected potential users;

"Conn. $V_P$ pow" is the average total power (in kW) of connected potential users;

"B&C Nodes" is the average number of branch-and-cut nodes.

"Root Time" is the time (in seconds) required for the root node of the branch-and-cut;

"Total time" is the total time (in seconds) required by the branch-and-cut.

In addition, the percentage gap of the best upper bound and heuristic solution values at the root node are computed as follows

$$\text{Gap U} = (U - Z^*)/Z^* \cdot 100$$

$$\text{Gap H} = (H - Z^*)/Z^* \cdot 100$$

where $U$ is the best upper bound value, $H$ is the best heuristic solution value found at root node, and $Z^*$ is the value of the optimal solution.

### 6.6.3 Basic Scenario

The first set of tests is performed by considering a plant with a very high capacity sufficient to serve all potential users and without any limitation on the number of potential users that can be connected.

The results for the basic scenario are reported in Table 6.3, which shows that all problems can be solved within a very short computing time by the solver. Moreover the formulation appears to be quite tight as indicated by the small values of the average gaps of both the upper bound and of the heuristic solution value. Since the Scenario does not limit considerably the number of users that can be connected we see that on average about 70 % of potential users are selected corresponding to more than 85% of the total power demand. Such users are clearly the ones that are both profitable and compatible with the physical constraints of the network resulting from the pressure drops and the pipe capacities.

Table 6.3: Results for Scenario 1. Plant with very high capacity and no limit on the number of connected potential users. Average results over five instances.

| $\lvert V_P\rvert/\lvert V_E\rvert$ ($n$) | $\lvert V_S\rvert$ ($n$) | Total $V_S$ pow (kW) | Total $V_P$ pow (kW) | Conn. $V_P$ (n) | Conn. $V_P$ (%) | Conn. $V_P$ pow (kW) | Conn. $V_P$ pow (%) | Gap U (%) | Gap H (%) | B&C Nodes (n) | Root Time (sec) | Total Time (sec) |
|---|---|---|---|---|---|---|---|---|---|---|---|---|
| 50 / 100 | 22.00 | 1561 | 3436 | 35 | 69.20 | 3041 | 88.52 | 0.24 | 0.00 | 0.0 | 0.16 | 0.16 |
| 100 /100 | 21.00 | 1621 | 7553 | 66 | 66.00 | 6243 | 82.65 | 0.73 | -0.31 | 19.8 | 0.43 | 0.54 |
| 150/100 | 23.60 | 1750 | 11671 | 104 | 69.20 | 10077 | 86.34 | 0.10 | -0.06 | 4.2 | 0.39 | 0.44 |
| 200/100 | 22.20 | 1578 | 15918 | 136 | 68.10 | 13487 | 84.72 | 0.16 | -0.25 | 17.6 | 0.75 | 0.95 |
| 100/200 | 44.40 | 3381 | 7513 | 71 | 71.40 | 6740 | 89.71 | 0.19 | 0.00 | 0.0 | 0.53 | 0.36 |
| 200/200 | 43.00 | 3689 | 14926 | 144 | 71.90 | 13380 | 89.65 | 0.16 | -0.04 | 6.2 | 0.83 | 0.90 |
| 300/200 | 43.20 | 3281 | 22941 | 204 | 68.07 | 19816 | 86.38 | 0.17 | -0.03 | 28.2 | 1.20 | 1.64 |
| 400/200 | 45.80 | 3149 | 24995 | 236 | 58.90 | 20108 | 80.45 | 0.14 | -0.43 | 69.0 | 2.12 | 3.40 |
| 150/300 | 65.20 | 4828 | 11011 | 113 | 75.07 | 10107 | 91.79 | 0.02 | 0.00 | 0.0 | 0.40 | 0.40 |
| 300/300 | 65.20 | 4994 | 22622 | 215 | 71.73 | 20140 | 89.03 | 0.22 | -0.21 | 23.2 | 1.54 | 1.94 |
| 450/300 | 66.00 | 5099 | 33736 | 331 | 73.47 | 30508 | 90.43 | 0.07 | -0.10 | 28.6 | 2.32 | 3.05 |
| 600/300 | 64.00 | 3707 | 35707 | 356 | 59.40 | 28817 | 80.70 | 0.18 | -0.19 | 81.6 | 3.92 | 7.19 |
| 200/400 | 89.20 | 6985 | 14854 | 149 | 74.40 | 13504 | 90.91 | 0.09 | -0.07 | 3.6 | 0.80 | 0.89 |
| 400/400 | 86.40 | 6188 | 29583 | 293 | 73.30 | 26848 | 90.76 | 0.18 | -0.06 | 13.6 | 3.50 | 4.25 |
| 600/400 | 91.40 | 6855 | 45611 | 444 | 74.03 | 41122 | 90.16 | 0.09 | -0.21 | 58.6 | 4.64 | 7.25 |
| 800/400 | 87.00 | 5323 | 47398 | 512 | 63.95 | 40040 | 84.48 | 0.10 | -0.18 | 375.8 | 6.54 | 23.22 |
| 250/500 | 109.60 | 7885 | 18841 | 187 | 74.88 | 17265 | 91.64 | 0.08 | -0.01 | 0.4 | 1.16 | 1.18 |
| 500/500 | 107.00 | 8284 | 38324 | 376 | 75.24 | 35023 | 91.39 | 0.08 | -0.07 | 39.2 | 4.87 | 6.16 |
| 750/500 | 108.80 | 8562 | 56134 | 551 | 73.44 | 50649 | 90.23 | 0.04 | -0.08 | 35.0 | 7.34 | 9.21 |
| 1000/500 | 109.60 | 6585 | 60132 | 629 | 62.92 | 50658 | 84.24 | 0.06 | -0.10 | 327.6 | 10.50 | 29.34 |

As previously mentioned, the average computing times required to solve the problems to optimality is considerably small and grows relatively slowly with the number of potential users as shown by Figure 6.7.

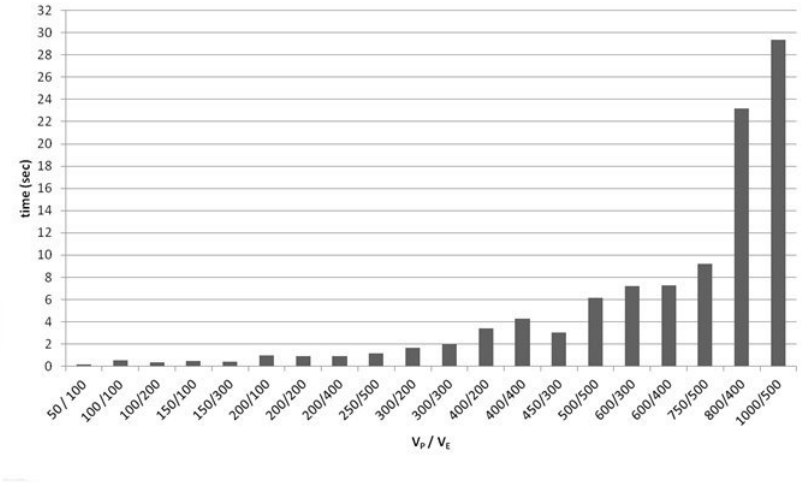


Figure 6.7: Computing time required to optimally solve the model as a function of the number of potential users of the network.

### 6.6.4 Scenarios 2 and 3

We conducted further tests by considering two additional scenarios to evaluate the model behavior and robustness in different conditions with respect to the basic. The two scenarios are defined by either limiting the total number of potential users that can be connected or the plant total capacity, as follows:

> Scenario 2: the plant capacity is not limited but at most half of the users in $V_P$ can be connected;
>
> Scenario 3: the plant capacity is reduced by 25% with respect to that used in Scenario 1 and no limit is set on the number of potential users that can be connected.

Scenario 2 represents the case in which budget restrictions impose a limit on the new users that can be connected. We simplified this requirement by considering just the number of users but a similar effect may be obtained by limiting any other measure related to the potential users that are connected in the optimal solution, such as the total investment cost, the total power or the total length of the pipes used. Scenario 3 instead represents a change either in the available capacity, e.g. due to a modification of the existing or designed plant. Such a scenario may also indirectly account for modifications of the consumption profile of the users that increases the concurrent demand requirement. Because the computing time required by the model is relatively short, we limited our analysis to the 20 instances with 500 existing nodes.

It is interesting to note that computational time is higher when the plant capacity is limited.

The results for Scenario 2 are given in Table 6.4 and show that the model is not sensibly affected by the additional constraint on the number of users. The computing times and the quality of upper bound and heuristics solutions are almost unchanged. We observe that, as expected, the user that are selected by the model are the largest one as their total demand is the 75 % of the potential demand.

Table 6.4: Results for Scenario 2. No limitation on plant capacity but at most 50% of potential users may be connected. Average results over five instances.

| $\|V_P\|/\|V_E\|$ ($n$) | $\|V_S\|$ ($n$) | Total $V_S$ pow (kW) | Total $V_P$ pow (kW) | Conn. $V_P$ (n) | Conn. $V_P$ (%) | Conn. $V_P$ pow (kW) | Conn. $V_P$ pow (%) | Gap U (%) | Gap H (%) | B&C Nodes (n) | Root Time (sec) | Total Time (sec) |
|---|---|---|---|---|---|---|---|---|---|---|---|---|
| 250/500 | 109.60 | 7885 | 18841 | 125 | 50.00 | 14261 | 75.69 | 0.17 | -0.15 | 5.0 | 1.36 | 1.61 |
| 500/500 | 107.00 | 8284 | 38324 | 250 | 50.00 | 28747 | 75.01 | 0.10 | -0.16 | 33.0 | 4.33 | 6.31 |
| 750/500 | 108.80 | 8562 | 56134 | 375 | 50.00 | 42074 | 74.95 | 0.03 | -0.14 | 48.0 | 8.20 | 12.43 |
| 1000/500 | 109.60 | 6585 | 60132 | 500 | 50.00 | 45113 | 75.02 | 0.08 | -0.12 | 124.0 | 18.93 | 33.38 |

The results for Scenario 3 are show in Table 6.5. In this case the reduction of plant capacity has a perceptible effect on both the total computing effort, as indicated by the increase in B&C nodes and total time, and on the quality of the heuristic solution. In addition, the number of users that are connected is drastically reduced.

Table 6.5: Results for Scenario 3. Reduction by 25% of the plant capacity and no limit on the number of potential users that may be connected. Average results over five instances.

| $\|V_P\|/\|V_E\|$ ($n$) | $\|V_S\|$ ($n$) | Total $V_S$ pow (kW) | Total $V_P$ pow (kW) | Conn. $V_P$ (n) | Conn. $V_P$ (%) | Conn. $V_P$ pow (kW) | Conn. $V_P$ pow (%) | Gap U (%) | Gap H (%) | B&C Nodes (n) | Root Time (sec) | Total Time (sec) |
|---|---|---|---|---|---|---|---|---|---|---|---|---|
| 250/500 | 109.60 | 7885 | 18841 | 56 | 22.40 | 8528 | 45.26 | 0.04 | -0.15 | 810.0 | 2.79 | 13.21 |
| 500/500 | 107.00 | 8284 | 38324 | 47 | 9.40 | 8965 | 23.39 | 0.04 | -0.47 | 1501.0 | 7.96 | 52.77 |
| 750/500 | 108.80 | 8562 | 56134 | 46 | 6.08 | 9271 | 16.52 | 0.02 | -0.37 | 1664.0 | 11.62 | 66.69 |
| 1000/500 | 109.60 | 6585 | 60132 | 38 | 3.80 | 7090 | 11.79 | 0.05 | -0.39 | 2453.0 | 18.63 | 109.02 |

In Table 6.6 we mimic the summary results of a what-if analysis on a single instance of the 250/500 set. The table compares the results of the three scenarios by also reporting the total value of the objective function in monetary units.

Table 6.6: An example of what-if analysis conducted on a single instance of the 250/500 test set.

| $\|V_P\|/\|V_E\|$ (n) | $\|V_S\|$ (n) | $V_S$ pow (kW) | Total $V_P$ pow (kW) | Total Scenario | Conn. $V_P$ (n) | Conn. $V_P$ (%) | Conn. $V_P$ pow (kW) | Conn. $V_P$ pow (%) | $Z^*$ (mu) |
|---|---|---|---|---|---|---|---|---|---|
| 250/500 | 111 | 10840 | 20509 | 1 | 199 | 79.60 | 19162 | 93.43 | 9,506,397 |
| | | | | 2 | 125 | 50.00 | 15398 | 75.08 | 8,484,102 |
| | | | | 3 | 60 | 24.00 | 9757 | 47.57 | 6,358,060 |

We note that the difference in total net present value of the revenue between Scenarios 1 and 2 is about 10% while clearly the starting investment cost for Scenario 2 is substantially smaller because of the smaller number of connected users. Such observation may be verified by considering the unit cost per connected customer and per connected kW that are in Scenario 2 larger by 42 and 11 %, respectively.

Similarly, the greatly reduced net present value of Scenario 3 is compensated by a consistent reduction of the initial investment associated with a smaller plant and much smaller number of connected users. Also in this case the unit revenue per connected user and kW are larger than those of Scenario 1 by 121 and 31 %, respectively.

Given the possibility of running new simulations in a few minutes of computing time the decision makers can examine in detail several alternative scenarios to carefully evaluate the best solution to implement taking into account all the performance measures that are relevant in the specific real-world context.

### 6.6.5 Testing Features on Randomly Generated Networks

We conducted further tests by considering new scenarios to evaluate the model behavior and robustness with the additional variables and constraints related to the features described in previous sections. The results are shown in Tables 6.7, 6.8, 6.9.

The additional data available in the tables are related to the "client contract change" scenario.

> "$|N_S|$" is the average number of convertible users (average number of users with an actual consumption smaller than the historical consumption);
>
> "$N_S$ pow" is the average convertible power (in kW) that can be subtracted by the convertible users to eventually feed new potential users;
>
> "Select $N_S$" is the average number of convertible users that has been selected by the model for the power reduction;
>
> "Select $N_S$ pow" is the average power that has been subtracted by the selected convertible users to feed up new potential users;

Scenario 4 represents a combination of the Scenario 3 previously described, together with the client contract change feature. In this case the plant capacity is the same of that used in Scenario 3 but at most half of the users in $V_P$ can be connected. The number of convertible users $V_N$ is half of the existing users. Hence, part of the potential users power $V_P$ *pow* can be satisfied by using part of the exceeding power $N_S$ *pow* of the available convertible users.

The results of scenario 4 are given in Table 6.7. It is possible to note that the number of connected potential users in Scenario 4 is higher than the number of potential users connected in Scenario 3. This is because in Scenario 4 there is additional power that can be obtained by an optimal subset of convertible users.

Note that in Scenario 4 the model can connect at most half of the available potential users, while in Scenario 3 there were not limits on the number of potential users that may be connected: despite that, the number of potential users connected in Scenario 4 is still higher than the number of potential users connected in Scenario 3.

With regard to the model robustness, we note that for this additional feature the computational time is higher, but the model is still quite fast.

Table 6.8 shows results for Scenario 5. This scenario is related to a basic network of 250 nodes and 100 potential users, which is connected to a complete potential network (a sort of new district where there is no district heating at all). The complete potential network is composed of 500 potential nodes (459 potential arcs) and an ascending number

of potential users (250, 500, 750, 1000). In this case the problem has a higher complexity since the model has to evaluate not only the optimal subset of potential users to be connected, but also all the possible pipe paths through which the potential users can be reached by the district heating system. The model contains all the decision variables and constraint related to all the feature together: potential users connection, client contract change decision, potential pipes connection, cost of different joints that affect the path choice.

For such Scenario the computational time becomes particularly high, but the analyses that can be made with such a combination of features are particularly strategic and can have a high impact on the Energy company decisions and investments.

In Table 6.9 we mimic the summary results of a what-if analysis on a single instance of the 250/500 set with the additional features related to the client contract change and the cost of different pipe connections. The table compares the results of further scenarios by also reporting the total value of the objective function in monetary units.

Scenario 6: reduction by 25% of the plant capacity, no limit on the number of potential users that may be connected, no limit on the number of convertible existing users that may change their contract.

Scenario 7: reduction by 25% of the plant capacity, at most half of the potential users can be connected, at most half of the convertible existing users may change their contract.

Scenario 8: reduction by 25% of the plant capacity, the model can connect at most half of the potential users that it connected in Scenario 6, no limit on the number of convertible existing users that may change their contract.

Scenario 9: reduction by 25% of the plant capacity, the model can connect at most half of the potential users that it connected in Scenario 8, at most half of the convertible existing users may change their contract.

Scenario 6 is similar to Scenario 3 of Table 6.6 as the plant capacity is reduced by 25% in both cases and there is no limit on the number of potential users that may be connected. In Scenario 6, however, there is the additional choice related to the client contract change.

We note that the net present value is almost the same for the two cases, but the number of connected potential users is higher in scenario 6: that is because part of the convertible existing users power has been used to connect further potential users. Hence it is possible to reach more potential clients at no additional costs.

If the company had to connect the additional potential users to the network without the convertible users feature, it would have had to build a new plant, as the current plant was already saturated. The net present value of Scenario 6 is not higher than the one of Scenario 3, because even though new potential users has been connected, there are costs associated to the power reduction of convertible users. Hence we can say it is possible to reach more potential users at no additional costs. The great saving in this case is related to the possibility to avoid an investment in a new plant.

In Scenario 9 no convertible users are selected. That is because there is a very tight limit on the number of potential users that may be connected: the costs related to the client contract change are higher than the revenues associated to the few potential users that may be connected through the additional power of the convertible users.

Table 6.7: Results for Scenario 4. Reduction by 25% of the plant capacity. At most 50% of potential users may be connected. At most 50% of existing users can change their contract. Average results for five instances

| $\lvert V_P\rvert/\lvert V_E\rvert$ ($n$) | $\lvert V_S\rvert$ ($n$) | $N_S$ (n) | Total $V_S$ pow (kW) | Total $N_S$ pow (kW) | Total $V_P$ pow (kW) | Conn. $V_P$ (n) | Conn. $V_P$ (%) | Conn. $V_P$ pow (kW) | Conn. $V_P$ pow (%) | Select $N_S$ (n) | Select $N_S$ (%) | Select $N_S$ pow (kW) | Gap U (%) | Gap H (%) | B&C Nodes (n) | Root Time (sec) | Total Time (sec) |
|---|---|---|---|---|---|---|---|---|---|---|---|---|---|---|---|---|---|
| 250/500 | 112 | 56.00 | 9912 | 6740 | 19086 | 70 | 28.00 | 10032 | 52.56 | 55 | 98.93 | 4180 | 0.02 | -0.12 | 134 | 2.87 | 5.86 |
| 500/500 | 109 | 54.30 | 9704 | 6598 | 36122 | 62 | 12.40 | 10583 | 29.30 | 54 | 99.45 | 4123 | 0.03 | -0.22 | 3377 | 7.25 | 50.19 |
| 750/500 | 109 | 54.40 | 10108 | 6873 | 56515 | 57 | 7.60 | 11120 | 19.68 | 54 | 99.26 | 4390 | 0.02 | -0.30 | 4506 | 11.11 | 94.66 |
| 1000/500 | 106 | 53.10 | 9708 | 6601 | 76038 | 50 | 5.00 | 10640 | 13.99 | 53 | 99.44 | 4173 | 0.03 | -0.70 | 4066 | 17.88 | 158.25 |

Table 6.8: Results for Scenario 5. Basic network of 250 nodes and 100 potential users, which is connected to a complete potential network. Reduction by 25% of the plant capacity and no limit on the number of potential users that may be connected. No limit on the existing users that can change their contract. The model has to evaluate also the cost of different joints as well as the optimal path to reach every selected potential user. Average results for five instances.

| $\lvert V_P\rvert/\lvert V_E\rvert$ ($n$) | $\lvert V_S\rvert$ ($n$) | $N_S$ (n) | Total $V_S$ pow (kW) | Total $N_S$ pow (kW) | Total $V_P$ pow (kW) | Conn. $V_P$ (n) | Conn. $V_P$ (%) | Conn. $V_P$ pow (kW) | Conn. $V_P$ pow (%) | Select $N_S$ (n) | Select $N_S$ (%) | Select $N_S$ pow (kW) | Gap U (%) | Gap H (%) | B&C Nodes (n) | Root Time (sec) | Total Time (sec) |
|---|---|---|---|---|---|---|---|---|---|---|---|---|---|---|---|---|---|
| 250/500 | 54 | 54 | 4911 | 3339 | 21318 | 80 | 32.00 | 8317 | 39.01 | 47 | 87.08 | 3004 | 0.77 | -26.42 | 1904 | 28.38 | 149.99 |
| 500/500 | 56 | 56 | 5044 | 3430 | 39489 | 87 | 17.40 | 8465 | 21.44 | 47 | 84.89 | 3002 | 9.76 | -100.00 | 9588 | 64.49 | 627.76 |
| 750/500 | 57 | 57 | 5205 | 3539 | 57641 | 74 | 9.87 | 9176 | 15.92 | 57 | 100.00 | 3539 | 5.39 | -94.48 | 30791 | 101.31 | 2557.08 |
| 1000/500 | 57 | 57 | 5187 | 3527 | 77167 | 68 | 6.80 | 9145 | 11.85 | 57 | 100.09 | 3527 | 6.45 | -100.00 | 15499 | 146.33 | 2761.89 |

Table 6.9: An example of what-if analysis conducted on a single instance of the 250/500 test set. The model has to choose the potential users to be connected as well as the existing users that can change their contract. The cost of different joints is also considered.

| $\lvert V_P\rvert/\lvert V_E\rvert$ (n) | $\lvert V_S\rvert$ (n) | $V_S$ pow (kW) | Total $V_N$ pow (kW) | Total $V_P$ pow (kW) | Total Scenario | $V_P$ (n) | Conn. $V_P$ (%) | Conn. $V_P$ pow (kW) | Conn. $V_P$ pow (%) | Select $V_N$ (n) | Select $V_N$ (%) | Select $V_N$ pow (kW) | Select $V_N$ pow (%) | $Z^*$ (mu) |
|---|---|---|---|---|---|---|---|---|---|---|---|---|---|---|
| 250/500 | 111 | 10840 | 6138 | 20509 | 6 | 84 | 33.6 | 12146 | 59.22 | 111 | 100.00 | 6138 | 100.00 | 6353424 |
| | | | | | 7 | 58 | 23.2 | 9613 | 46.87 | 55 | 49.55 | 3605 | 58.73 | 5515649 |
| | | | | | 8 | 42 | 16.8 | 7673 | 37.41 | 25 | 22.52 | 1666 | 27.14 | 4795219 |
| | | | | | 9 | 29 | 11.6 | 5806 | 28.31 | 0 | 0.00 | 0 | 0.00 | 3980588 |

## 6.7 Conclusions and Future Developments

An optimization approach for the optimal incremental design of district heating networks has been presented. The proposed mathematical model represents a valuable tool to support strategic decision analyses in the field: it has been conceived to incorporate the essential hydraulic characteristics of a real network together with the economic elements that allow to evaluate long-term scenarios. The model resulted fast to solve even for large networks and very robust with respect to variations of some parameters.

The future development will be in the direction of enriching the model so as to incorporate additional features that may be relevant in real-world applications. First of all, more complex network topologies such as those including either some loops in the backbone infrastructure of the network or multiple plants, need to be fully examined. We performed a preliminary testing on this type of networks and we obtained very encouraging results showing the capability of solving realistic sized networks. In addition several constraints or cost components may be considered, such as:

- the cost of the insertion of new tees in the potential network,
- the cost of pumping,
- the choice of the optimal diameters of the potential pipes,
- the choice of the optimal size of heat exchangers at potential users when it is possible to reduce their initial power demand,

Other interesting directions for future developments can be open by including in the optimization process also the creation of the potential network to be fed as an input to the current model. In such a case, the potential network is virtually a complete graph including all possible potential topologies from which the optimal one has to be selected. Because of the substantial increase in the difficulty of the resulting problems it will be appropriate to develop solution methods which belong to the field of matheuristics, where mathematical programming models are integrated into general heuristic solution frameworks that permit to consider complex problems within a reasonable amount of computing time.

An implementation of the proposed model has been incorporated by Optit srl, an accredited spinoff company of the University of Bologna, into a software tool for the strategic network design of DH networks. The tool, called Opti-TLR, is based on a public domain GIS for the representation of the network and of the solutions and solves the model through IBM ILOG Cplex. Opti-TLR (see Figure 6.8) has been used in the last three years in several projects of DH network design by several mayor utility companies in Italy.

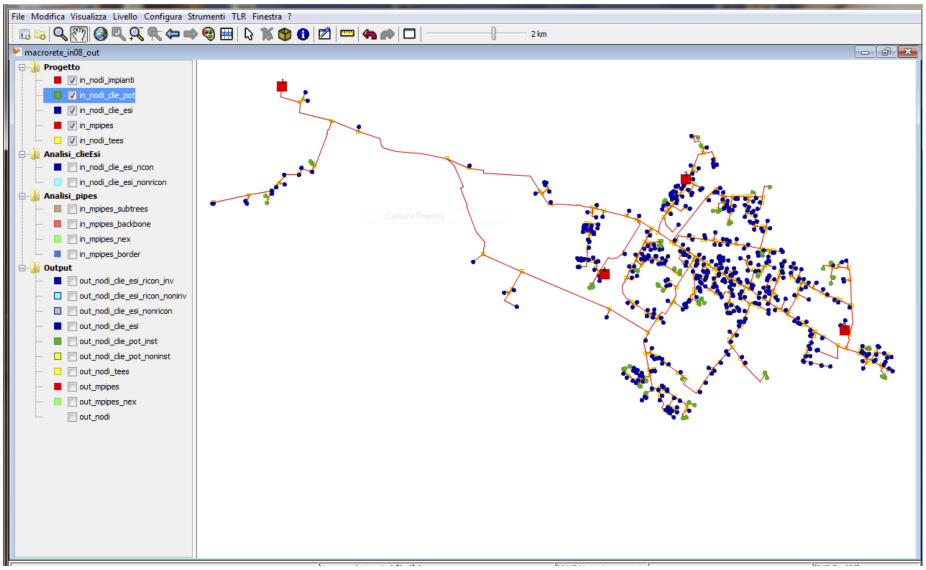


Figure 6.8: A screenshot of Opti-TLR: a Decision Support Tool for the design of DH networks which incorporates an implementation of the model described in this document.

## Acknowledgments

Research partially funded by Ministero dell'Università e della Ricerca, Italy. A preliminary research activity carried out within Progetto Innovami was partially funded by Regione Emilia-Romagna, Italy.

# Bibliography


[1] R. Aringhieri and F. Malucelli. Optimal operations management and network planning of a district heating system with a combined heat and power plant. *Annals OR*, 120(1–4):173–199, 2003.

[2] A. Benonysson, B. Bøhm, and H. F. Ravn. Operational optimization in a district heating system. *Energy Conversion and Management*, 36(5):297–314, 1995.

[3] B. Bøhm, M. Lucht, Y. Park, K. Sipil, S. Ha, K. Won-tae, K. Bong-kyun, T. Koljonen, H. Larsen, M. Wigbels, and M. Wistbacka. Simple models for operational optimization. *Contract*, 524110:0010, 2002.

[4] B. Bøhm, H. Pálsson, H. V. Larsen, and H. F. Ravn. Equivalent models for district heating systems. In *7th International Symposium on District Heating and Cooling*, pages 1–16, 2008.

[5] M. Fischetti, A. Lodi, and D. Salvagnin. Just MIP it! In V. Maniezzo, T. Stuetzle, and S. Voss, editors, *Matheuristics*, volume 10 of *Annals of Information Systems*, pages 39–70. Springer US, 2010.

[6] H. V. Larsen, H. Palsson, B. Bøhm, and H. F. Ravn. An aggregated dynamic simulation model of district heating networks. *Energy Conversion and Management*, 43 (8):995–1019, 2002.

[7] H. V. Larsen, B. Bøhm, and M. Wigbels. A comparison of aggregated models for simulation and operational optimisation of district heating networks. *Energy Conversion and Management*, 46(7–8):1119–1139, 2004.

[8] A. Loewen, M. Wigbels, W. Althaus, A. Augusiak, and A. Renski. Structural simplification of complex DH networks-part 1 (in german). *Euroheat and Power*, 30(5): 42–44, 2001.

[9] A. Loewen, M. Wigbels, W. Althaus, A. Augusiak, and A. Renski. Structural simplification of complex DH networks-part 2 (in german). *Euroheat and Power*, 30(6): 46–51, 2001.

[10] O. Pálsson. *Stochastic modeling, control and optimization of district heating systems.* PhD thesis, Inst. for MatematiskStatistik og Operationsanalyse, Technical University of Denmark, 1993.

[11] Y. S. Park, W. T. Kim, and B. K. Kim. State of the art report of Denmark, Germany and Finland. Simple models for operational optimization. Technical report, Department of Mechanical Engineering, Technical University of Denmark, 2000.

[12] M. Reini, D. Buoro, C. Covassin, A. De Nardi, and P. Pinamonti. Optimization of a distributed trigeneration system with heating micro-grids for an industrial area. *Distributed Generation and Alternative Energy Journal*, 26(2):7–34, 2011.

[13] F. Wernstedt, P. Davidsson, and C. Johansson. Simulation of district heating systems for evaluation of real-time control strategies. In *1st European Simulation and Modelling Conference*, 2003.

[14] H. Zhao. *Analysis, modelling and operational optimization of district heating systems.* Centre for District Heating Technology, Laboratory of Heating and Air Conditioning, Technical University of Denmark, DK-2800 Lyngby, Denmark, 1995.

[15] H. Zhao and J. Holst. Study on a network aggregation model in dh systems. *Euroheat and Power*, 27(4-5):38–44, 1998.

# Part III

# Electrical Energy Side Mathematical Programming Applications

# Chapter 7

# Power Systems Storage and Lead Acid Batteries Fundamentals

In this chapter we introduce the main theory in the field of storage technology for off-grid systems. This is made to build the most important background that will be useful to understand the mathematical models and computational tests that will be presented in the following Chapter 8.

Section 7.1 will present a brief introduction to motivate the proposed study and underline the key issues in terms of storage integration in off-grid systems. The following Section 7.2 will be dedicated to a description of the most important battery properties that will be considered in our mathematical model. Section 7.3 will discuss the kinetic battery representation to take into account the chemical processes involved in the battery charge and discharge operations, while Section 7.4 will explain in more detail the main degradation issues involved in the charge/discharge operations. The last Section 7.6 will discuss some formulations for the definition of a battery degradation cost.

## 7.1 Introduction

Storage technologies and storage integration are currently key issues for most of the researchers working in the energy field, especially when they have to deal with the increasing integration of renewable energy.

Off-grid power systems in particular have received a wide attention around the world as they allow to bring electricity to remote rural areas at lower costs than grid extension. They are based on one or more renewable energy sources (i.e. PV or wind) together with a conventional power generator to provide backup when it is necessary. Sometimes and in certain parts of the world such as Africa villages, the conventional generator can be absent and the community will commit its energy needs just to the renewable availability, allowing a portion of unmet demand. In this latter case the presence of a storage unit becomes essential to eventually store the exceeding energy and provide it when it is needed: this way it is possible to cover a higher portion of demand. However, beyond these extreme cases, storage units are usually integrated in offgrid systems as they represent an alternative energy source to the conventional generator use which induces high operations costs due to the fuel consumption in addition to the CO2 emissions. For these reasons the possibility to store the renewable Energy is generally highly appealing. Especially in Off-Grid applications batteries perform several important tasks such as absorbing short-

term intermittence of the renewable resources, extending the electrical service hours to night time periods and giving the system an autonomy of many hours or even several days without any power generation.

As storage units in general and batteries in particular requires important investment costs, the main question that arises from this current scenario is how storage operations might be carried out in a more economical way, as there are important degradation issues involved in such technologies; issues that are generally overlooked both during the system design and during the hourly operation management of the system. And since these batteries technologies implies operations costs due to degradation issues, are they still cost effective for the general operating costs of a system? These kind of questions can be well studied through the Mathematical Optimization techniques. In particular linear programming can be very useful in defining whether certain choices are cost effective or not and, if not, understanding under which conditions they can become cost effective and how to make a better use of the available alternatives.

Our research was motivated by a field project on operation of off-grid storage in Rwanda carried on at Durham University In particular, after a mathematical modeling definition, some computational tests using real world data from a site in Rwanda will be presented in Chapter 8. The main objective is to show how the battery use changes with different degradation cost structures. The key of this step is the definition of a battery degradation cost that will be introduced in Section 7.2) and that will take us towards sensitivity analyses in Chapter 8, to explore how much battery costs have to come down before the decisions become subtle and what trade offs there are, looking forward to when the battery technology is more economical. In particular we will investigate when batteries become more economical in a forecasted scenario in which diesel price will continue to increase and battery costs drop, as well as when battery price become interesting as a function of the declared lifetime throughput. These analyses will also give us answers on the best type of use for batteries that lies in a certain range of price. It will be the case that with the current technology, the optimized use of batteries will suggest to keep them just for backup and emergency, but as the costs change we will see how deeper cycles and intensive use become more convenient.

## 7.2 Main Battery Properties

In order to build a linear programming model that can be strongly focused on the battery degradation optimization, it is very important to be aware of what factors affect the battery lifetime and which are the most important battery properties to consider. For that purpose there is a wide literature related to chemical analyses and laboratory tests (Jarno et al. [5]), methodological papers related to battery lifetime prediction (Monika et al. [11], Peng and Pedram [12]), general guidelines on battery optimal management (Atcitty et al. [1]) as well as useful literature reviews about battery degradation processes from a chemical and material point of view (Kanevskii and Dubasova [7]). None of these papers are aimed at developing degradation cost fictions in a form suitable for inclusion in optimization models, but they represent a good starting point to have an overview of battery properties and degradation processes. There are also other useful works that give good inputs about battery degradation cost definition and calculation (Michael et al. [10]) as well as general battery lifetime modeling Bindner et al. [2].

The main battery properties that we need to consider inside an operational management optimization problem are: max charge power $h^t_{char}$ (kWh) that defines the maximum

amount of power that can be absorbed by the battery in every time step t; max discharge power $h^t_{dis}$ (kWh) that defines the maximum amount of energy that can be withdrawal from the battery in every time step t; nominal voltage $V$ (V) which is the reference voltage provided by manufacturers; minimum state of charge $S$ (kWh) below which the battery must not be discharged to avoid permanent damage; maximum charge rate $\alpha$ (A/Ah), that is the maximum allowable charge rate measured in amp per amp-hours of unfilled capacity; maximum charge current $I$ (A) which is the absolute maximum charge current regardless of the state of charge; nominal capacity $Q_{max}$ (kWh) that indicates the rated capacity of the battery; square root of the roundtrip efficiency $Eff$ (%) which indicates the percentage of the energy going into the battery that can be drawn back out. Note that the roundtrip efficiency of the battery represents the total efficiency of charging and discharging. The square root gives the efficiency in one direction. This assumes the battery efficiency is symmetric. It may be that more is lost when charging than when discharging, but for modeling purposes, symmetry is always assumed.

The nominal capacity is often measured by Ah (number of Amperes that can be taken from battery multiplied by time how long this current can be taken). As our model is focused on energy flows defined in kWh, we will calculate the battery capacity as battery voltage multiplied by Ah ($V * A * h = Wh$) assuming a constant battery voltage.

## 7.3 Charge/Discharge Processes and Kinetic Modeling

There are two main ways to think about charge/discharge processes of batteries. The simplest one - and the most commonly used in literature - is the one-tank model with a fixed capacity and no limit to the charge and discharge rates. A more detailed approach to determine the amount of energy that can be absorbed by or withdrawn from the battery bank on each time step, is the Kinetic Battery Model described in Manwell and McGowan [9]. This latter approach is the one we will use in our study.

The kinetic battery model is based on the concepts of electrochemical kinetics and it represents a battery as a two tank system. The first tank contains *available energy*, that is energy that is readily available for conversion to electricity. The second tank contains *bound energy*, that is energy that is chemically bound and therefore not immediately available for withdrawal. The following Figure 7.1 illustrates the concept:

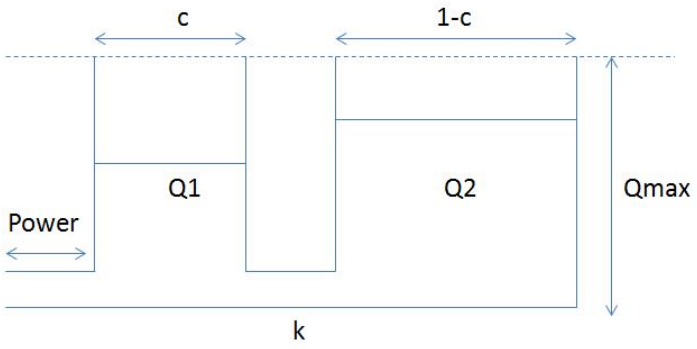


Figure 7.1: Two-tanks kinetic battery model representation

The total amount of energy stored in the battery at any time t $Q^t_j$ is the sum of the

available energy $Q1^t$ and bound energy $Q2^t$.

In order to describe this two tank system we will need three parameters in our mathematical model: the maximum battery capacity ($Q_{max}$) which is the total amount of energy the two tanks can contain; the capacity ratio (c) which is the ratio of the size of the available energy tank to the combined size of both tanks; the rate constant (k) which relates to the conductance between the two tanks, it is a measure of how quickly the battery can convert bound energy to available energy or vice-versa and it is analogous to the size of the pipe between the tanks. These values can be derived from battery data provided by manufacturers. In particular it is necessary to fit data from the battery capacity curve (which shows the discharge capacity of the battery in Ah versus the discharge current in A) to the kinetic battery model with a numerical algorithm (i.e. simulated annealing, see Saul et al. [13] for further details).

In our mathematical model we will define the value of $Q1^t$ and the maximum charge and discharge power in every time step as well as the battery constants using the kinetic battery model formulas available in Manwell and McGowan [9].

As described in Lambert et al. [8], if we model the battery as a two-tank system rather than a single-tank system we can get two effects. The first one is that the battery will never be fully charged or discharged all at once. The second one is that the battery ability to charge and discharge will depend on its recent charge and discharge history and not only on its current state of charge. Hence the Kinetic Battery Model approach will allow us a more detailed representation of the battery behavior.

## 7.4 Main Considerations on Battery Degradation Issues

The life of a battery can be measured by the number of times it can be cycled before it is no longer able to deliver sufficient energy to satisfy the load requirements of the system IEEE1013-2007 [3]. There are two main definitions of a battery *cycle*. A *full cycle* refers to a sequence of discharge-charge operations that takes a fully charged battery down during discharge and then back to full charge again. On the contrary a *partial cycle* refers to a sequence of discharge-charge that can start and/or end with a not fully charged battery.

In Kaise et al. [6] several stress factors were identified, which were defined as quantities that, either directly or indirectly, affect the battery life, even though they are not themselves ageing mechanism that cause irreversible degradation. The found major stress factors are discharge rate, time at low state of charge, Ah throughput, charge factor, time between full charge, partial cycling and temperature.

In general the number of cycles of battery operation depends on the factors that can be grouped in: cell design, use and operating temperature IEEE1013-2007 [3]. Particularly, we are going to focus on the following stress factors Svoboda et al. [14]:

- Depth of discharge. The published cycle-life values are usually given at several different depth of discharge. The shallower the depth of discharge the greater the cycle-life IEEE1361-2003 [4]
- Number of cycles. As the life of the battery can be measured by the number of times it can be cycled, the higher the number of cycles is during the battery use, the shorter the battery lifetime will be.
- Ah throughput. It is expressed as the cumulative energy discharged per year and it represents the type of operation: it can be used to distinguish between a back up

battery operation and between a full cycling operation.

- Time between fully charged states. This is the average time in days between recharging the battery to a full state of charge. Generally a value of 90% as full state of charge criteria is chosen for practical reasons.

- Insufficient recharge (partial cycles). Insufficient time at the available charge rate results in an undercharged battery. Failure to properly recharge a battery limits its capacity. A discharge cycle that starts with a battery full of energy is less damaging than the same discharge cycle that starts with a battery less full of energy (different battery contents at the beginning of a discharge cycle have different impacts on the battery wearing).

## 7.5 Battery Lifetime and Lifetime Throughput

The battery lifetime is usually calculated through an approximated value that is called lifetime throughput. We described in the following lines this kind of approach.

The lifetime of a battery is generally calculated as a function of three values: the number of batteries in the battery bank, the lifetime throughput and the annual throughput.

Figure 7.2 shows a screenshot of the Homer software interface, that contains a good example of a battery's lifetime curve and data.

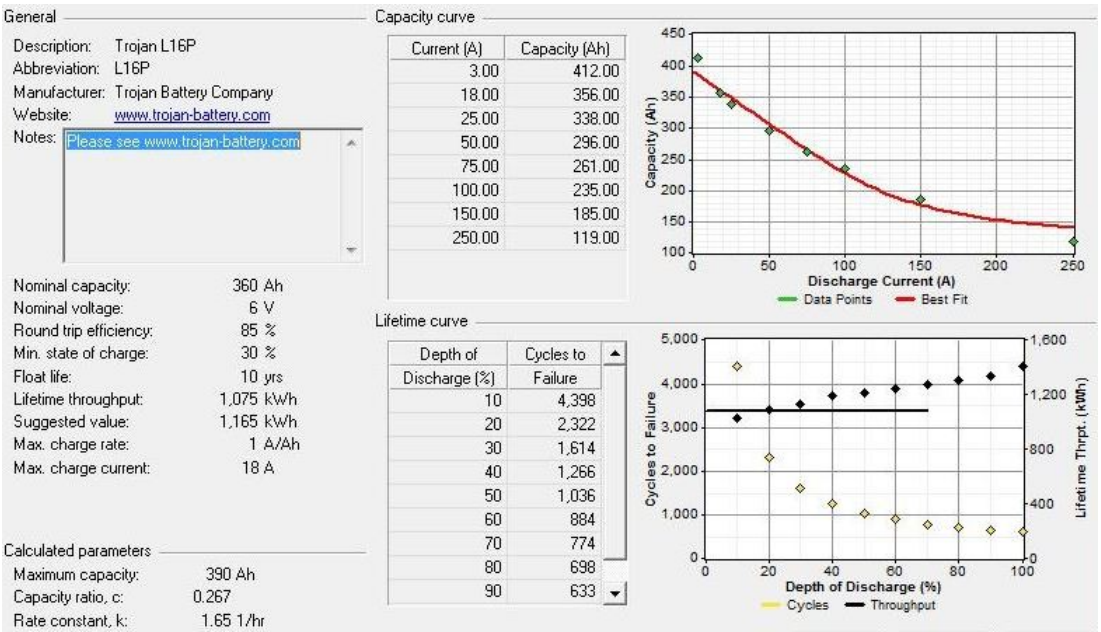


Figure 7.2: A screenshot of the Homer software interface: battery data and battery curves provided by manufacturers. Example of a Trojan battery L16P

The values entered in the table of cycles-to-failure versus depth-of-discharge appear as white diamonds. For each of those $n$ points, it is possible to calculate a value of the lifetime throughput $LT_n$ (where $n$ corresponds to each line of the table) using the following equation:

$$LT_n = Q_{max} * d_n * f_n \tag{7.1}$$

where:
$Qmax$ is the battery capacity (kWh)
$f_n$ is the number of cycles to failure of the table's line $n$
$d_n$ is the depth of discharge of the table's line $n$ (%)

The resulting set of points appear as black diamonds on the lifetime curve of Figure 7.2. Then the lifetime throughput $LT$ of the battery is obtained by averaging the $n$ values of lifetime throughput $LT_n$ in the allowable range of depth of discharge.

$$LT = \sum_{l=1}^{n} LT_n/n \tag{7.2}$$

Note that the allowable range is determined using the minimum state of charge: for instance, if the minimum state of charge is 30%, then the battery will only experience depths of discharge between 0% and 70%. That means that, for this example, in the Lifetime Throughput calculation, we will only use the first 7 values available in the table of cycles-to-failure versus depth-of-discharge (and we will averaging dividing by 7 and not by 10)

### 7.5.1 Numerical Example of Lifetime Throughput Calculation

Consider a battery with a minimum state of charge of 30%, a maximum capacity of 360 $Ah$, a voltage of 6 $V$ and values of cycles to failure versus depth of discharge listed in the following Table 7.1:

Table 7.1: Cycles-to-failure versus depth-of-discharge

| depth-of-discharge | cycles-to-failure |
|---|---|
| 0.1 | 4398 |
| 0.2 | 2322 |
| 0.3 | 1614 |
| 0.4 | 1266 |
| 0.5 | 1036 |
| 0.6 | 884 |
| 0.7 | 774 |
| 0.8 | 698 |
| 0.9 | 633 |
| 1 | 600 |

We can define for every line $n$ of the table the value of $LT_n = Q_{max} * d_n * f_n$ (where $d_n$ is the depth of discharge in line $n$ and $f_n$ is the cycles to failure value in line $n$). The following Table 7.2 contains the value of $LT_n$ for every line $n$ in the third column (for example, the first line LT value is $(6 * 360/1000) * 0.1 * 4398 = 950$):

Table 7.2: Lifetime throughput calculations for every depth of discharge

| depth-of-discharge | cycles-to-failure | LT |
|---|---|---|
| 0.1 | 4398 | 950 |
| 0.2 | 2322 | 1003 |
| 0.3 | 1614 | 1046 |
| 0.4 | 1266 | 1094 |
| 0.5 | 1036 | 1119 |
| 0.6 | 884 | 1146 |
| 0.7 | 774 | 1170 |
| 0.8 | 698 | 1206 |
| 0.9 | 633 | 1230 |
| 1 | 600 | 1296 |

Now we can calculate the Lifetime Throughput by averaging the $LT_n$ values calculated in the table above. But we need to remember that the battery has a minimum state of charge of 30% so we will not average all the values shown in the table: we will average the values from 0.1 to 0.7 depth of discharge (in fact 100% - 30% = 70%).

Hence the Life Time Throughput will be calculated as follow:

$$LT = \frac{950 + 1003 + 1046 + 1094 + 1119 + 1146 + 1170}{7} = 1075 \tag{7.3}$$

The battery life (years of life) $LY$ can be derived from the lifetime throughput defined above, using the following equation:

$$LY = \frac{N * LT}{AT} \tag{7.4}$$

where N is the number of batteries in the battery bank, while $AT$ is the annual throughput. The annual throughput is a value that can be calculated at the end of the time horizon (generally one year) and it is equal to the summation of the charge power values ($kWh$) in every time step $t$. As highlighted before, we must remember the energy losses that occur during the charge/discharge process, so for every time step $t$ we need to multiply every charge power by the square root of the roundtrip efficiency of the battery $Eff_j$.

## 7.6 Battery Degradation Cost Definitions

In order to run an optimization model we will need to build an objective function that is a cost minimization one. Thus, every degradation issue will have to be treated in the objective function multiplying the related decision variables by a representative battery degradation cost.

In the present study we will refer to two ways to calculate the battery degradation cost. One related to the battery throughput which refers to a cost per kWh out the battery and the other one related to the battery cycles to failure which refers to an average cost per cycle. Further descriptions of these two costs follow.

### 7.6.1 Cost per kWh

The battery degradation cost can be defined as the cost of the energy through the battery bank. We can assume the battery bank will require replacement once its total throughput equals its lifetime throughput. Each $kWh$ of throughput brings the battery bank closer to needing replacement. From that point of view, the battery degradation cost per $kWh$ $BDC_{kWh}$ can be defined using the following equation:

$$BDC_{kWh} = \frac{C_{rep}}{LT * Eff_j} \tag{7.5}$$

Where:
$C_{rep}$ replacement cost of the battery ($)
$LT$ the lifetime throughput of the battery (kWh)
$Eff_j$ the square root of the roundtrip efficiency of the battery (%)

This cost can be used every time the battery is discharging as a cost per $kWh$ out the battery.

### 7.6.2 Cost per Cycle

The second way to calculate the battery degradation cost is related to the cycles to failure. We can use the lifetime curve provided by manufacturers and we can calculate the cost per cycle for every depth of discharge n as a fraction of the battery capital cost $C_{rep}$ and the remaining cycles to failure $f_n$ as shown in formula (7.6).

$$BDC^n_{cycle} = \frac{C_{rep}}{f_n} \tag{7.6}$$

See in Table (7.3) a numerical example related to a Troian battery L16P with a capital cost of 300 $.

Table 7.3: Cycle cost associated to every depth of discharge

| depth-of-discharge | cycles-to-failure | cycle cost |
|---|---|---|
| 0.1 | 4398 | 0.07 |
| 0.2 | 2322 | 0.13 |
| 0.3 | 1614 | 0.19 |
| 0.4 | 1266 | 0.24 |
| 0.5 | 1036 | 0.29 |
| 0.6 | 884 | 0.34 |
| 0.7 | 774 | 0.39 |
| 0.8 | 698 | 0.43 |
| 0.9 | 633 | 0.47 |
| 1 | 600 | 0.50 |

Figure 7.3 shows the trend of the cycle cost as function of the depth of discharge. The trend in this case is almost linear and can be successfully approximated and then inserted

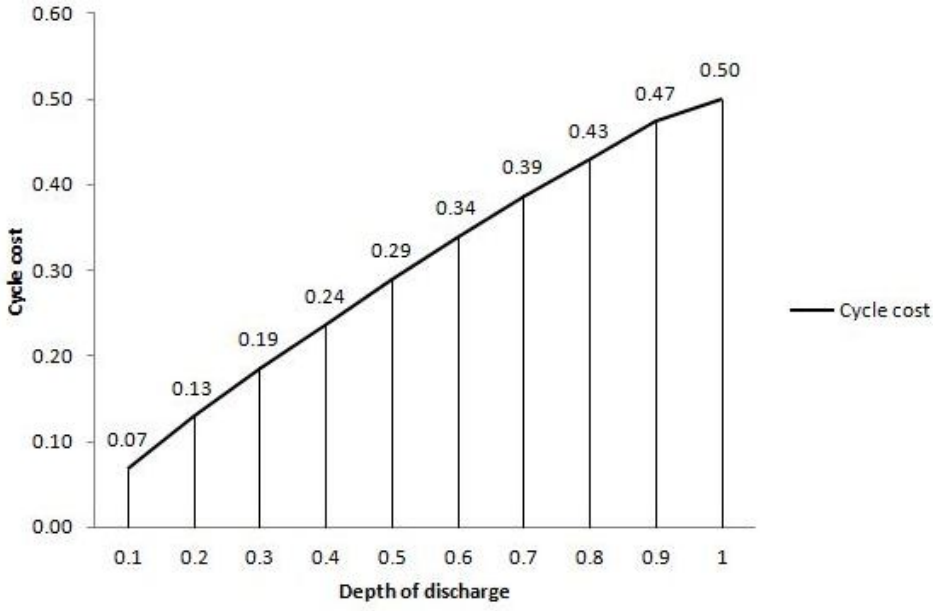


Figure 7.3: Representation of the cycle cost as function of the depth of discharge for a Troian battery L16P

in a linear programming model. The idea is that say we have different depth of discharge values and different cycle life values, we calculate the cost per cycle for each depth of discharge. We calculate the value for the whole battery bank (capital cost) and then store up the costs of every discharge cycle until we get to the max capital cost: then the battery has to be replaced.

# Bibliography


[1] S. Atcitty, P. C. Butler, G. P. Corey, and P. C. Symons. Optimal management of batteries in electric systems, Mar. 5 2002. US Patent 6,353,304.

[2] H. Bindner, T. Cronin, P. Lundsager, J. F. Manwell, U. Abdulwahid, and I. Baring-Gould. *Lifetime modelling of lead acid batteries*. 2005.

[3] IEEE1013-2007. Recommended practice for sizing lead-acid batteries for stand alone photovoltaic (pv) systems. Technical report, IEEE, 2007.

[4] IEEE1361-2003. Guide for selection, charging, test and evaluation of lead-acid batteries used in stand alone photovoltaic (pv) systems. Technical report, IEEE, 2003.

[5] D. D. Jarno, R. Bart, and D. J. N. Frans. Characterization of li-ion batteries for intelligent management of distributed grid-connected storage. *IEEE Transactions on Energy Conversion*, 26, 2010.

[6] R. Kaise, G. Bopp, H. Wenzl, N. Renewable, N. Wimot, A. Carr, M. L. Gall, G. E. D. Cadarache, C. Tselepis, C. Rodrigues, and I. Technology. Work package 4.3: benchmarking processes and recommendations, 2005.

[7] L. S. Kanevskii and V. S. Dubasova. Degradation of lithium-ion batteries and how to fight it. a review. *Russian Journal of Electrochemistry*, 41(1):1, 2005.

[8] T. Lambert, P. Gilman, and P. Lilienthal. Micropower system modeling with homer. *Integration of alternative sources of energy*, 1, 2006.

[9] J. F. Manwell and J. G. McGowan. Lead acid battery storage model for hybrid energy systems. *Solar Energy*, 50, 1993.

[10] K. Michael, B. Theodor, U. Andreas, and G. Andersson. Defining a degradation cost function for optimal control of a battery energy storage system. In *PowerTech*, 2013.

[11] C. Monika, N. rajendra, B. Rajni, and W. Herman. Utility energy storage life degradation estimation method. In *Innovative Technologies for an Efficient and reliable Electricity Supply*, 2010.

[12] R. Peng and M. Pedram. An analytical model for predicting the remaining battery capacity of lithium-ion batteries. *IEEE Transactions on Very Large Scale Integration Systems*, 14, 2006.

[13] A. T. Saul, T. V. William, and P. F. Brian. *Numerical Recipes in C++: The Art of Scientific Computing*. Cambridge Univ Pr (Sd).

[14] V. Svoboda, H. Wenzl, R. Kaiser, A. Jossen, I. Baring-Gould, J. Manwell, P. Lundsager, H. Bindner, T. Cronin, P. Nørgård, et al. Operating conditions of batteries in off-grid renewable energy systems. *Solar Energy*, 81(11):1409–1425, 2007.

# Chapter 8

# MILP Models for Optimal Battery Management in Off Grid Systems

The present chapter will discuss mathematical formulations to build linear programming models that can be used to find the optimal hourly management of Solar Off-Grid Systems, focusing on batteries degradation issues and allowing the integration of existing design softwares (i.e. Connolly et al. [9]) with more aware battery modeling. One of the main questions we want to answer to is whether it is possible to find a good balance between storage needs and cost reduction needs and how does this affect the system design choices and the system operational reliability.

The chapter starts with a brief literature review in Section 8.1 where the main works in the field of mathematical programming for the battery degradation modeling are discussed. In Section 8.2 we will present a basic mathematical model that defines the hourly optimal management of an off-grid system, minimizing the energy costs of the conventional generator production and allowing an optimal use of the available renewable energy, through optimized battery charge/discharge operations. Then in Section 8.3 this first basic model will be further developed adding features to mathematically describe the main battery degradation issues involved in the charge/discharge cycles and reduce some of the major stress factors. Computational experiments on a real world site in Rwanda and sensitivity analyses will be discussed in Section 8.4. The next two sections will be dedicated to further developments of the proposed model. We will add features to allow further analyses in different scenarios. Section 8.5 will discuss how the preliminary design of an off-grid system can change when battery degradation issues are considered, with particular regard to the additional PV production required to guarantee a healthier battery lifetime. Then Section 8.6 will study a different Scenario in which the demand flexibility makes it possible to run systems without generator but with a better battery use, by disconnecting some flexible loads. Conclusions and future developments will be illustrated in Section 8.7

## 8.1 Literature Review

The batteries degradation issues have received a wide attention in literature, although linear programming approaches are quite rare and mostly dedicated to system design problems (Di et al. [10], Chedid and Saliba [8], Pascal et al. [20]) or to operational management and scheduling problems (Bo and Mohammad [6]) without any particular attention to battery degradation processes and battery use optimization.

The majority of works is focused on grid connected systems with arbitrage and investment decisions (Faisal and Heikki [11], Mohamed and Koivo [18]), even though there are some studies related to islanded systems as well (Bakirtzis and Dokopoulos [5], Hugo et al. [14]), but the battery degradation issues are not considered.

Other papers use dynamic programming and heuristics and metaheuristics approaches (i.e. genetic algorithms and neural networks) to study the optimal operations management of grid connected energy systems with storage (Jen-Hao et al. [15], Yann et al. [26],) and some of them take into account the reduction of battery stress during operations (Maly and Kwan [17], Saeed et al. [22], Angel et al. [3]).

There is a wide literature related to battery control in the electric vehicle field, where the main purpose is to define the optimal scheduling of vehicle charging (Lombardi et al. [16], Anderson et al. [1], Hoke et al. [13]). These studies belong to a different field where the issues related to the renewable availability and integration in offgrid systems don't need to be considered.

Some studies are more focused on battery control and degradation issues, but they are generally related to grid connected systems and the battery modeling usually turns out to be very simple. In fact the battery control is made using very strong assumptions as inputs, for instance, defining a priori an upper bound on the maximum number of allowable cycles (Shinya et al. [24], Shinya et al. [23]) or defining upper bounds and lower bounds on the state of charge of the battery (Rakesh and Ratnesh [21]).

An optimization model can give more complete results if it is built in such a way that number of cycles and state of charge (as well as other degradation properties) are considered as variables rather than as input parameters. This way deeper analyses on balancing cost of using battery against benefits can be done and the optimal trend of use for the battery can be found without affecting the final results with assumptions that tend to limit the model decisions. The key point is that if one can assign costs to battery cycles of different natures, then the optimization approach will be more directly related to minimizing the true costs of operating the battery. This will be the major focus of the study proposed in the present chapter.

## 8.2 A Mathematical Model for the Battery Optimal Management in Off Grid Systems with Renewable Integration

In this section we introduce a mathematical formulation for the battery optimal management in Off-Grid systems while in the following section we will discuss features to take into account the main degradation issues. Figure 8.1 shows the energy flows among the different units that will represent decision variables in our optimization model. When the conventional generator is on it can send energy directly to the final users ($x^t_{pd}$) or to the storage units. Since the storage belongs to the DC side and the conventional generator belongs to the AC side, we need a converter unit (rectifier) so that the flow from the conventional generator to the storage will be split into a flow $x^t_{pr}$ from the conventional generator to the rectifier and another flow $x^t_{rj}$ from the rectifier to the storage.

The final demand can be met also using the energy stored in the battery. In this case the flow must be split too since the demand belongs to the AC side and the storage belongs to the DC side. We have a flow from the storage to the inverter $x^t_{jv}$ and a flow from the inverter to the final demand $x^t_{vd}$. Note that the converter units may have different

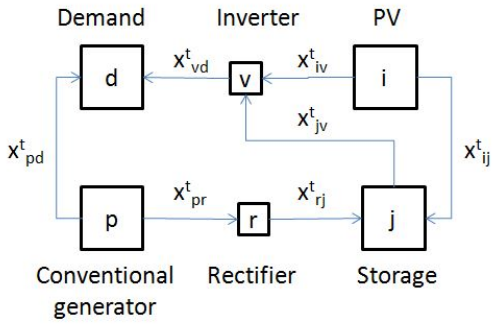


Figure 8.1: Off-grid power system block diagram and simplified energy flows for the linear programming model

Table 8.1: Continuous decision variables

| | |
|---|---|
| $x^t_{ij}$ | energy that flows from the renewable source i to the storage unit j in time t |
| $x^t_{iv}$ | energy that flows from the renewable source i to the inverter v in time t |
| $x^t_{jv}$ | energy that flows from the storage unit j to the inverter v in time t |
| $x^t_{vd}$ | energy that flows from the inverter v to the final users d in time t |
| $x^t_{rj}$ | energy that flows from the rectifier r to the storage unit j in time t |
| $Q^t_j$ | battery energy content in time t |
| $Q1^t$ | available energy in the battery in time t |

Table 8.2: Semi continuous decision variables

| | |
|---|---|
| $x^t_{pd}$ | energy that flows from the conventional generator p to the final users d in time t |
| $x^t_{pr}$ | energy that flows from the conventional generator p to the rectifier r in time t |

efficiency values in case they are inverter or rectifier.

There is also the possibility to send energy from the renewable source to the final users: in this case there is a flow $x^t_{iv}$ from the renewable source i to the inverter v and a flow $x^t_{vd}$ from the inverter v to the final users d.

Note that we will need to consider the total flow into the battery ($x^t_{rj}$ plus $x^t_{ij}$) and the flow out from the battery ($x^t_{jv}$) as mutually exclusive flows, since it is not physically allowed for the same battery unit to do charge and discharge cycles at the same time.

We assume that the voltage is constant and equal to the nominal voltage (instead of considering a battery with an internal resistance that causes the voltage to rise above the nominal voltage during charging, and drop below the nominal voltage during discharging.) We also assume that the battery has a constant round-trip energy efficiency, independent of the rate of charge/discharge and independent of the state of charge.

We consider a time step t of one hour. Note that the interval time t is related to what happen at the beginning of every time step.

Let us consider the system represented in Figure 8.1, the decision variables listed in Tables 8.1, 8.2 and the parameters listed in Table 8.3. The resulting mathematical model for the basic hourly operation management problem follows.

Table 8.3: Parameters

| | |
|---|---|
| $T$ | programming period |
| $0 < t \leq T$ | interval time (one hour h) |
| $d^t$ | final users demand defined for period t (kWh) |
| $R^t$ | renewable energy forecast production in period t (kWh) |
| $K_p$ | cost of the energy produced by the conventional generator ($/kWh) |
| $PP_p$ | conventional generator minimum production (kWh) |
| $PC_p$ | conventional generator capacity (kW) |
| $\lambda_v$ | efficiency of the inverter v (%) |
| $\lambda_r$ | efficiency of the rectifier r (%) |
| $Qmax$ | battery capacity (kWh) |
| $Eff_j$ | square root of the roundtrip efficiency of the battery j (%) |
| $S_j$ | minimum state of charge of the battery j (%) |
| $c$ | battery capacity ratio (unitless) |
| $k$ | battery rate constant (1/h) |
| $N$ | number of cells in the battery bank (n) |
| $V$ | nominal voltage of the battery (V) |
| $I$ | battery maximum charge current (A) |
| $\alpha$ | battery maximum charge rate (A/Ah) |

**OBJECTIVE**

$$\min \sum_t C_G^t + C_B^t \tag{8.1}$$

The objective function (8.1) aims at minimizing the energy cost $C_G^t$ of the conventional generator and the total degradation costs $C_B^t$ related to the battery use.

The conventional generator cost is given by $C_G^t = \sum_t (x_{pd}^t + x_{pr}^t) * K_p$. It minimizes the cost of energy that flows from the conventional generator to the final users $x_{pd}$ and from the conventional generator to the battery $x_{pr}$, by multiplying the $kWh$ out the conventional generator by the energy cost per $kWh$ $K_p$.

The battery total degradation cost $C_B^t$ is defined as a function of one or more battery stress factors $s$ and their related costs. Hence $C_B^t = f(s)$ where $f(s)$ can be a function of: the lowest depth of discharge reached along a representative period $C_B^t = f(Qm)$; the battery energy content at the end of a discharge cycle $C_B^t = f(Q_{end})$; the battery energy content at the beginning of a discharge cycle $C_B^t = f(Q_{start})$; the number of cycles along a representative time horizon $C_B^t = f(N)$; the amount of energy out the battery $C_B^t = f(x_{jv})$.

The mathematical modeling for all of these battery degradation functions will be further explained in following sections, to show how the objective function and constraints of this basic mathematical model can be modified to take into consideration one or more battery stress factors.

Note that if we impose $C_B^t = 0$ we will obtain an optimization result that reflects the actual current Off-Grid systems behavior focused just on diesel costs minimization regardless of battery degradation issues.

**CONSTRAINTS**

**Meet demand**

$$x_{pd}^t + x_{vd}^t = d^t \quad \forall t \tag{8.2}$$

Constraint (8.2) reflects the fact that the final users demand must be completely met with one of the two flows.

**Conventional generator properties**

$$(x_{pd}^t + x_{pr}^t = 0) || (PP_p \leq x_{pd}^t + x_{pr}^t \leq PC_p) \quad \forall t \tag{8.3}$$

From an operational point of view we must respect a minimum plant production $PP_p$ and a maximum plant capacity $PC_p$. For this purpose the semi continuous variables $(x_{pd}^t + x_{pr}^t)$ can be inserted in a disjunction constraint (8.3). The use of semi-continuous variables will allow us to avoid the explicit use of binary variables (i.e. variables that are equal to 1 if the plant is on and equal to 0 if the plant is off) and improve the model speed.

**Converter units efficiency**

$$x_{vd}^t = (x_{iv}^t + x_{jv}^t) * \lambda_v \quad \forall t \tag{8.4}$$

$$x_{rj}^t = x_{pr}^t * \lambda_r \quad \forall t \tag{8.5}$$

Constraint (8.4) and (8.5) are used to take into account the loss of energy due to the inverter efficiency $\lambda_v$ and the rectifier efficiency $\lambda_r$.

**Renewable source capacity**

$$x_{iv}^t + x_{ij}^t \leq R^t \quad \forall t \tag{8.6}$$

Constraint (8.6) is inserted to control the flows from the renewable source: their summation must respect the maximum forecast production of the renewable source in time $t$.

**Initial values of battery variables**

$$Q_j^t = Q_j^{max} \quad \forall t = 0 \tag{8.7}$$

$$Q_1^t = c * Q_j^{max} \quad \forall t = 0 \tag{8.8}$$

Constraints (8.7) and (8.8) define the initial values ($t = 0$) of the battery content $Q_j^t$ (the battery is assumed completely charged) and of the variable $Q_1^t$ that will be used inside the max charge and discharge constraints. The parameter $c$ is the battery capacity ratio defined as input.

**Minimum battery charge level**

$$Q_j^t \geq S_j \quad \forall t \tag{8.9}$$

The battery properties impose that the battery content can't be less than a minimum value as expressed in constraint (8.9) where $S_j$ is the minimum state of charge defined as input.

**Charge and discharge processes management**

The last following constraints define the charge and discharge processes through the Kinetic Battery Model formulas introduced in the previous paragraph.

$$Q_j^t = (Q_j^{t-1} - (x_{jv}^t * \frac{1}{Eff_j}) + x_{rj}^t + x_{ij}^t \quad \forall t > 0 \tag{8.10}$$

Constraint (8.10) defines the current value of the battery energy content for every time step t taking into account the loss of energy due to the discharge process $Eff_j$

**Battery max discharge**

$$x_{jv}^t \leq h_{dis}^t * Eff_j \quad \forall t \tag{8.11}$$

Constraint (8.11) contains the max discharge power formula where $h^t_{dis}$ is expressed by the following equation according to the Kinetic Battery Model formulation:

$$h^t_{dis} = \frac{Q^t_1 * k * e^{-k*\delta t} + Q^t_j * k * c * (1 - e^{-k*\delta t})}{1 - e^{-k*\delta t} + c * (k * \delta t - 1 + e^{-k*\delta t})}$$

**Battery max charge**

$$x^t_{rj} + x^t_{ij} \leq h^t_{char} \quad \forall t \tag{8.12}$$

Constraint (8.12) contains the max charge formula where $h^t_{char}$ is expressed by the following formula:

$$h^t_{char} = [Min(H^t_1, H^t_2, H_3)] * \frac{1}{Eff_j}$$

According to the Kinetic Battery Model formulation the values of $H_1$ $H_2$ and $H_3$ are the following:

$$H^t_1 = \frac{Q_{max} * k * c - Q^t_1 * k * e^{-k*\delta t} - Q^t_j * k * c(1 - e^{-k*\delta t})}{1 - e^{-k*\delta t} + c * (k * \delta t - 1 + e^{-k*\delta t})} \tag{8.13}$$

$$H^t_2 = \frac{(1 - e^{-\alpha*\delta t}) * (Q^{max}_j - Q^t_j)}{\delta t} \tag{8.14}$$

$$H_3 = N * I * V/1000 \tag{8.15}$$

Note that $H_3$ is not time dependent since it is the absolute maximum charge power allowed for the battery.

**Q1 step by step value**

$$Q^t_1 = Q^{t-1}_1 * e^{-k*\delta t} + \frac{(Q^t_j * k * c + P^t) * (1 - e^{-k*\delta t})}{k} + \frac{P^t * c * (k * \delta t - 1 + e^{-k*\delta t})}{k} \tag{8.16}$$

$$P_t = x^t_{ij} + x^t_{rj} - x^t_{jv} \tag{8.17}$$

The last constraint (8.16) defines the value of $Q_1$ for every time step t according to the Kinetic Battery Model formulation.

## 8.3 Battery Stress Factors Modeling

In this section we will explain how to model different battery stress factors and how the basic model presented in previous section can be modified by adding variables and constraints to take into consideration different battery degradation issues.

### 8.3.1 Daily Depth of Discharge

Let us assume that the battery wearing is mainly due to a cost on the depth of discharge. Let us assume also that the battery use for Off-Grid solar applications has a daily trend with daily discharge-charge operations. That is related to the fact that the general Off-Grid systems behavior for solar applications is to store the exceeding renewable energy during the day in order to extend the electrical service hours during night time periods when the PV production is zero. Computational tests presented in Section 8.4 will show such daily trends for solar applications.

Under the above assumptions we can improve the battery lifetime by focusing on the daily depth of discharge and placing a cost per $kWh$ on it. What we will obtain through this trick is shifting the battery use curve towards the higher part of a diagram so that the deeper discharge in every day will be minimized. Note we are not imposing a lower bound on the state of charge a priori as we want to find the optimal value towards which the lowest state of charge should settle in every day, by varying the battery degradation cost.

From a mathematical and computational point of view, in order to do that we need a new decision variable $Qm^g$ that will represent the lowest state of charge in every day $g$. Then we can insert the following constraint:

$$Q_j^t >= Qm^g \quad \forall g, \quad \forall t : t = \{[(g-1)*24]...[(g-1)*24+23]\} \tag{8.18}$$

We impose that for every day $g$, the value of $Q_j^t$ along 24 hours, must be greater than or equal to a value $Qm^g$ that will be maximized by the objective function. In this way we will avoid the deeper daily discharge and we will keep the battery state of charge on higher levels.

Note that $t$ has to be defined from 1 to T (with T equal to the number of hours) while $g$ has to be defined from 1 to G (with G equal to the number of days). Hence the total period T is split into daily intervals through the formulation $t = \{[(g-1)*24]...[(g-1)*24+23$. The model will therefore find the optimal lowest state of charge in every single day.

If needed, it is possible to modify the length of the time intervals sequence, by considering sequences of 12 hours, or sequences of 6 hours, or longer sequences of 48 hours and so on. It is only necessary to change the range according to the specific needs. For instance, in wind applications the daily trend might be not suitable and the range of time might be shorter according to the particular wind resource behavior. Appropriate preliminary computational tests can give good answers on the most suitable range to adopt. As we are presenting a study related to solar applications, we found that the battery use has a strong daily trend and computational experiments that will be showed in Section 8.4 will demonstrate that. Hence for our purposes a range of 24 hours is appropriate.

In order to apply a cost on the daily depth of discharge, we need to add it inside the objective function: this new term of cost is represented by the summation of the $Qm^g$ in every day $g$ multiplied by a representative battery degradation cost per $kWh$. It has a

negative sign, as the lower the battery content is (hence the lower the value of $Qm$ is), the higher the related cost should be.

So the objective function will become:

$$\min \sum_t (x_{pd}^t + x_{pr}^t) * K_p - \sum_g Qm^g * BDC_{kWh} \tag{8.19}$$

where the term $-\sum_g Qm^g$ has been inserted and $BDC_{kWh}$ represents a Battery Degradation Cost per $kWh$, as introduced in Section 7.4.

### 8.3.2 Partial Cycles

The daily depth of discharge formulation presented in previous Section 8.3.1, can be suitable to reduce the number of partial cycles as well. If the battery curve will be shifted towards the higher part of the diagram, this will have two main effects: the direct effect is that the deeper discharge in every day will be penalized by the degradation cost as explained in previous section; the indirect effect of this procedure is that as the battery curve will be shifted up, we will obtain a higher number of cycles that end with a fully charged battery (that means in other words that we will reduce or even annul the number of partial cycles). An example to better understand such behavior is depicted in Figure 8.2: the curve related to case01 can be shifted little by little and as this happen, a higher number of cycles will end with a fully charged battery, hence the number of partial cycles is minimized. In particular, in case01 there are 4 partial cycles, in case02 there are again 4 partial cycles but the depth of discharge is a little bit shallower; in case03 there are 2 partial cycles and a shallower depth of discharge; in case04 there are no partial cycles and a very light depth of discharge. Note that in practical problems a value of 90% as a full state of charge criteria is chosen for practical reasons as explained in Svoboda et al. [25].

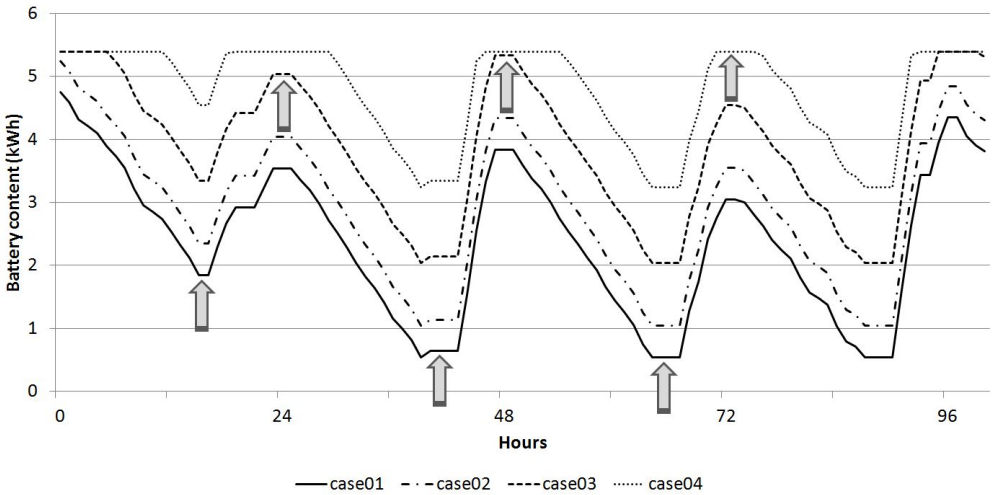


Figure 8.2: Example of a battery curve that is shifted towards the higher part of the diagram. The direct effect is the depth of discharge minimization. The indirect effect is the reduction of partial cycles (which are cycles that starts and/or end with a not fully charged battery).

Computational experiments presented in Section 8.4 will show such behavior. Sensitivity analyses with different costs per $kWh$ will show in which conditions it is possible to substantially reduce the number of partial cycles.

### 8.3.3 Counting Battery Cycles

In order to better model the battery degradation, we are interested in defining the exact time t on which a discharge action is finishing: if we can identify the end of a cycle and the state of charging of the battery, we can for instance minimize the number of cycles in our objective function, or we can impose that when a charge is starting, then it must carry on until a fully charged battery. Both procedures might be interesting to reduce the battery degradation.

In order to do that from a linear programming point of view, we need to link three types of binary variables.

- $\theta^t$ 1 if the battery is charging in time t, 0 otherwise
- $\theta^t_{down}$ 1 if a charging is starting or a discharging is finishing, 0 otherwise
- $\theta^t_{up}$ 1 if a charging is finishing or a discharging is starting, 0 otherwise

If on time t a sequence of charging actions is starting, that means that on time $t-1$ a sequence of discharging actions has just finished. Hence from a mathematical point of view, we can say that:

- if in time t the storage is on a charging sequence ($\theta^t = 1$) and on time t-1 it was on a discharging sequence ($\theta^{t-1} = 0$), then in time t a charging sequence is starting ($\theta^t_{down} = 1$);
- if in time t the storage is on a discharging sequence ($\theta^t = 0$) and on time t-1 it was on a charging sequence ($\theta^{t-1} = 1$), then in time t a discharging sequence is starting ($\theta^t_{up} = 1$);
- if in time t the storage is on a charging sequence ($\theta^t = 1$) and on time t-1 it was on a charging sequence too ($\theta^{t-1} = 1$), then there are no changing in the state of charge ($\theta^t_{down} = 0$ and $\theta^t_{up} = 0$);
- if in time t the storage is on a discharging sequence ($\theta^t = 0$) and on time t-1 it was on a discharging sequence too ($\theta^{t-1} = 0$), then there are no changing in the state of discharge ($\theta^t_{down} = 0$ and $\theta^t_{up} = 0$).

These considerations can be expressed by the following constraint:

$$\theta^t - \theta^{t-1} = \theta^t_{down} - \theta^t_{up} \quad \forall t > 0 \tag{8.20}$$

We also need to impose that the beginning of a charge event can't happen together with the beginning of a discharge event, that means the $\theta^t_{down}$ and the $\theta^t_{up}$ can't be equal to one at the same time.

$$\theta^t_{down} + \theta^t_{up} <= 1 \quad \forall t \tag{8.21}$$

It is necessary to link the new binary variables to the existing decision variables in order to get correct results from our mathematical model. We need to link in particular the variable $\theta^t$ to the flows into the battery in time t, $x^t_{ij}$ and $x^t_{rj}$.

$$x^t_{ij} + x^t_{rj} \leq Q_{max} * \theta^t \quad \forall t \tag{8.22}$$

Finally we need to add another constraint in order to link the binary variable $\theta^t$ to the flows out the battery. If the binary variable $\theta^t$ is equal to 1, it means that the battery is charging and therefore the flows out the battery itself must be equal to zero. Thus, to let the model work properly, we need to insert a "mutually exclusive flows" constraint as follows:

$$x^t_{jv} <= Q_{max} * (1 - \theta^t) \quad \forall t \tag{8.23}$$

What we can do in the objective function is minimize the number of cycles multiplying the variable $\theta^t_{up}$ by a representative cost per cycle as outlined in Section 7.4.

$$\min \sum_t (x^t_{pd} + x^t_{pr}) * K_p + \sum_t \theta^t_{up} * BDC_{cycle} \tag{8.24}$$

### 8.3.4 Define the Content of Energy at the End/Beginning of a Cycle

A more detailed way to study battery degradation issues is not only focusing on the number of cycles, but considering also the energy content at the beginning or at the end of every cycle. For that purpose we can define two new decision variables as follow:

$Q^t_{end}$ which define the energy content in the battery at the end of a discharge cycle;

$Q^t_{start}$ which define the energy content in the battery at the beginning of a discharge cycle;

In order to define the value of $Q_{end}$ we need to insert the following constraints:

$$Q^t_{end} \leq \theta^t_{down} * Q_{max} \quad \forall t \tag{8.25}$$

$$Q^t_{end} \leq Q^t_j \quad \forall t \tag{8.26}$$

Through the constraint (8.25) we impose that the variable $Q_{end}$ will assume a value greater than zero only when the variable $\theta^t_{down}$ will be equal to one, as we want to look for the energy content only when a cycle is finishing. The constraint (8.26) imposes that the variable $Q_{end}$ can't be greater than the energy content in time t, thus if we maximize the variable $Q_{end}$ in the objective function, it will always be equal to the battery energy content $Q^t_j$. But thanks to the constraint 8.25 this will happen only when the cycle is finishing, that is when the variable $\theta^t_{down}$ is equal to 1.

The objective function will become the following:

$$\min \sum_t (x^t_{pd} + x^t_{pr}) * K_p + \sum_t (Qmax - Q^t_{end}) * BDC_{kWh} \tag{8.27}$$

where $(Qmax - Q^t_{end})$ represents the amount of space in the battery at the end of a discharge cycle on which a degradation cost is applied. The lower the value, the shallower the depth of discharge. $BDC_{kWh}$ is the battery degradation cost per $kWh$ introduced in Section 7.4.

Similarly, for the battery energy content at the beginning of a discharge cycle $Q_{start}$ we can add the following constraints:

$$Q^t_{start} \leq \theta^t_{up} * Q_{max} \quad \forall t \tag{8.28}$$

$$Q^t_{start} \leq Q^t_j \quad \forall t \tag{8.29}$$

Then the objective function will become as follow:

$$\min \sum_t (x^t_{pd} + x^t_{pr}) * K_p + \sum_t (Qmax - Q^t_{start}) * BDC_{kWh} \tag{8.30}$$

where $(Qmax - Q^t_{start})$ represents the amount of space in the battery at the beginning of a discharge cycle to be minimized. The lower the value, the higher the battery energy content at the beginning of a cycle (that means the battery starts a discharge in a fully charged condition).

### 8.3.5 Cost per kWh Throughout the Battery

One of the quickest ways to take into consideration the battery degradation is applying a degradation cost on the flows out the battery $x^t_{jv}$ as follow:

$$\min \sum_t (x^t_{pd} + x^t_{pr}) * K_p + \sum_t x^t_{jv} * BDC_{kWh} \tag{8.31}$$

## 8.4 Computational Experiments and Sensitivity Analyses

### 8.4.1 Introduction to Sensitivity Analyses

Broadly speaking the objective of the following computational tests and sensitivity analyses is to see whether the battery technology is worthy at the current state of art of technology and, if not, in which conditions it becomes valuable.

As the battery degradation cost definition comes with an intrinsic uncertainty (due to manufacturer data uncertainty), the most interesting thing to do is making sensitivity analyses using different values of such cost and comparing it with a reference cost, to see how different trade offs affect the optimization model decisions. In particular, since the main energy alternative to meet the demand of an offgrid system is represented by a diesel generator, we will study how the battery behavior depends on the ratio of the battery degradation cost and the diesel cost. In fact if the system is going to use the battery less (because of the battery degradation cost applied on the depth of discharge, for instance), then sometimes it will have to run the conventional generator more. The key

is also whether it is still worthy to use the battery when there is a conventional generator with a lower cost per $kWh$.

Batteries degradation costs are high at present, so we will study a range of costs to understand how behavior of system will depend on lower degradation costs in a future world with better batteries (i.e. a forecasted scenario in which battery costs drop and diesel costs will continue to increase).

Such tests will also tell us how much the battery replacement cost should drop as a function of the declared lifetime throughput, to make the battery use more convenient.

### 8.4.2 A Rolling Optimization Procedure for Big Instances

We made some previous tests and we found out that every day trend is affected by the model decisions of the next three days ahead, but after the fourth day the results of the first one become constant. We call this condition "edge effect" as there is and edge of three days before getting a stable result of the first day. Figure 8.3 shows an example of such behavior. That means we don't need to run an optimization grouping too many days together as we can look ahead of just three days to eliminate the edge effect. For this reason we can solve the model through a rolling optimization procedure by testing 6 days each time, keeping the results of the first 3 days of every run and use the values of the variables $Q_t$ and $Q1_t$ at the end of the third day, as the starting values for the next 6 days run and so on. This way we can link every optimization and we can run big instances of the problem that otherwise would be computationally hard to solve for a wide time horizon (i.e. one year) especially with the addition of binary variables.

However, it is important to underline that we can solve the current model in few seconds for instances of one month length. Hence we don't need any rolling procedure to run monthly instances of the model.

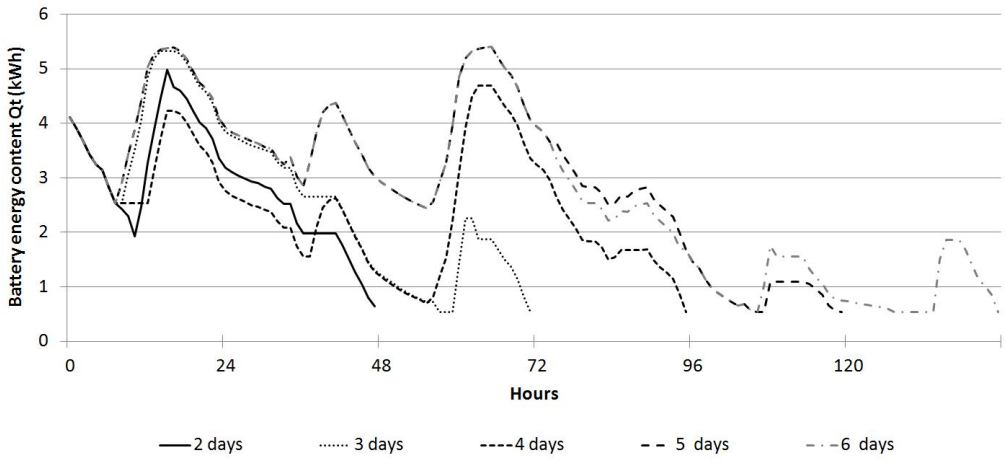


Figure 8.3: Example of the edge effect. Different optimizations run adding one day each time to see variations in final results.

### 8.4.3 Data

Tests have been made using real world data of demand and renewable production from a site in Rwanda Anuta et al. [4]. We tested an offgrid system with a set of data showed in

Table 8.4 and an average very common battery for solar applications. The offgrid system data shown in Table 8.4 come from the real world application in Rwanda. The site is provided with a 1.3 kW solar PV array.

The diesel cost in $\$/kWh$ is given by $(\$/Liter) * (L/kWh)$ where we considered a cost per liter equal to 1.6 $ (values for the African sites tested in Anuta et al. [4]) and an average diesel production of 0.330 $L/kWh$.

Battery data are provided by manufacturer documentation, as well as the kinetic battery constants are derived by the capacity curves and lifetime curves. Table 8.5 shows the battery lifetime data expressed as depth of discharge versus cycles to failure that is generally provided by manufacturers. The column "Lifetime throughput" shows the calculated throughput for each depth of discharge using the formula 7.1, while the column "Cycle cost" shows the calculated cost per every cycle using the formula 7.6. The global lifetime throughput of the battery is obtained by averaging the values of each line, as well as the battery cycle cost can be obtained by averaging the cycle costs of each line.

Table 8.4: Data for computational tests

| | | |
|---|---|---|
| GENERATOR DATA | | |
| $D$ | 0.48 | conventional generator diesel cost ($/kWh) |
| $PC$ | 1 | conventional generator capacity (kW) |
| $PP$ | 0.2 | conventional generator minimum production (%) |
| CONVERTER DATA | | |
| $\lambda_v$ | 0.90 | inverter efficiency (%) |
| $\lambda_r$ | 0.85 | rectifier efficiency (%) |
| BATTERY DATA | | |
| $Eff$ | 0.89 | square root of the roundtrip efficiency of the battery (%) |
| $S$ | 0.2 | battery minimum state of charge (%) |
| $c$ | 0.151 | battery capacity ratio (unitless) |
| $k$ | 9.51 | battery rate constant (1/h) |
| $Ah$ | 225 | battery capacity (Ah) |
| $V$ | 12 | battery nominal voltage (V) |
| $I$ | 67.5 | battery charge current (A) |
| $\alpha$ | 1 | battery maximum charge rate (A/Ah) |
| $C_{rep}$ | 900 | battery purchase cost ($) |
| $LT$ | 1344 | battery lifetime throughput (kWh) |
| $BDC_{kWh}$ | 0.7 | battery degradation cost ($/kWh) |
| BATTERY BANK DATA | | |
| $N$ | 2 | number of cells in the battery bank (n) |
| $Qmax$ | 5.4 | battery bank capacity (kWh) |
| $V^{bank}$ | 24 | battery bank nominal voltage (V) |
| $C^{bank}_{rep}$ | 1800 | battery bank purchase cost ($) |
| $Q^{bank}_{lifetime}$ | 2688 | battery bank throughput (kWh) |

Note that in Table 8.4 battery data are shown for a single battery. As in the real world case we have 2 cells in the battery bank that means that the battery capacity has to be multiplied by 2 as well as the voltage and the resulting lifetime throughput will be

Table 8.5: Battery bank lifetime table (depth of discharge versus cycles to failure) with lifetime throughput calculations

| Depth-of-discharge (%) | Cycles-to-failure (n) | Lifetime throughput (kWh) |
|---|---|---|
| 10 | 5700 | 3078 |
| 25 | 2100 | 2835 |
| 35 | 1470 | 2778 |
| 50 | 1000 | 2700 |
| 60 | 830 | 2689 |
| 70 | 700 | 2646 |
| 80 | 600 | 2592 |
| 90 | 450 | 2187 |

double as shown in the section "battery bank data" of Table 8.4. However, this doesn't change the Battery Degradation Cost $BDC_{kWh}$ as the double cost at the numerator will be neutralized by a double throughput at the denominator. The cycles to failure per every depth of discharge remain the same.

### 8.4.4 Tests on the Lowest State of Charge in Every Day. Results Discussion

The following diagrams and tables show the results obtained performing the optimization using an Intel Pentium processor SU4100 1.30 GHz PC, with 4GB of memory; the MILP models are solved through the branch-and-cut algorithm implemented in the IBM Cplex 12.2 solver.

The model has been run for the months of August from the 1st to the 31st and we show the resulting battery energy content $Q_j$ in 20 mainly representative days in the middle, from the 8th to the 27th of August. We made different analyses applying different kinds of costs in the objective function. In particular, in this section $D$ represents the diesel cost per $kWh$ and $LW$ represents a degradation cost per $kWh$ on the lowest state of charge in every day. We tested different ratios of per $kWh$ battery degradation cost to diesel cost.

Figure 8.4 shows two extreme cases that represent the starting point for sensitivity analyses. The worse situation is represented by a battery that is deeply used where no degradation charge is applied: this situation is showed by the black bold curve which is related to an optimization run applying a cost only on the conventional plant generation, hence the model makes a deep use of the battery to minimize the conventional generator costs. This trend shows the main battery degradation issues: high number of cycles, very deep discharge mode and partial cycles with a battery not fully charged for most of the time. Another interesting thing to note is that from this battery curve it is clear that an actual general battery use for solar Off-Grid systems is made of one main daily deep cycle, thus it makes sense to focus on a cost of the lowest state of charge per every day as explained in Section 8.3.1.

The other extreme scenario depicted in Figure 8.4 is the one that shows a very little use of the battery, mainly for backup and emergency. This scenario is represented by the traced line, obtained applying a very high degradation cost per $kWh$ on the lowest state of charge in every day. In particular, the cost per $kWh$ applied in this scenario is for present

day battery costs. It is equal to the battery degradation cost $BDC_{kWh}$ calculated through the formula 7.5 which is a function of the battery replacement cost, lifetime throughput and efficiency. This shows that, for Off-Grid applications, the current battery technology is still not mature enough as battery replacement costs are currently too high compared with their throughput properties.

Within the two extreme scenarios outlined above, we made some sensitivity analyses to find out in which range the battery degradation cost defined in 7.5 should settle to allow a healthier battery life and how the battery curves change and shift in the diagram as a function of different degradation cost values. As already stated in Section 8.4.1, we will compare the battery degradation cost with a reference that is the diesel cost, as it represents the main alternative source of energy available in the system. For a clearer visualization we will show the results enlargement of these sensitivity analyses for some more representative fragments of the battery trend. The gray circles in Figure 8.4, indicate the most interesting fragments that will be enlarged in the following pictures to show the battery trend with different degradation costs applied.

Figure 8.5 shows enlargements of the fragments number 1, 2, 3 and 4 identified by the gray circles in Figure 8.4. We apply different degradation costs on the lowest state of charge in every day (LW cost). Degradation costs are defined as a percentage of the fixed diesel cost. We reduce the LW cost little by little to see how the battery trend changes from the very little use (backup and emergency use) to the deeper use (storage purpose).

It is important to note how the application of a cost on the lowest state of charge in every day is able to shift the battery curve towards the higher section of the diagram, allowing both shallower depth of discharge and an almost fully charged battery at the end of every cycle. Hence, through the application of a degradation cost on the lowest state of charge in every day, we get a direct effect that is to avoid deep discharge cycles, and an indirect benefit that is an almost fully charged battery at the end of every cycle (which is beneficial for the battery).

In fragments 1 and 3 we get overlapped curves for LW values equal to the 50-60-70 % of the diesel cost D. In fragment 4 we get almost overlapped curves as well for LW values equal to the 50-60-70 %. There is an evidence that this is a particular range of degradation costs within which the depth of discharge is shallower and the battery is almost fully charged at the end of a cycle (see the peak of the curves). Fragment 2 in particular shows how close these three curves are (even when they are not overlapped) and how they can shift the battery curve in such a way that the battery ends in a fully charged state at the end of the cycle. Lower values of LW costs (see for instance the curve with LW equal to 40% of the diesel cost) give as results deeper and partial cycles that are not beneficial for the battery life. Higher values of LW costs (i.e. LW values greater than or equal to 80% of the diesel cost) tend to a smaller use of the battery, more for backup and emergency activities rather than storage purposes.

The use of the diesel generator to satisfy the final user demand can change as the battery degradation costs become higher. In fragment 1 for instance, when there are no battery degradation costs (black line) we saw the diesel production was zero as the demand was satisfied through a deep use of the battery. As we applied the LW cost, we saw the use of the traditional generator became higher. However, in the range of LW costs within the 50-60-70%, the additional diesel production was very limited. In the fragment 1 for

instance we found the diesel generator was on at 18.00 (0.22 $kWh$) and 22.00 of the 9th (0.29 $kWh$) and at 10.00 of the 10th (0.28 $kWh$), for a total additional production of 0.79 $kWh$. If the LW cost is higher (i.e. greater than 80% of the diesel cost) then the diesel generator production increases strongly. In the fragment 1, for the dot curve (80% of the diesel cost) we saw the diesel generator was on at 18.00 of the 9th (0.2 $kWh$), 19.00 of the 9th (0.17 $kWh$), 22.00 of the 9th (0.29 $kWh$), 10.00 of the 10th (0.28 $kWh$), 18.00 of the 10th (0.2 $kWh$) and 21.00 of the 10th (0.21 $kWh$) for a total additional production of 1.35 $kWh$.

An interesting thing we noted is that sometimes, in the range of LW costs within the 50-60-70%, the curve shifting brings a beneficial shallower depth of discharge and a fully charged battery, at no diesel extra costs. Fragment 3 is an example of such behavior. The diesel generator was always off for the curves related to the 50-60-70%. While there was an additional diesel production of 1.6 $kWh$ for the curve related to the 80%.

In Table 8.6 there is a summary of the total additional diesel production required in the different cases tested for the whole 20 days of August (from the 8th to the 27th).

Table 8.7 summarizes the main stress factor values for the different battery degradation costs along the 20 days shown in the previous diagrams. Note that partial cycles are all the charge/discharge operations that start with a not fully charged battery and/or end with a not fully charged battery. For practical reasons we consider a fully charged battery when the energy content is greater than or equal to 90% of the total battery capacity (that is an almost fully charged battery)

In Figures 8.6, 8.7, 8.8, 8.9, 8.10 the different battery stress factors values (see Section 7.4) for the different battery degradation costs are shown together with the related diesel costs. As we apply a battery degradation cost, then the battery use tends to become shallower allowing a reduction of the stress factors, but that requires a higher use of the conventional generator. However, it is clear how the interval of battery degradation costs within 50-60-70% is the one in which the diesel costs remain steady on medium-low values. As the battery degradation cost increases to 80% and more then the additional diesel production increases considerably. Note that both in the tables and figures the total diesel cost is split into the amount of energy that flows directly to satisfy the demand and the amount of energy that has to flow towards the battery. This latter energy is the result of the conventional generator minimum production constraint: as outlined in the mathematical model formulation, when the conventional generator is on, it has to produce a minimum amount of energy. If the final user demand is less than the conventional generator minimum production, then there is an excess of energy that has to be stored inside the battery.

Table 8.8 shows an annual projection of data for a broader vision of the battery use and estimated lifetime as a consequence of the different patterns studied above. The lifetime throughput in $kWh$ for the different scenarios has been obtained from the battery data, considering the lowest depth of discharge reached at different battery degradation costs. The estimated lifetime in years is obtained through the following formulation

$$\frac{Q_{lowSoC}}{Q_{out}} \tag{8.32}$$

where $Q_{lowSoC}$ is the lifetime throughput at the lowest depth of discharge reached along the period and $Q_{out}$ is the annual energy out the battery.

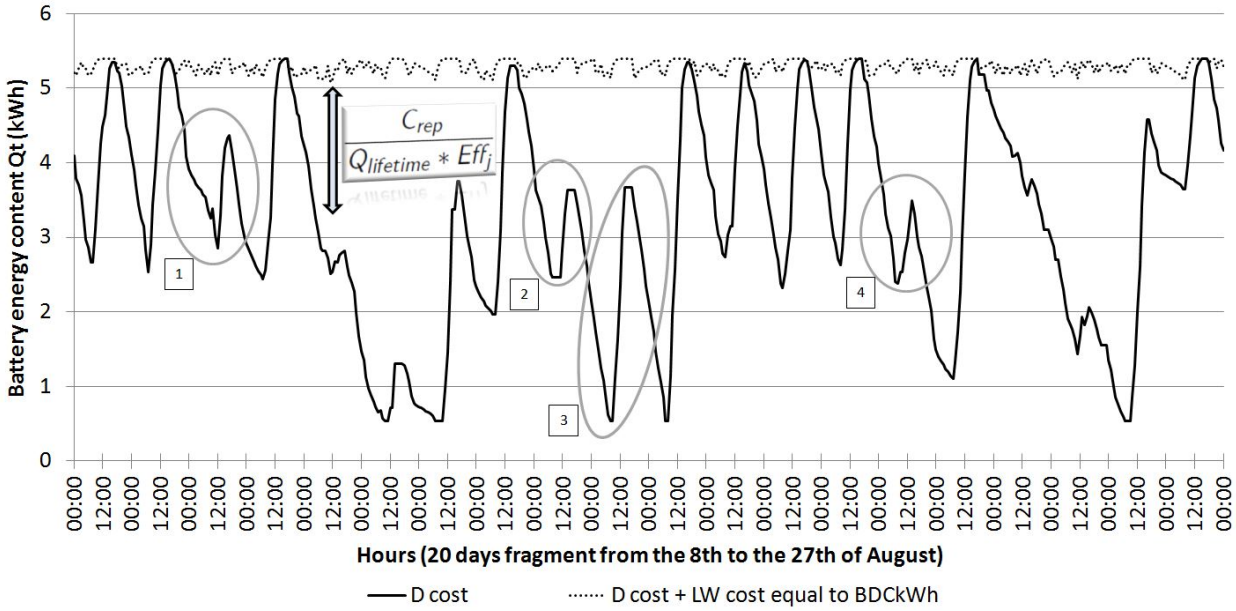


Figure 8.4: Two extreme cases of battery use: the deeper use without any battery degradation cost (black line) and the very little use due to a very high battery degradation cost (dot line). $D$ is the diesel cost per $kWh$ while $LW$ is the cost per $kWh$ applied to the lowest state of charge in every day.

Table 8.6: Results summary along a representative period of 20 days - additional diesel production and diesel costs in different scenarios with different battery degradation costs applied to the daily depth of discharge

| Battery degradation cost LW (% of D cost) | Diesel Prod towards demand (kWh) | Diesel cost towards demand ($) | Diesel Prod towards battery (kWh) | Diesel cost towards battery ($) | Tot diesel production (kWh) | Tot diesel cost ($) |
|---|---|---|---|---|---|---|
| 80 | 16.87 | 8.1 | 1.25 | 0.6 | 18.12 | 8.7 |
| 70 | 11.53 | 5.53 | 1.1 | 0.53 | 12.63 | 6.06 |
| 60 | 11.27 | 5.41 | 0.98 | 0.47 | 12.25 | 5.88 |
| 50 | 11.1 | 5.33 | 0.96 | 0.46 | 12.06 | 5.79 |
| 40 | 7.25 | 3.48 | 0.53 | 0.25 | 7.78 | 3.73 |
| 0 | 2.48 | 1.19 | 0 | 0 | 2.48 | 1.19 |

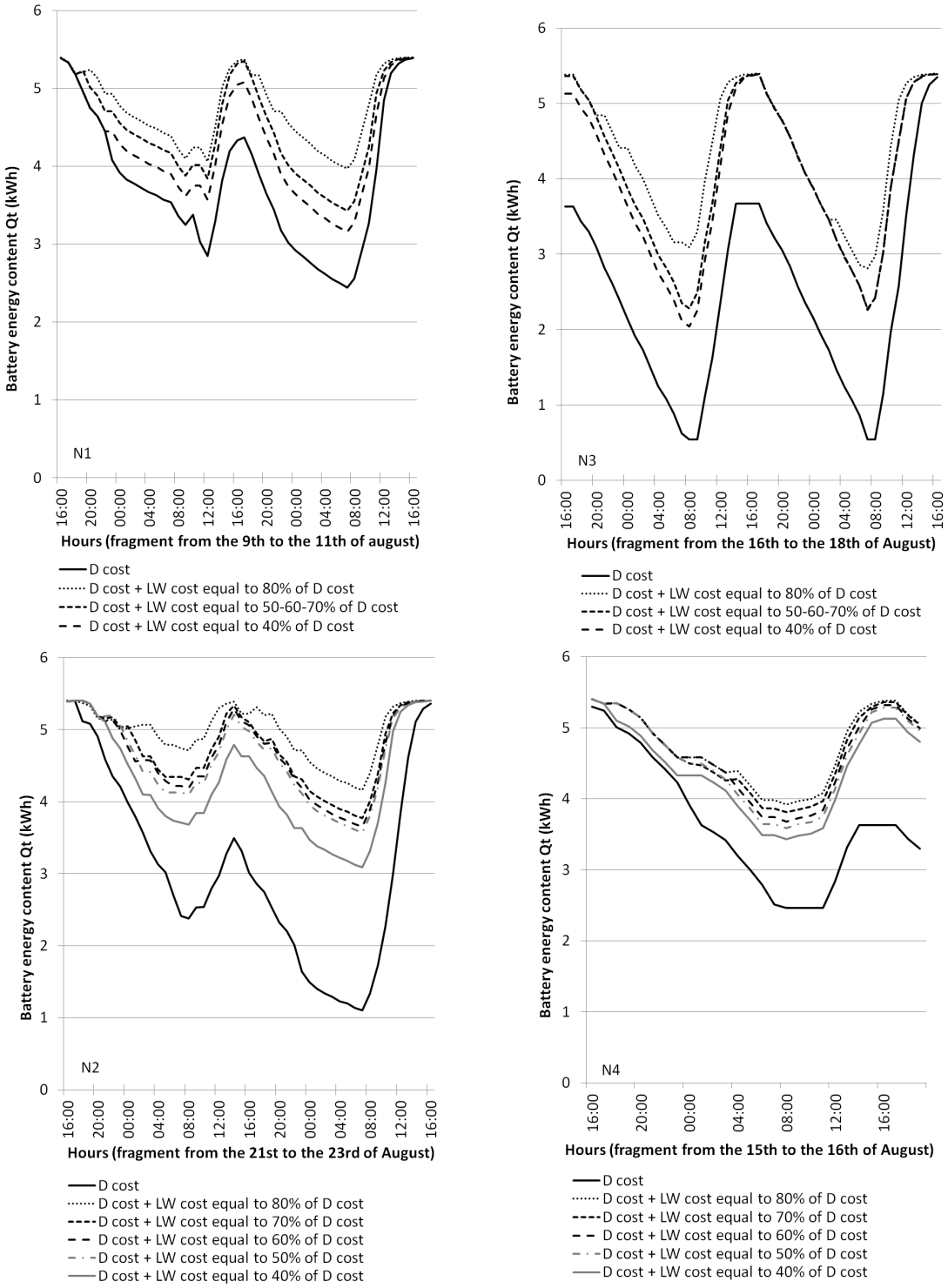


Figure 8.5: Enlargement N1, N2, N3 and N4 of sensitivity analyses with different battery degradation costs (LW) applied to the daily depth of discharge as a function of the diesel cost (D).

Table 8.7: Results summary along a representative period of 20 days - battery stress factors in different scenarios with different battery degradation costs applied to the daily depth of discharge

| Battery degradation cost LW (% of D cost) | Energy out the battery (kWh) | Lowest SoC reached (%) | Average Time between full charged (days) | Highest time between full charged (days) | Time at low SoC (below 35%) (%) | Partial cycles (n) |
|---|---|---|---|---|---|---|
| 80 | 24.88 | 48 | 1 | 1 | 0 | 1 |
| 70 | 30.81 | 58 | 1 | 1 | 0 | 1 |
| 60 | 31 | 58 | 1 | 1 | 0 | 1 |
| 50 | 31.08 | 58 | 1 | 1 | 0 | 1 |
| 40 | 34.98 | 70 | 1.3 | 3 | 5 | 10 |
| 0 | 40.01 | 80 | 2.1 | 4 | 35 | 16 |

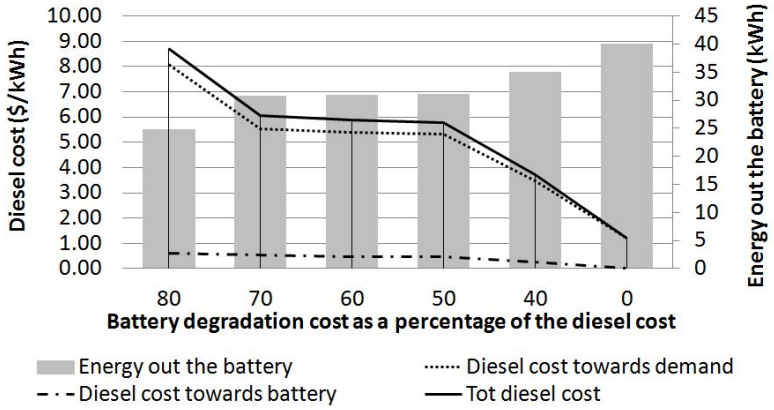


Figure 8.6: Stress factor analyses along 20 representative days. Energy out the battery and diesel costs trend with different battery degradation costs applied to the daily depth of discharge. The higher the column is the worse the stress factor is.

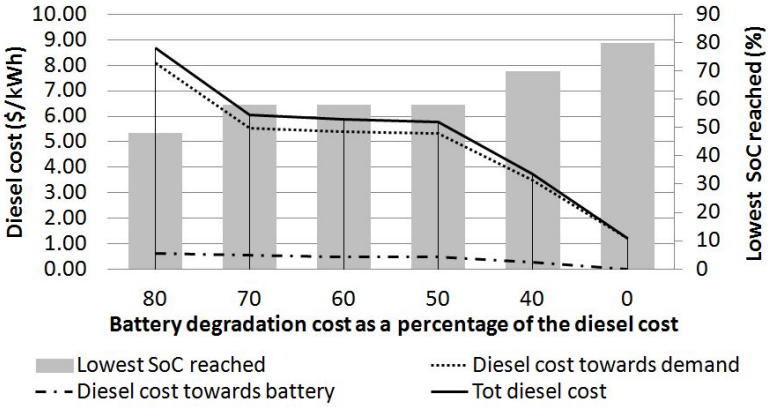


Figure 8.7: Stress factor analyses along 20 representative days. Lowest state of charge reached and diesel costs trend with different battery degradation costs applied to the daily depth of discharge. The higher the column is the worse the stress factor is.

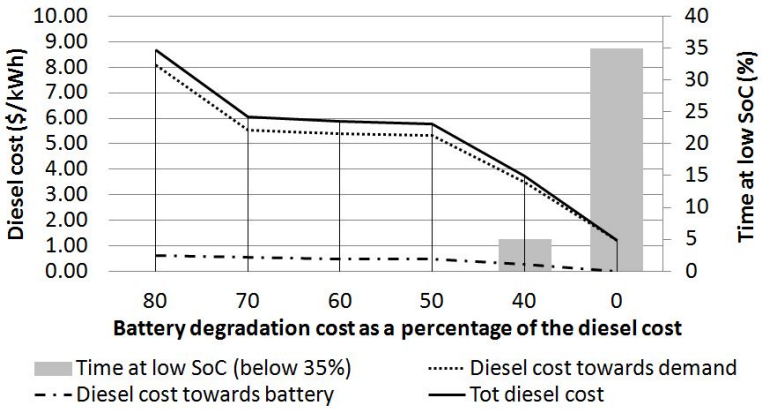


Figure 8.8: Stress factor analyses along 20 representative days. Time at the lowest state of charge and diesel costs trend with different battery degradation costs applied to the daily depth of discharge. The higher the column is the worse the stress factor is.

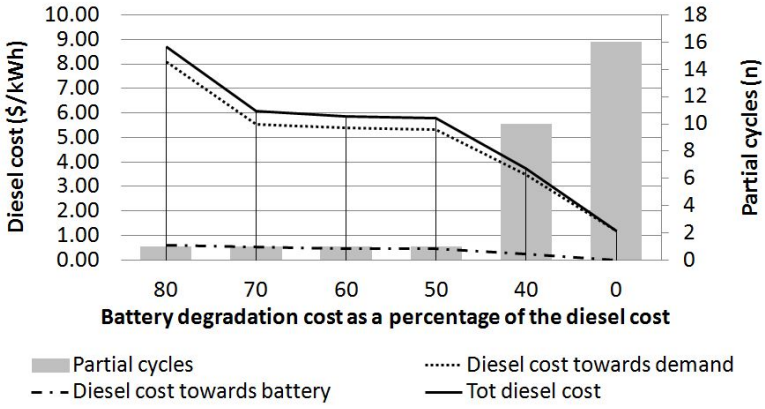


Figure 8.9: Stress factor analyses along 20 representative days. Number of partial cycles and diesel costs trend with different battery degradation costs applied to the daily depth of discharge. The higher the column is the worse the stress factor is.

Table 8.8: Annual projection of the battery estimated lifetime in the different scenarios with different battery degradation costs applied to the daily depth of discharge. Estimated values at the lowest state of charge reached along the period.

| Battery degradation cost LW (% of D cost) | Lowest SoC reached (%) | Average annual energy out (kWh) | Throughput at lowest SoC (kWh) | Estimated lifetime (years) |
|---|---|---|---|---|
| 80 | 0.5 | 448 | 2700 | 6 |
| 70 | 0.6 | 543 | 2689 | 5 |
| 60 | 0.6 | 543 | 2689 | 5 |
| 50 | 0.6 | 543 | 2689 | 5 |
| 40 | 0.7 | 630 | 2646 | 4.2 |
| 0 | 0.8 | 720 | 2592 | 3.6 |

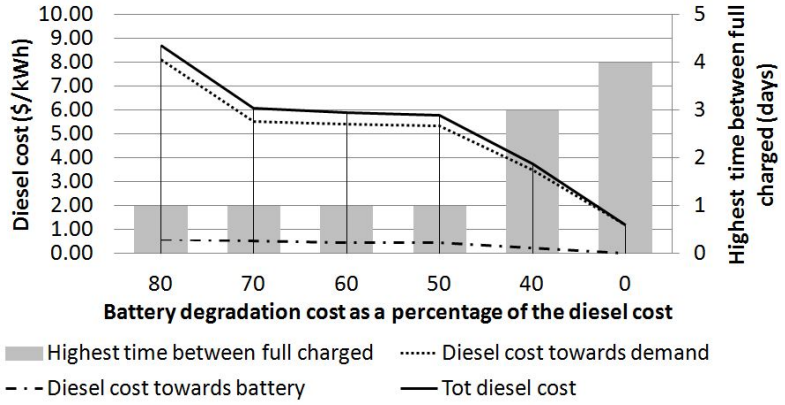


Figure 8.10: Stress factor analyses along 20 representative days. Time between fully charged states and diesel costs trend with different battery degradation costs applied to the daily depth of discharge. The higher the column is the worse the stress factor is.

### 8.4.5 Conclusions

As a conclusion, for Off-Grid application the battery technology is still no mature enough and it should move towards a degradation cost reduction where the battery degradation cost $BDC_{kWh}$ defined in 7.5 should settle at least around 70% of the diesel costs. In other words, that means that, given the current diesel costs $K$, the lifetime throughput $LT$ and the efficiency $Eff$ of a battery, then the battery replacement cost $C_{rep}$ should satisfy the relationship:

$$C_{rep} = LT * Eff * 0.7 * K \tag{8.33}$$

The formula 8.33 can be a guideline during battery choice and purchase. Higher battery costs can be accepted in systems where the battery is going to be used mostly for backup and emergency purposes. At the current state of technology PV-Storage is not feasible without government incentives. Batteries can be more convenient in Off-grid applications for rural and remote areas, where the diesel costs are much higher due to handling and transportation activities required because of the lack of fuel availability. However, looking at a future in which diesel prices will increase and the battery technology will improve, we can reasonably expect that the ratio between the battery degradation costs and the diesel costs will drop. Figure 8.11 for instance shows the increasing diesel prices trends in Rwanda along the last years. Prices has increased quite a lot since 2000 and we can expect further increase in the near future.

Table 8.9: Diesel prices trend in Rwanda along the last years. Source: World Development Indicators (WDI), September 2014 (http://knoema.com)

| Year | Diesel price ($/L) |
|---|---|
| 1991 | 0.79 |
| 1992 | 0.88 |
| 1998 | 0.72 |
| 2000 | 0.84 |
| 2002 | 0.84 |
| 2004 | 0.99 |
| 2006 | 1.08 |
| 2008 | 1.37 |
| 2010 | 1.62 |
| 2012 | 1.73 |

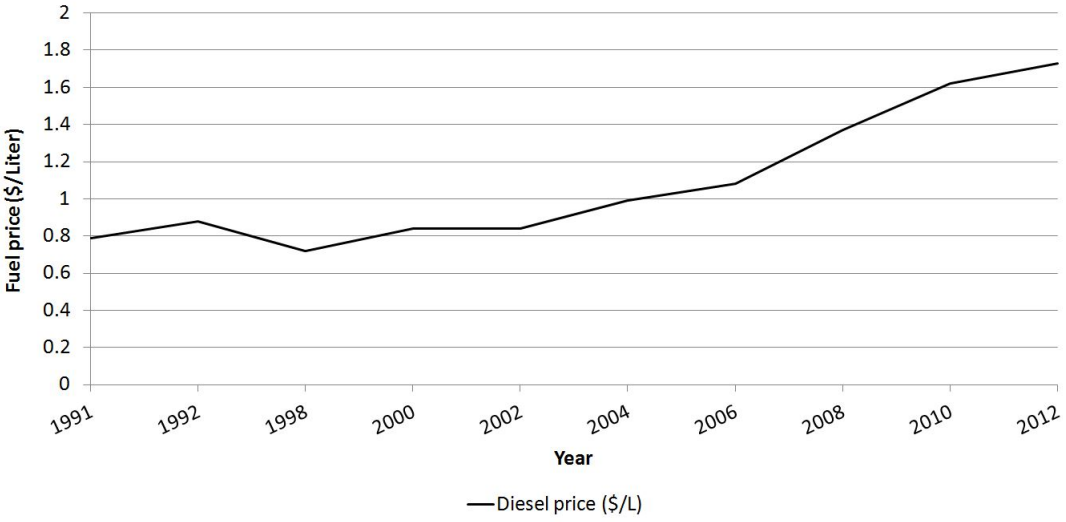


Figure 8.11: Increasing diesel prices trend in Rwanda along the last years. Source: World Development Indicators (WDI), September 2014 (http://knoema.com)

### 8.4.6 Tests on the Number of Cycles. Results Discussion

In this section we will show one of the tests made adding the cycle cost to the optimization run. The related mathematical modeling has been already explained in detail in Section 8.3.3. The objective is to minimize the number of cycles along the period, together with the diesel costs and the lowest state of charge through a combined optimization. We noted in previous tests that a battery degradation cost equal to the 70% of the diesel cost, is enough both to avoid deep discharge and tho shift the battery curve in such a way that every charge operation ends with a fully charged battery (that means the number of partial cycles tend to be null): hence, we can apply a cost per cycle regardless of the state of charge at the end of a charge operation, as we can reasonably expect that every cycle will end with an almost fully charged battery. That is why we need a combined optimization: the battery degradation cost on the lowest state of charge in every day will guarantee a fully charged battery at the end of every discharge operation and the cost per cycle will reduce the number of battery cycles for a further improvement in the battery lifetime. Note that in practical problems a value of 90% as a full state of charge criteria is chosen for practical reasons as explained in Svoboda et al. [25].

As already outlined in Section 7.4 the cost per cycle $BDC_{cycle}$ can be calculated for every depth of discharge $n$ as

$$BDC^{n}_{cycle} = \frac{C_{rep}}{f_n} \tag{8.34}$$

We saw in previous computational tests that a battery degradation cost equal to 70% of the diesel cost is the most representative value, hence we run an optimization considering a battery replacement cost equal to $[LT * Eff * 0.7 * K]$. In our real world case this corresponds to a replacement cost for the battery bank equal to 803$. This gives an average cost per cycle CY equal to 0.76 $/cycle as shown in table 8.10

Table 8.10: Battery bank cycle costs considering a battery bank replacement cost equal to 803 $

| Depth of discharge (%) | Cycles to failure (n) | Lifetime throughput (kWh) | Cycle cost ($/cycle) |
|---|---|---|---|
| 10 | 5700 | 3078 | 0.14 |
| 25 | 2100 | 2835 | 0.38 |
| 35 | 1470 | 2778 | 0.55 |
| 50 | 1000 | 2700 | 0.80 |
| 60 | 830 | 2689 | 0.97 |
| 70 | 700 | 2646 | 1.15 |
| 80 | 600 | 2592 | 1.34 |
| | | | Average cycle cost 0.76 |

Figure 8.12 shows the battery trend after the optimization, while Tables 8.11 and 8.12 summarize the resulting diesel costs and battery stress factors. An interesting thing to note in Figure 8.12 is how the model tends to penalize just the partial cycles (that are particularly bad for the battery health) by making longer discharge operations that allow it to jump the partial cycle sections. The combined cost on the lowest state of charge helps maintaining the curve properly shifted avoiding deep discharge. The annual projection for the battery lifetime estimation is shown in Table 8.13. As the cycles has been reduced, the shallower use of the battery had to be balanced by a higher use of the conventional

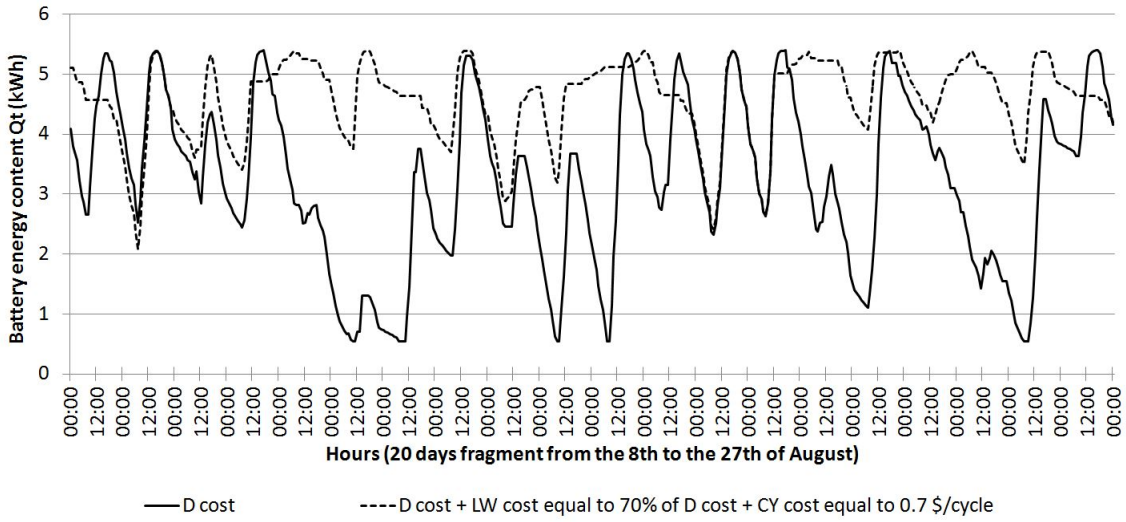


Figure 8.12: Battery trend with a cycle cost applied to reduce the number of cycles and a daily depth of discharge cost applied to minimize the daily depth of discharge

Table 8.11: Results summary along a representative period of 20 days - additional diesel production and diesel costs in the different scenarios (with and without a cycle cost and a daily depth of discharge cost).

| Battery degradation cost LW (% of D cost) | Battery degradation cost CY ($/cycle) | Diesel Prod towards demand (kWh) | Diesel cost towards demand ($) | Diesel Prod towards battery (kWh) | Diesel cost towards battery ($) | Tot diesel production (kWh) | Tot diesel cost ($) |
|---|---|---|---|---|---|---|---|
| 70 | 0.7 | 20.05 | 9.62 | 2.4 | 1.15 | 22.45 | 10.78 |
| 0 | 0 | 2.48 | 1.19 | 0 | 0 | 2.48 | 1.19 |

Table 8.12: Results summary along a representative period of 20 days - battery stress factors in the different scenarios (with and without a cycle cost and a daily depth of discharge cost).

| Battery degradation cost LW (% of D cost) | Battery degradation cost CY ($/cycle) | Energy out the battery (kWh) | Lowest SoC reached (%) | Average Time between full charged (days) | Highest time between full charged (days) | Time at low SoC (below 35%) (%) | Partial cycles (n) |
|---|---|---|---|---|---|---|---|
| 70 | 0.7 | 21.96 | 60 | 1.3 | 3 | 0 | 2 |
| 0 | 0 | 40.01 | 80 | 2.1 | 4 | 35 | 16 |

generator which brings a high increase in the diesel costs. But on the other hand the estimated battery lifetime after the optimization is even double.

Table 8.13: Annual projection of the battery estimated lifetime in the different scenarios (with and without a cycle cost and a daily depth of discharge cost). Estimated values at the lowest state of charge reached along the period.

| Battery degradation cost LW (% of D cost) | Battery degradation cost LW ($/cycle) | Lowest SoC reached (%) | Average annual energy out (kWh) | Throughput at lowest SoC (kWh) | Estimated lifetime (years) |
|---|---|---|---|---|---|
| 70 | 0.7 | 0.6 | 395 | 2689 | 6.8 |
| 0 | 0 | 0.8 | 720 | 2592 | 3.6 |

### 8.4.7 Conclusions

The number of cycles minimization together with the lowest state of charge minimization tends mainly to reduce the number of partial cycles and the amount of energy throughout the battery. That gives as result a strong improvement in the battery lifetime, but it involves much higher diesel costs.

We would also like to underline that more work needs to be done in the cycle cost definition, as the manufacturer data that provide the depth of discharge versus cycles to failure, come with an intrinsic uncertainty that need to be treated. We however show that a mathematical formulation that take into account the number of cycles can exist and might be used. From that point of view the scientific production should also move towards a better definition of numbers and data for such field as at the current state of the art the major limit of such analyses is represented by the lack of precise numbers and data to put on a model.

## 8.5 Optimal Additional PV Production

### 8.5.1 Modeling Introduction

The proposed model can be further developed adding features to extend the sensitivity analyses. In this section we will discuss some of the results obtained by increasing the PV production. In particular, the mathematical model can be modified to get the optimal value of PV production. This value, combined with the different battery degradation costs, can give as output an optimized battery trend together with a reduction of the conventional generator use. For that purpose the model has been modified as follows. A new continuous decision variable $R^t_{add}$ has been created to define the additional PV production required in time t. Then the constraint 8.6 has been modified as follow

$$x^t_{iv} + x^t_{ij} \leq R^t + R^t_{add} \quad \forall t \tag{8.35}$$

Finally a new constraint to maintain the renewable production equal to zero during night hours has been added.

$$R^t_{add} = 0 \quad \forall g, \quad \forall t : t = \{[(g-1)*24-5]...[(g-1)*24+6]\} \tag{8.36}$$

### 8.5.2 Computational Experiments. Results Discussion

Figure 8.13 shows the resulting battery trends for the different battery degradation costs, once that the optimal additional PV production has been found by the model.

Figures 8.14 and 8.15 show the single battery trend together with the actual and modified renewable production to better understand in which time slots the model suggests a higher PV availability. The average additional PV production is showed in Table 8.14.

To summarize the results, what we found is that the average battery trend is improved when the degradation cost is applied. That means we get a battery trend where the depth of discharge is shallower and we annul the partial cycles, getting only more beneficial full cycles that start and end with a fully charged battery. We get overlapped curves in the range of battery degradation costs within 40-50-60-70-80% of the diesel cost. While in the previous tests without any additional PV, the overlapped range was within 50-60-70%. That means the additional PV can somehow relax the battery degradation cost upper limit, allowing the purchase of more expensive batteries, with a degradation cost that can increase until the 80% of the diesel cost.

Furthermore, we also noted that in the range of battery degradation costs within 40-50-60-70-80% of the diesel cost, the total diesel production and related costs were zero. Hence in this range we can run the system at no diesel costs, but with a healthier battery life. While diesel costs increase a lot when the battery degradation cost applied is higher (i.e. 90% of the diesel cost).

Tables 8.14, 8.15 and 8.16 summarize the results showing the suggested additional PV production in different scenarios, the battery stress factors and the annual projection of the battery lifetime respectively.

Table 8.14: Average additional PV production suggested by the model in different scenarios and related diesel costs. Comparison with the basic scenario with no battery degradation costs applied and no additional PV

| Battery degradation cost LW (% of D cost) | Average additional PV production (kWh) | Total diesel cost ($) |
|---|---|---|
| 90 | 0.2 | 10.43 |
| 40-50-60-70-80 | 0.4 | 0 |
| 0 | 0 | 1.19 |

Table 8.15: Results summary along a representative period of 20 days. Battery stress factors in the different scenarios as a consequence of the additional PV production. Comparison with the basic scenario with no battery degradation costs and no additional PV

| Battery degradation cost LW (% of D cost) | Average additional PV production (kWh) | Energy out the battery (kWh) | Lowest SoC reached (%) | Average Time between full charged (days) | Highest time between full charged (days) | Time at low SoC (below 35%) (%) | Partial cycles (n) |
|---|---|---|---|---|---|---|---|
| 90 | 0.2 | 11.29 | 20 | 1 | 1 | 0 | 0 |
| 40-50-60-70-80 | 0.4 | 33.22 | 50 | 1 | 1 | 0 | 0 |
| 0 | 0 | 40.01 | 80 | 2.1 | 19 | 35 | 16 |

Table 8.16: Annual projection of the battery estimated lifetime in the different scenarios as a consequence of the additional PV production. Comparison with the basic scenario with no battery degradation costs and no additional PV. Estimated values at the lowest state of charge reached along the period

| Battery degradation cost LW (% of D cost) | Average additional PV production (kWh) | Lowest SoC reached (%) | Average annual energy out (kWh) | Lifetime Throughput (kWh) | Estimated lifetime (years) |
|---|---|---|---|---|---|
| 90 | 0.2 | 0.2 | 203 | 2835 | 14 |
| 40-50-60-70-80 | 0.4 | 0.5 | 598 | 2700 | 4.5 |
| 0 | 0 | 0.8 | 720 | 2592 | 3.6 |

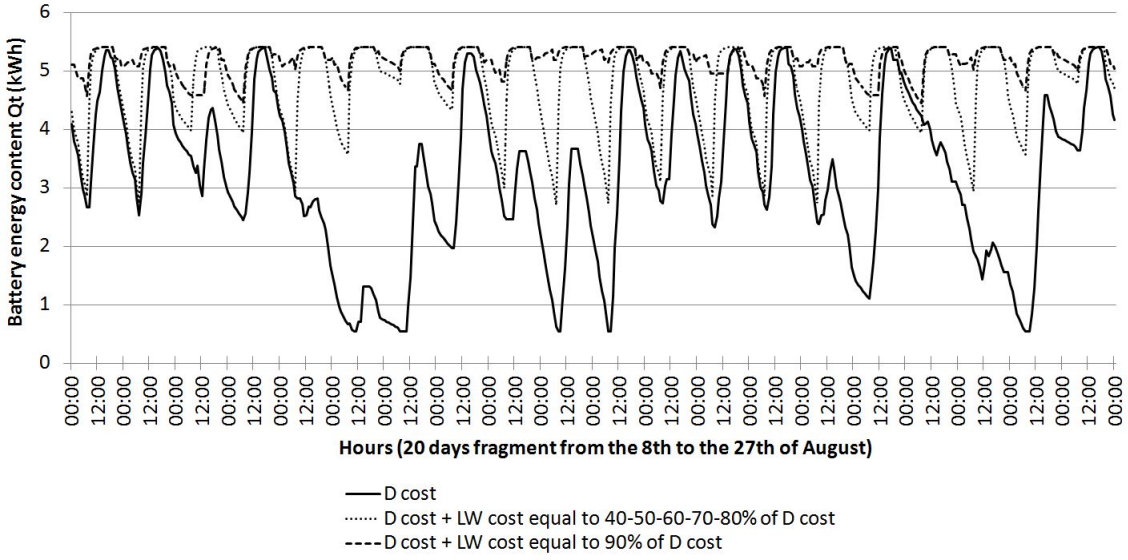


Figure 8.13: Battery trend in different scenarios as a consequence of the additional PV production suggested by the model.

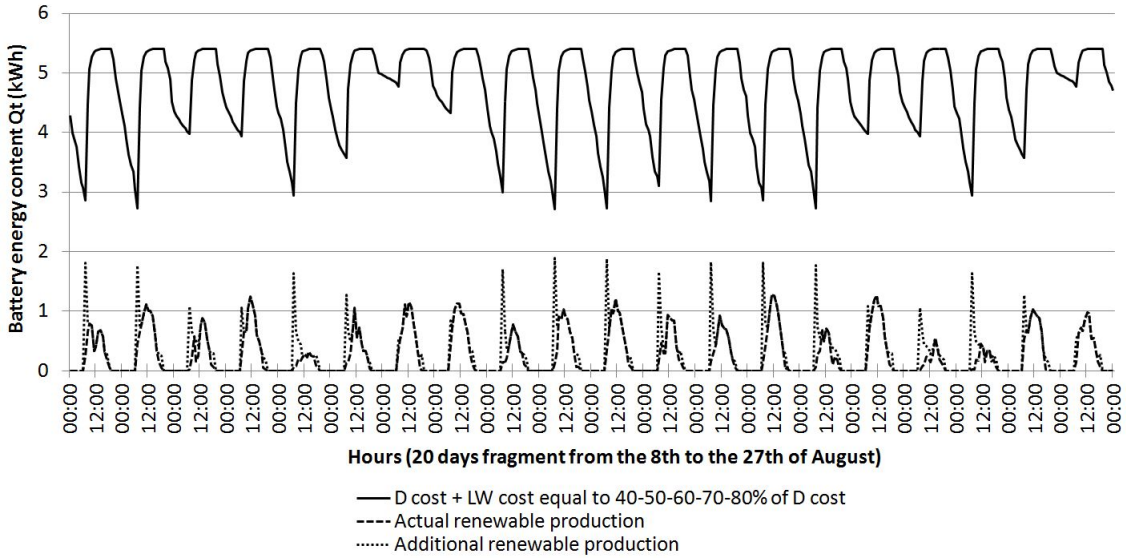


Figure 8.14: Battery trend as a consequence of the additional PV production suggested by the model together with curves related to the actual PV production and the additional suggested PV production. Scenario with LW cost equal to 40-50-60-70-80% of the D cost (overlapped curves)

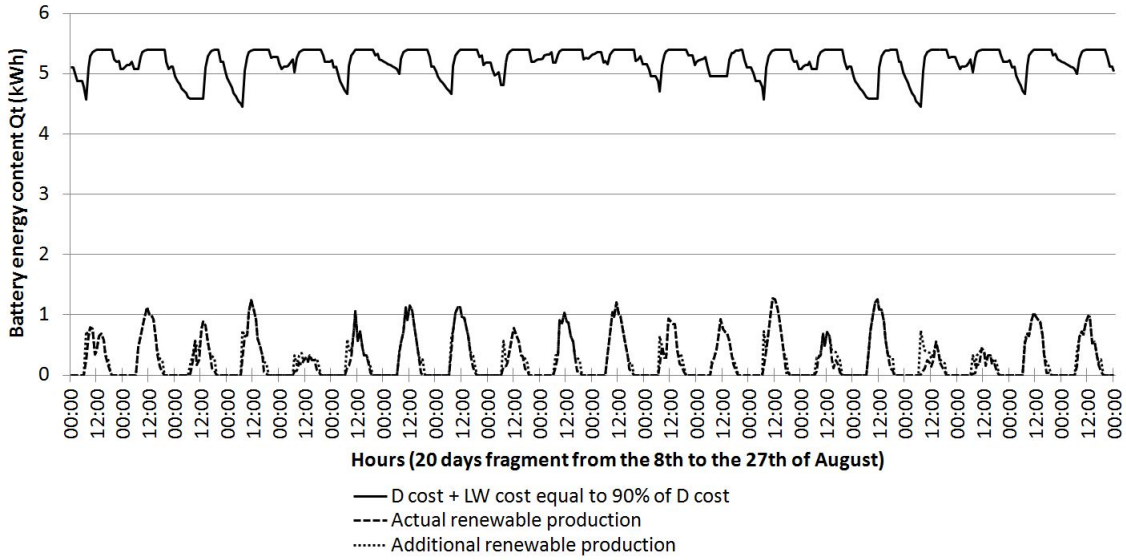


Figure 8.15: Battery trend as a consequence of the additional PV production suggested by the model together with curves related to the actual PV production and the additional suggested PV production. Scenario with LW cost equal to 90% of the D cost

### 8.5.3 Conclusions

To summarize, compared to the Scenario with no additional PV and no battery degradation costs, in this new Scenario with additional PV production and battery degradation costs, the battery use is improved, the diesel costs decrease to zero and the battery replacement cost $C_{rep}$ can increase as follow

$$C_{rep} = LT * Eff * 0.8 * K \tag{8.37}$$

where $LT$ and $Eff$ are the battery lifetime throughput and square root of the roundtrip efficiency respectively, while $K$ is the diesel cost per kWh.

We noted that a healthier battery use can be achieved by an oversized PV plant. That means that if we take into account the battery degradation issues during the operational management of a system, then this can bring to different choices in the preliminary design of the system itself. In this case we showed for instance how the PV plant needed to be built with a different bigger size to guarantee a better lifetime of the integrated battery. Designing a system taking into consideration the battery degradation issues brings to a higher suggested PV installation.

As in previous sections we found that at the current state of the technology battery prices are too high compared to their throughput and efficiency properties, considering the additional tests of the current section, we can say it may be better to invest on more PV panels rather than bigger batteries. This is particularly true if we also consider the rapidly falling global PV prices in the last years. See for instance Figure 8.16 which shows an example of the rapidly falling global PV prices in East Africa.

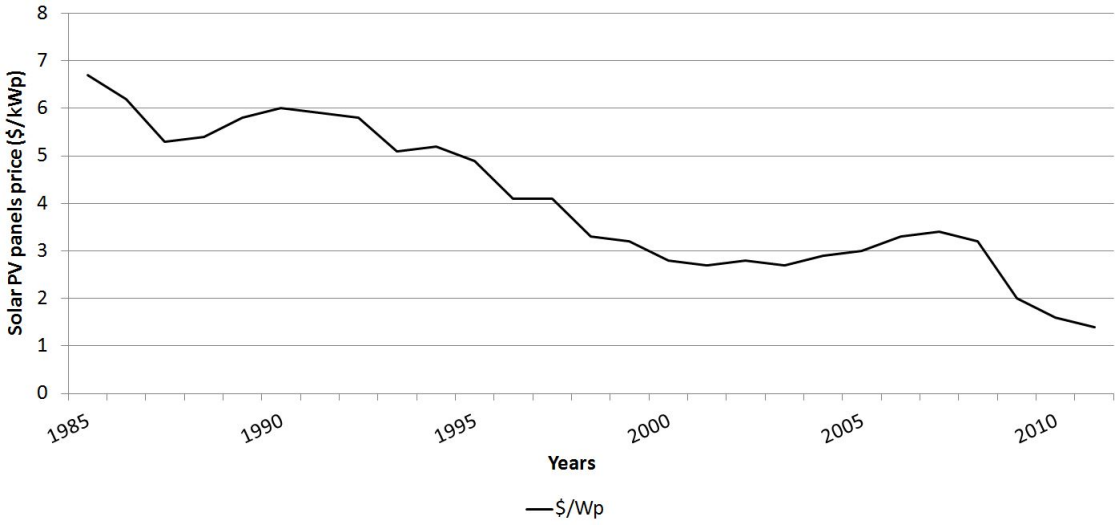


Figure 8.16: Rapidly falling global PV prices in East Africa. Pricing trend of solar PV panels from 1985 to 2011. Source: 1985-2010 data from Paula Mints, Principal Analyst, Solar Services Programme, Navigant. 2011; based on current market data

## 8.6 Loads Disconnection for Sites with No Generator

### 8.6.1 Introduction to African Social Aspects

In this section we will further develop the proposed model to analyze "shortage conditions". These are related to extreme situations in which the conventional generator is assumed to be unavailable. It is the case of most African rural islanded villages where the conventional generator can be missing because of the lack of fossil fuels in the country. Hence communities have to commit the Energy needs just to the renewable resources and storage technologies. In such cases the social aspects of the particular country become very important and they should be included in the analyses together with the technical requirements we discussed in previous sections.

One of the social aspects that characterize African sites in general and the Rwanda sites we are studying in particular, is that 100% power is not a necessity. It is necessary to have it during critical periods, i.e. for essential activities during parts of the day or for lighting at night etc, but compared to other developed countries (i.e. Italy or UK etc), African power demand is much more flexible. Hence, at this stage, it is important not to take out the social element as it is crucial and pure technical optimization can give results that are not practical for such systems.

A wide literature is available in the field of the social and anthropological aspects of Energy. Many interesting studies are related to the way through which people in different countries, conditions and cultures make use of the available Energy resources modifying their needs according to the particular situation in which they grew up and live. Even though these are very interesting and fascinating subjects, a dedicated deep discussion would fall outside the main topic of the present Thesis. Hence we will focus on mathematical formulations that may be useful to meet such social aspects, but for further anthropological readings, the suggestion is to refer to the existing literature available among the scientific production.

More detailed descriptions about African Energy situation in general and Rwanda case in particular can be found in Gupta and Sood [12] and Anuta et al. [4]. For further in depth analyses on social aspects of Energy needs in underdeveloped countries it is also possible to refer to a wide scientific production that comes from the Durham Energy Institute of the Durham University (UK) and its "Society and Energy Research Cluster". The latter in particular developed new theoretical approaches to current energy research challenges based on the conception of energy systems as "socio-technical"; that is, on the understanding that energy systems are co-produced through relations between constituent social and technical elements.

### 8.6.2 Flexible Demand Modeling

To take into account the Rwanda Energy social aspects related to the lack of fossil fuels and to the demand sites flexibility, it is possible to modify the proposed mathematical model by allowing some capacity shortage. That means we will move towards the use of a relaxed "demand meeting constraint", by allowing a portion of unmet demand.

It is necessary to disaggregate the global hourly demand $d^t$ into the different types of loads $l$ that are required in every time step $t$. Hence the global demand $d^t$ will be modified in $d_l^t$, the energy demand of load $l$ in time $t$. A new continuous decision variable $w_l^t$ will be created, to define the amount of $kWh$ of load $l$ that is better to disconnect in time $t$. A representative penalty cost of disconnection $C_l^t$ will be assigned to every load $l$ according

to the different loads priorities, in such a way that most critical loads will have a higher penalty than the most flexible ones.

The objective function will be modified by removing the diesel costs per $kWh$ and adding the new term of cost related to the loads disconnection as follow:

$$\min \sum_t C_L^t + C_B^t \tag{8.38}$$

where the cost of loads disconnection $C_L^t$ has been added in place of the conventional generator cost $C_G^t$ that has been removed to take into consideration sites with no generator. The cost of load disconnection is given by the amount of load $l$ disconnected in time $t$ times the penalty associated to load $l$ according to its priority: $C_L^t = w_l^t * C_l^t$

$C_B^t$ is a battery wearing cost defined as a function $f(s)$ of one or more battery stress factors $s$ as already explained in previous sections.

Then the set of constraints should be modified as follow

$$x_{vd}^t = \sum_l D_l^t - w_l^t \quad \forall t \tag{8.39}$$

$$w_l^t \leq D_l^t \quad \forall t, l \tag{8.40}$$

Constraint 8.39 is a modified version of the basic model constraint 8.2: the flow $x_{pd}^t$ related to the conventional generator has been removed, the demand $d^t$ has been disaggregated into different loads demand $D_l^t$ and the possibility of disconnect part of loads has been added through the variable $w_l^t$. Constraint 8.40 says that for every load $l$, the disconnected power must be less than or equal to the demand of that particular load. Such constraint might be modified by adding different and lower upper bounds to further limit the available power for disconnection; that might be useful to meet some particular needs of the specific site studied.

### 8.6.3 Computational Experiments

In order to run the model it is necessary to disaggregate the demand into different loads with different priorities. A list of the main equipments available in the Rwanda site are listed in Table 8.17.

As real world data are not available, we generated random loads values for every time step $t$ in such a way that the random values summation in every time $t$ is equal to the total demand $d^t$ that we already used in our previous sensitivity analyses. We generated random values for four different types of representative loads ($l = 4$) with four different priorities. Hence the loads listed in Table 8.17 are grouped into four priority classes 1, 2, 3, 4 from the most flexible loads belonging to class 1 to the less flexible loads belonging to class 4.

The load disconnection cost is difficult to estimate. Some studies suggest that the cost of disconnection should be equal to the value of lost load (VOLL) assigned by the customers (i.e. Centolella et al. [7], Anderson and Taylor [2]) and that it depends on the duration of the event (Oseni and Pollitt [19]).

Table 8.17: Main equipments for the Rwanda site and related priorities. 1 is for the most flexible loads, 4 is for the less flexible loads. 2 and 3 correspond to intermediate flexibilities

| Equipment | Priority |
|---|---|
| Centrifuge | 3 |
| Desktop computer | 3 |
| Fridge Freezer | 3 |
| Hematology analyzer | 4 |
| Humalyzer | 4 |
| Laptops | 1 |
| LED Bulbs | 3 |
| Microscope | 4 |
| Mobile Phone chargers | 1 |
| Photocopier | 2 |
| Printers | 2 |
| Rotator | 3 |
| Satellite modem | 2 |
| Security light | 4 |
| Sterilizer | 4 |
| TV | 1 |

For our computational tests purposes, the values of $C_l^t$ were fixed as listed in the Table 8.18 so that the costs of disconnection are higher than any other kind of generation, that means higher than diesel costs and battery degradation costs (considering a standard battery degradation cost equal to 70% of the diesel cost). As a guideline, the penalty cost of disconnection should not be too high, otherwise the model will not disconnect anything, but at the same time it should not be too low, otherwise the model will disconnect almost everything. From some previous tests we found reasonable values lie just around the diesel and battery degradation costs, with slightly higher values.

Moreover each value reflects the flexibility of the load in such a way that the less flexible loads, for example night lighting, are more expensive than the more flexible loads, like the TV or equipments in a rest room. Loads of type L4 with a high priority, are characterized by a *bigm* penalty that is a very high value so that such loads will never be disconnected for any reason.

The upper diagram in Figure 8.17 shows the resulting battery trend after the optimization run by minimizing the battery degradation cost (fixed at 70% of the diesel cost from previous analyses described in Section 8.4.4) together with the load disconnection penalty costs. The bottom diagram shows the demand trend and the total load disconnection trend. The disconnected loads belong to classes L1, L2 and L3, with a very small amount of disconnection for loads of type L3 and a higher amount of disconnection for loads of type L1 and L2.

Thanks to the load disconnection it is still possible to run the off-grid system and improve the battery use, even though the conventional generator is missing.

Table 8.19 shows the battery stress factors comparison between the basic scenario with no battery optimization and the scenario that takes into account the battery degradation cost and the load disconnection possibility.

Table 8.20 shows the estimated lifetime in the two cases. Note that in this case we are not using the conventional generator at all and the load disconnection is limited to the most flexible loads. Hence, the Scenario conditions are quite extreme, but we can still make a better use of the battery and get an improvement in its degradation issues and lifetime.

Table 8.18: Representative penalty costs of disconnection for different loads with different priorities

| Load type | $C_l^t$ ($/kWh) |
|---|---|
| L1 | 0.6 |
| L2 | 0.7 |
| L3 | 0.8 |
| L4 | $bigm$ |

Table 8.19: Results summary along a representative period of 20 days - battery stress factors. Comparison between the basic Scenario with no battery degradation costs and no loads disconnection and the Scenario which consider both a battery degradation cost and load disconnection

| Battery degradation cost LW (% of D cost) | Loads disconnection (Y/N) | Energy out the battery (kWh) | Lowest SoC reached (%) | Average Time between full charged (days) | Highest time between full charged (days) | Time at low SoC (below 35%) (%) | Partial cycles (n) |
|---|---|---|---|---|---|---|---|
| 70 | Yes | 32.15 | 40 | 1.2 | 3 | 0 | 5 |
| 0 | No | 40.01 | 80 | 2.1 | 4 | 35 | 16 |

Table 8.20: Annual projection of the battery estimated lifetime in the different scenarios. Comparison between the basic Scenario with no battery degradation costs and no loads disconnection and the Scenario which considers both a battery degradation cost and load disconnection. Estimated values at the lowest state of charge reached along the period.

| Battery degradation cost LW (% of D cost) | Loads disconnection (Y/N) | Lowest SoC reached (%) | Average annual energy out (kWh) | Throughput at lowest SoC (kWh) | Estimated lifetime (years) |
|---|---|---|---|---|---|
| 70 | Yes | 0.4 | 579 | 2778 | 4.8 |
| 0 | No | 0.8 | 720 | 2592 | 3.6 |

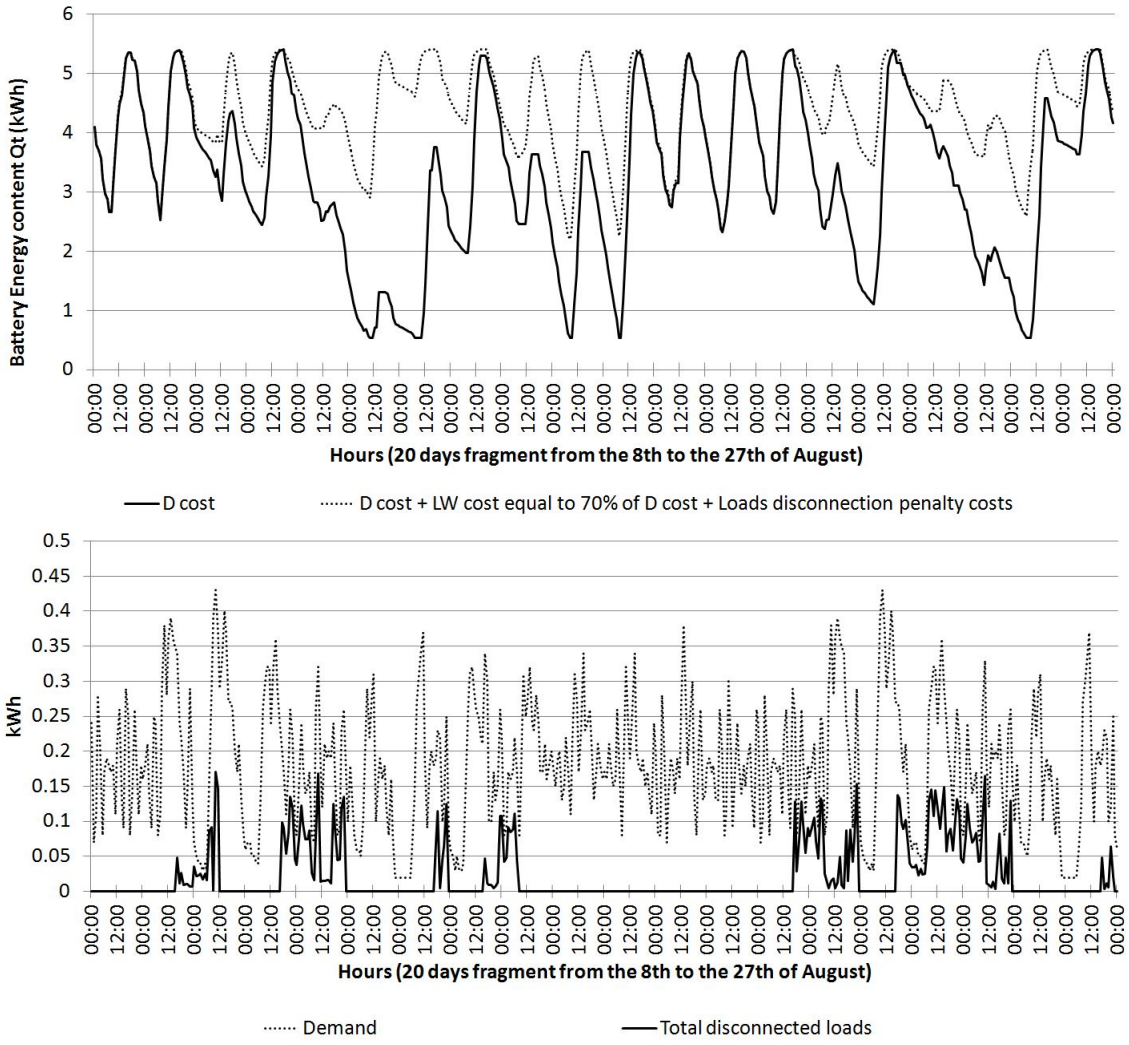


Figure 8.17: Battery trend as a consequence of the loads disconnection. Comparison between the basic scenario with no battery degradation costs and no load disconnection and the new scenario that take into account both the battery degradation cost and the load disconnection

Table 8.21: Total disconnected power for different loads classes along a representative period of 20 days

| Load type | $C_l^t$ ($/kWh) | Disconnected Power (kWh) |
|---|---|---|
| L1 | 0.6 | 8.39 |
| L2 | 0.7 | 0.83 |
| L3 | 0.8 | 0.72 |
| L4 | $bigm$ | 0 |

A further test has been made by combining the load disconnection and an additional PV production.

We found in Section 8.5 that the optimal additional PV production was equal to 0.4 $kWh$. With such additional production the diesel costs were zero and the off-grid system had the possibility to work without any conventional generator.

Let us suppose now that some hypothetical budget limits impose to increase the PV system of an amount that is less than the optimal additional production found in Section 8.5. We can still run our off-grid system without any conventional generator by allowing the loads disconnection previously explained.

Figure 8.18 shows the results obtained running an optimization with an additional PV production equal to the 70% of the optimal production found in Section 8.5, that means an additional PV production equal to 0.3 $kWh$. In this case the battery trend is better than the trend we got in Figure 8.17 (where no additional PV production was considered) as there are no partial cycles at all. We can also see that the total disconnected loads are less than the loads that have been disconnected in Figure 8.17. That is because the test represented in Figure 8.17 has been run with the actual PV production while the test represented in Figure 8.18 has been run with an additional PV production. Hence in the latter case the system can count on more renewable and therefore it is possible to reduce the disconnected loads.

Table 8.22 summarize the loads disconnection obtained in this test.

Table 8.22: Total disconnected power for different loads classes along a representative period of 20 days with an additional PV production of 0.3 $kWh$

| Load type | $C_l^t$ ($/kWh) | Disconnected Power (kWh) |
|---|---|---|
| L1 | 0.6 | 0.15 |
| L2 | 0.7 | 0.02 |
| L3 | 0.8 | 0.01 |
| L4 | $bigm$ | 0 |

Table 8.23: Results summary along a representative period of 20 days - battery stress factors. Comparison between the basic Scenario and the Scenario that takes into account a battery degradation cost, the load disconnection and an additional PV production equal to 0.3 $kWh$

| Battery degradation cost LW (% of D cost) | Loads discon (Y/N) | Additional PV production (kWh) | Energy out the battery (kWh) | Lowest SoC reached (%) | Average Time between full charged (days) | Highest time between full charged (days) | Time at low SoC (below 35%) (%) | Partial cycles (n) |
|---|---|---|---|---|---|---|---|---|
| 70 | Yes | 0.3 | 33.22 | 50 | 1 | 1 | 0 | 0 |
| 0 | No | 0 | 40.01 | 80 | 2.1 | 4 | 35 | 16 |

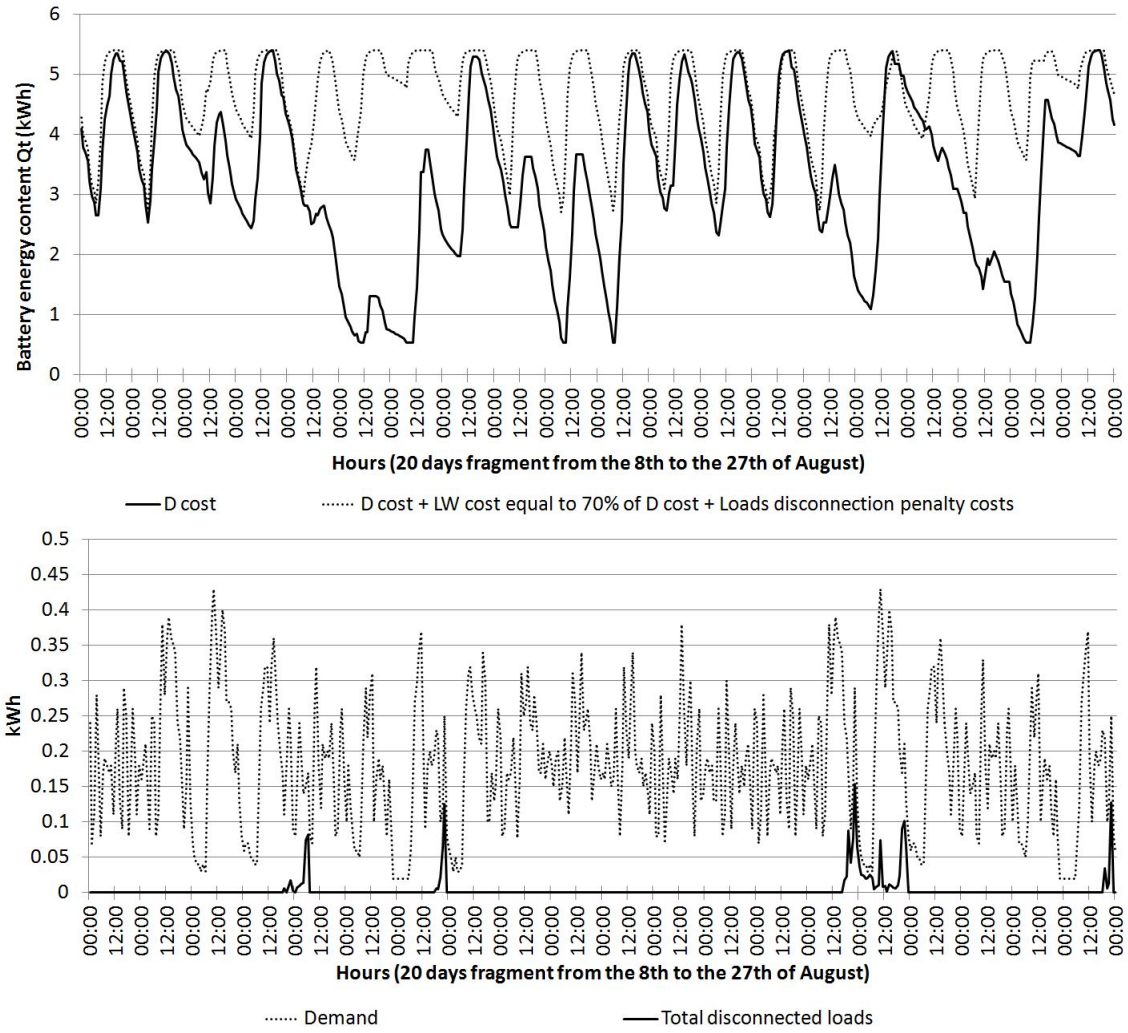


Figure 8.18: Battery trend and loads disconnection along a representative period of 20 days. Comparison between the basic Scenario and the Scenario that takes into account a battery degradataion cost, the load disconnection and an additional PV production equal to 0.3 $kWh$

Table 8.24: Annual projection of the battery estimated lifetime. Comparison between the basic Scenario and the Scenario that takes into account a battery degradataion cost, the load disconnection and an additional PV production equal to 0.3 $kWh$. Estimated values at the lowest state of charge reached along a representative period of 20 days.

| Battery degradation cost LW (% of D cost) | Loads disconnection (Y/N) | Additional PV production (kWh) | Lowest SoC reached (%) | Average annual energy out (kWh) | Throughput at lowest SoC (kWh) | Estimated lifetime (years) |
|---|---|---|---|---|---|---|
| 70 | Yes | 0.3 | 0.5 | 598 | 2700 | 4.5 |
| 0 | No | 0 | 0.8 | 720 | 2592 | 3.6 |

### 8.6.4 Conclusions

In this section we further improved the model by including a representation of the load flexibility in terms of cost, allowing the system to disconnect loads with different priorities, when the demand is greater than the energy generation at certain time. Simulation results proved that the load disconnection can be used as a mechanism to protect the batteries from over-discharging and improper use in general. Moreover, the load flexibility can be useful to find a better design for the off-grid power supply, by reducing the capacity of the battery and therefore reducing the investment costs through the purchase of smaller and cheaper storage units.

## 8.7 Conclusions and Future Developments

A model for the battery degradation analyses and optimization has been presented. The contribution of the study is both a methodological one and an analytical one. From a methodological point of view we presented mathematical ways and tricks to represent off-grid systems and battery degradation issues inside an optimization model. It is important to note that we didn't make any assumption on the allowable depth of discharge or on the maximum number or allowed cycles but we found a way to get optimized values as output rather than imposing them as input (the latter way is what generally people do in literature). From an analytical point of view we used the proposed model (and the additional features in different combinations) to make sensitivity analyses on the battery prices and degradation costs showing the state of the art of the technology and how this might improve moving towards different prices. We also showed how the battery use can change taking into consideration the most important degradation issues such as depth of discharge and number and type of cycles.

At the current state of technology batteries are convenient for backup and emergency uses, no matter how they are classified. Both deep-cycle batteries and shallow cycles batteries, at the current prices, turned out to be not worthy for the deep use required by Off-Grid systems. Battery prices should move towards a reduction so that the battery replacement cost $C_{rep}$ should satisfy the relationship $C_{rep} = LT * Eff * 0.7 * K$ where $LT$ and $Eff$ are the battery lifetime throughput and square root of the roundtrip efficiency respectively, while $K$ is the diesel cost per $kWh$. Remember that the diesel represents the main alternative energy source for the system and a better use of the battery can require a higher use of diesel, hence it is important to find out the best trade-off between battery lifetime improvement and the related higher diesel costs.

This relationship could be a guideline when purchasing a battery to understand its degradation issues and forecast its behavior and lifetime. However, in remote sites where the diesel cost is higher due to additional transportation and handling operations, the use of storage becomes more valuable as long as the global diesel cost can increase at least up to the 20-30%.

We also saw how the installation of additional PV power can be useful both to further reduce the use of the backup conventional generator and to allow the purchase of more expensive batteries. In such cases the battery replacement cost can increase as follow: $C_{rep} = LT * Eff * 0.8 * K$.

In general we can say an optimization model like the one we studied, can be very useful to extend analyses on a wide range of batteries and evaluate their convenience in terms of prices and degradation costs.

In conclusion, it is clear that a hybrid system design should take into consideration battery degradation issues and costs: such issues are frequently overlooked while our analyses showed clearly how much they can influence the design and the general operating cost of a system.

As for future development, the model is going to be integrated with a demand responsive formulation that can extend the load disconnection analyses, shifting loads of sites or by programming a battery management system that limits output power at specific time of the day. More batteries types with different properties, costs, throughput and efficiency shall be investigated.

# Bibliography


[1] H. Anderson, B. Alexander, P. Annabelle, and S. Kandler. Electric vehicle charge optimization including effects of lithium-ion battery degradation. In *Vehicle Power and Propulsion Conference*, 2011.

[2] R. Anderson and L. Taylor. The social cost of unsupplied electricity: a critical review. *Energy Economics*, 8(3):139–146, 1986.

[3] U. Angel, p. Thomas, and G. J. Rudolph. Stochastic modeling of rechargeable battery life in a photovoltaic power system. In *Energy Conversion Engineering Conference and Exhibit*, 2000.

[4] O. Anuta, A. Crossland, B. McNeil, N. Wade, and S. Dargan. Techno-economic study on the performance of pv systems in schools and health centres in rural rwanda. Technical report, 2013.

[5] A. G. Bakirtzis and P. S. Dokopoulos. Short term generation scheduling in a small autonomous system with unconventional energy sources. *IEEE Transactions On Power Systems*, 3(3):1230 – 1236, 1988.

[6] L. Bo and S. Mohammad. Short-term scheduling of battery in a grid-connected pv-battery system. *IEEE Transactions On Power Systems*, 20(2):1053 – 1061, 2005.

[7] P. Centolella, M. Farber-DeAnda, L. Greening, and T. Kim. Estimates of the value of uninterrupted service for the mid-west independent system operator. *Carmel, IN: Midwest ISO*, 2006.

[8] R. Chedid and Y. Saliba. Optimization and control of autonomous renewable energy systems. *International Journal Of Energy Research*, 20, 1996.

[9] D. Connolly, H. Lund, B. V. Mathiesen, and M. Leahy. A review of computer tools for analysing the integration of renewable energy into various energy systems. *Applied Energy*, 87(4):1059–1082, 2010.

[10] Z. Di, W. Yanzhi, C. Naehyuck, and P. Massoud. Optimal design and management of a smart residential pv and energy storage system. In *Design, Automation and Test in Europe Conference and Exhibition*, 2014.

[11] A. M. Faisal and N. K. Heikki. System modelling and online optimal management of microgrid with battery storage. In *International Conference on Renewable Energies and Power Quality*, 2007.

[12] G. Gupta and H. Sood. A short paper research on energy resources in rwanda and alternative solution regarding the lack of fossil fuels in the country. *Research Reaction & Resolution International Journal of All Academic Research*, page 10.

[13] A. Hoke, A. Brissette, D. Maksimovic, D. Kelly, A. Pratt, and D. Boundy. Maximizing lithium ion vehicle battery life through optimized partial charging. In *Innovative Smart Grid Technologies (ISGT), 2013 IEEE PES*, pages 1–5. IEEE, 2013.

[14] M. Hugo, K. Peter, F. Pedro, A. V. Zita, and H. M. Khodr. Optimal scheduling of a renewable micro-grid in an isolated load area using mixed-integer linear programming. *Renewable Energy*, 35, 2010.

[15] T. Jen-Hao, L. Shang-Wen, L. Dong-Jing, and H. yong Qing. Optimal charging discharging scheduling of battery storage systems for distribution systems interconnected with sizeable pv generation systems. *Power Systems, IEEE Transactions*, 28, 2013.

[16] P. Lombardi, M. Heuer, and Z. Styczynski. Battery switch station as storage system in an autonomous power system: optimization issue. In *Power and Energy Society General Meeting, 2010 IEEE*, pages 1–6. IEEE, 2010.

[17] D. K. Maly and K. S. Kwan. Optimal battery energy storage system (bess) charge scheduling with dynamic programming. *IEEE Proc. Sci. Meas. Technol.*, 142(6):453 – 458, 1995.

[18] F. A. Mohamed and H. N. Koivo. Online management of microgrid with battery storage using multiobjective optimization. In *Power Engineering, Energy and Electrical Drives, 2007. POWERENG 2007. International Conference on*, pages 231–236. IEEE, 2007.

[19] M. O. Oseni and M. G. Pollitt. The economic costs of unsupplied electricity: Evidence from backup generation among african firms. Technical report, Faculty of Economics, University of Cambridge, 2013.

[20] M. Pascal, C. Rachid, and O. Aleandre. Optimizing a battery energy storage system for frequency control application in an isolated power system. *IEEE Transaction On Power Systems*, 24(3):1469 – 1477, 2009.

[21] P. Rakesh and S. Ratnesh. Quantifying the impact of battery constraints on microgrid operation using optimal control. In *Innovative Smart Grid Technologies Conference*, 2014.

[22] K. R. Saeed, C. R. Sean, and E. W. Ralph. Maximizing the life of a lithium-ion cell by optimization of charging rates. *Journal of The Electrochemical Society*, 157(12): A1302 – A1308, 2010.

[23] K. Shinya, N. Hide, T. Ittetsu, and S. Kazutoshi. Analysis on battery storage utilization in decentralized solar energy networks based on a mathematical programming model. In *Soft Computing and Intelligent Systems and 13th International Symposium on Advanced Intelligent Systems*, 2012.

[24] K. Shinya, T. Ittetsu, F. Masahiro, and S. Kazutoshi. A battery degradation aware optimal power distribution on decentralized energy network. In *New Circuits and Systems Conference*, 2012.

[25] V. Svoboda, H. Wenzl, R. Kaiser, A. Jossen, I. Baring-Gould, J. Manwell, P. Lundsager, H. Bindner, T. Cronin, P. Nørgård, et al. Operating conditions of batteries in off-grid renewable energy systems. *Solar Energy*, 81(11):1409–1425, 2007.

[26] R. Yann, B. Seddik, B. Franck, and P. Stephane. Optimal power flow management for grid connected pv systems with batteries. *IEEE Transactions On Sustainable Energy*, 2(3):309 – 320, 2011.